Identification of POT-3 and its role in telomere length maintenance in *Caenorhabditis elegans*

Xupeng Yu

A thesis submitted for the degree of PhD
at the
University of St Andrews

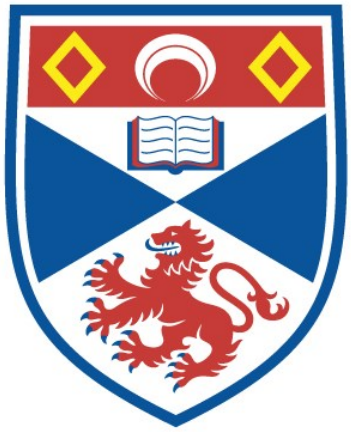

2024

Full metadata for this thesis is available in
St Andrews Research Repository
at:
https://research-repository.st-andrews.ac.uk/

Identifier to use to cite or link to this thesis:

DOI: https://doi.org/10.17630/sta/885

This item is protected by original copyright

This item is licensed under a
Creative Commons Licence

https://creativecommons.org/licenses/by/4.0/

Candidate's declaration

I, Xupeng Yu, do hereby certify that this thesis, submitted for the degree of PhD, which is approximately 40,000 words in length, has been written by me, and that it is the record of work carried out by me, or principally by myself in collaboration with others as acknowledged, and that it has not been submitted in any previous application for any degree. I confirm that any appendices included in my thesis contain only material permitted by the 'Assessment of Postgraduate Research Students' policy.

I was admitted as a research student at the University of St Andrews in October 2019.

I received funding from an organisation or institution and have acknowledged the funder(s) in the full text of my thesis.

Date 30/04/2024 Signature of candidate _____

Supervisor's declaration

I hereby certify that the candidate has fulfilled the conditions of the Resolution and Regulations appropriate for the degree of PhD in the University of St Andrews and that the candidate is qualified to submit this thesis in application for that degree. I confirm that any appendices included in the thesis contain only material permitted by the 'Assessment of Postgraduate Research Students' policy.

Date 30/04/2024 Signature of supervisor _____

Permission for publication

In submitting this thesis to the University of St Andrews we understand that we are giving permission for it to be made available for use in accordance with the regulations of the University Library for the time being in force, subject to any copyright vested in the work not being affected thereby. We also understand, unless exempt by an award of an embargo as requested below, that the title and the abstract will be published, and that a copy of the work may be made and supplied to any bona fide library or research worker, that this thesis will be electronically accessible for personal or research use and that the library has the right to migrate this thesis into new electronic forms as required to ensure continued access to the thesis.

I, Xupeng Yu, confirm that my thesis does not contain any third-party material that requires copyright clearance.

The following is an agreed request by candidate and supervisor regarding the publication of this thesis:

Printed copy

No embargo on print copy.

Electronic copy

No embargo on electronic copy.

Date 30/04/2024 Signature of candidate _____

Date 30/04/2024 Signature of supervisor _____

Underpinning Research Data or Digital Outputs

Candidate's declaration

I, Xupeng Yu, understand that by declaring that I have original research data or digital outputs, I should make every effort in meeting the University's and research funders' requirements on the deposit and sharing of research data or research digital outputs.

Date 30/04/2024 Signature of candidate _____

Permission for publication of underpinning research data or digital outputs

We understand that for any original research data or digital outputs which are deposited, we are giving permission for them to be made available for use in accordance with the requirements of the University and research funders, for the time being in force. We also understand that the title and the description will be published, and that the underpinning research data or digital outputs will be electronically accessible for use in accordance with the license specified at the point of deposit, unless exempt by award of an embargo as requested below.

The following is an agreed request by candidate and supervisor regarding the publication of underpinning research data or digital outputs:

No embargo on underpinning research data or digital outputs.

Date 30/04/2024 Signature of candidate _____

Date 30/04/2024 Signature of supervisor _____

Table of Contents

List of Figures

List of Tables

Acknowledgements

I would like to express my sincere gratitude to those who have contributed to the completion of my PhD thesis.

Firstly, I would like to start by thanking my supervisor Dr. Helder Ferreira for his guidance, expertise, and mentorship throughout my doctoral studies. He always guides me to the road to see the bigger picture. His profound insights and support have not only shaped the content of this thesis but have also contributed significantly to my growth as a scientist. His mentorship extends beyond the laboratory, as he has been a great friend, providing care and emotional support during the whole times.

Secondly, I would like to thank my colleagues and lab mates. In particular, I am grateful to Janie Olver, who is the best colleague and friend one can ever have. She created the supporting and loving environment for us. The brainstorm and emotional support between us been a source of inspiration in our studies. I also extend my thanks to Dr. Shirley Graham, Mariya Shtumpf, and Emma Brydges for their indispensable contributions to this research. Without their participation, this study would not have been possible.

Thirdly, I would like to thank the University of St Andrews for providing the necessary resources, including laboratory facilities and access to academic literature. Their support was pivotal in conducting this research. I also appreciate the support provided by the BSRC staff, whose efforts have fostered a conducive research environment. Moreover, I would like to thank China Scholarship Council for its generous fund.

Finally, I would like to thank my family and friends for their support all the time. I would like to express my deep appreciation to my parents, Zizhi Yu and Shi'e Jiang. They support my higher education over many years and are always there for me whenever I need them. I would like to thank my flatmate Dr Qilin Shangguan for managing household responsibilities, allowing me to focus on my studies. I also want to express my gratitude to all my friends: Dr Yang Yang, Puchong Paopan, Uthumphorn Kankeb, Boontharee Chomhom, Huanhuan Wu, Chen Xu, Haotian Chi, Kaixuan Cui. It's my luck to meet you all.

St Andrews is a magical place that I would call it my home. It has changed the way I see, the way I think, and the way I live. After four years, it is time for me to thrive and shine. I will forever cherish the time I spent here and the people I met here.

Funding

This work was supported by grants from the China Scholarship Council (reference 201904910787).

Research Data/Digital Outputs access statement

Research data underpinning this thesis are available at:

https://doi.org/10.17630/3810da11-c9f8-44be-9338-18f590738065

Abstract

Telomeres, consisting of repetitive DNA sequences, cap linear chromosomes, to prevent replicative erosion and inappropriate DNA damage responses. Human Protection of Telomeres 1 (POT1) directly interacts with single-stranded telomeric DNA, safeguarding chromosomal ends and contributing to telomere length regulation. In *Caenorhabditis elegans*, four human POT1 homologs, namely POT-1, POT-2, POT-3, and MRT-1, are present. MRT-1 is essential for telomerase-dependent telomere maintenance and acts as a 3' to 5' exonuclease. POT-1 and POT-2 repress telomerase activity and influence telomeric overhang length. However, POT-3 was less well understood.

Here, we show that the loss of POT-3 function leads to elongated telomere length and an increased level of circular extrachromosomal telomeric DNA (C-circles). This is consistent with POT-3 behaving as a paralog of POT-2. Interestingly, POT proteins display intricate phenotypic relationships between each other. When quantifying brood size, *pot-3* acts epistatically with *pot-2* in a POT-1 dependent manner. The extremely long telomeres of *pot* mutants provided an opportunity to study the inheritance of telomere length in *C. elegans.* Telomere length inheritance in *C. elegans* was observed to be a stochastic process, instead of being exclusively parental, with telomeres inherited from both male and hermaphrodite parents, regardless of their length. When worms inherit telomeres of different lengths, long telomeres remain stable while short ones elongate rapidly. Moreover, *mrt-1* and *trt-1* strains, previously thought to act in the same telomere regulation pathway, display differential responses in fertility span and telomere length shortening to the loss of POT-2 or/and POT-3. These results highlight the complexity of the interplay between these telomeric proteins. This study unveils the role of POT-2 and POT-3 in telomere length and fertility regulation, opening new avenues for future cancer research. Telomere inheritance identification in *C. elegans* also contributes to the study of telomere inheritance in other organisms.

Abbreviations

9-1-1	Rad9-Rad1-Hus1
ACD	adrenocortical dysplasia protein homologue
ALT	alternative lengthening of telomere
APBs	ALT-associated PML bodies
ATR	ataxia telangiectasia and Rad3-related
AUC	area under curve
BR	broad range
BSA	Bovine serum albumin
Cdc13	cell division cycle 13
CGC	Caenorhabditis Genetics Center
CST	Ctc1/Stn1/Ten1
DCK1	dyskerin
DDR	DNA damage response
DF	diluted factor
EDTA	ethylenediaminetetraacetic acid
EMSA	electrophoretic mobility shift assays
Exo1	Exonuclease 1
FISH	fluorescence in situ hybridization
Flow-FISH	fluorescent in situ hybridization with flow cytometry
G4	G-quadruplex
HIM	high incidence of males
HJRL	Holliday junction resolvase-like domain
hnRNPA1	heterogeneous nuclear ribonucleoprotein A1
HR	homologous recombination
hTR	human non-coding RNA templates
ICL	interstrand cross-link
IF	Immunofluorescence
kb	kilobase
LTR	non-long terminal repeat
ND-10	nuclear domain-10
NGM	Nematode Growth Medium
NHEJ	non-homologous DNA end joining
OB	oligonucleotide/oligosaccharide binding
OD	optical density

PFA	paraformaldehyde
PML	Promyelocytic leukemia
POT	The Protection of telomere
Q-FISH	Quantitative fluorescence *in situ* hybridization
qPCR	quantitative PCR
RAP1	repressor/activator protein 1
RCA	rolling circle amplification
RPA	replication protein A
SDS	sodium dodecyl sulphate
STELA	Single Telomere Length Analysis
TER1	telomerase RNA
TERRA	telomeric repeat-containing RNA
TERT	telomerase reverse transcriptase
TeSLA	Telomere Shortest Length Assay
TIN2	TRF1-interacting nuclear factor 2
T-loops	Telomeric loops
TMMs	Telomere Maintenance Mechanisms
TRD	telomere rapid deletion
TRF	terminal restriction fragment
TRF	telomere repeat binding factors
T-SCEs	telomere sister chromatid exchanges
UV	ultraviolet
Ver	Verrocchio
WGS	whole-genome sequencing

Chapter 1 : General introduction

1.1 Telomere and telomere ends in the ssDNA overhangs

Telomeres, crucial components of chromosomes, consist of tandemly repeated DNA sequences found in most eukaryotes (Jiang et al. 2018; Giardini et al. 2014). Telomeres were first discovered in 1938 by Muller, who identified their function as protective caps at the ends of chromosomes in the fruit fly *Drosophila melanogaster* (Muller 1938; Harald Biessmann and Mason 1997).

The repetitive DNA sequence within telomeres was initially identified by Moyzis et al. in 1988 from a human recombinant repetitive DNA library. This sequence is highly conserved across many species like mammals, fish, birds, and invertebrates (Moyzis et al. 1988). In numerous organisms, including humans, the telomere sequence is $(TTAGGG)_n$. Therefore, this is a sequence that has remained conserved for over 400 million years (Meyne, Ratliff, and Moyzis 1989).

The primary role of telomeres is to safeguard the chromosome ends from being recognised as DNA breaks, thereby preventing the triggering of DNA damage repair and attack from different enzymes (Giardini et al. 2014). These mechanisms involve the recruitment of various proteins and enzymes to repair DNA lesions, which can lead to telomere fragmentation and chromosome fusion (Giardini et al. 2014; Biessmann and Mason 1997). Enzymatic attack on telomeres can result in the loss of genetic information (Verdun and Karlseder 2007).

1.1.1 Structure of telomeric DNA

Telomeric DNA has a unique structure, comprising double-stranded DNA with a single-stranded G-rich 3’ tail (Nandakumar and Cech 2013). The foundational understanding of the telomeric DNA sequence and its features traces back to Blackburn and Gall's seminal work in 1978, conducted on the ciliated protozoan *Tetrahymena thermophila* (Blackburn and Gall 1978).

In most vertebrates, including humans and mice, telomeric DNA is typified by G-rich repetitive sequences, specifically a hexanucleotide repeat $(TTAGGG)_n$ (Meyne, Ratliff, and Moyzis 1989; Greider 1996; Wellinger and Sen 1997). The length of these repetitive sequences can vary notably between individual chromosome ends and even among different cells within an organism. For instance, in human cells, the telomeric DNA can range from 0.5 to 15 kilobase (kb) in length, depending on the tissue type (Aubert and Lansdorp 2008). This length variability

is influenced by factors such as the age of the cell source and the replicative history of the cells, indicating that the telomeric DNA undergoes replication distinct from that of the rest of the chromosome.

Furthermore, size variance of telomeric DNA extends across species. In mice, the length of telomeric DNA can vary from approximately 2.5 kb to 100 kb, significantly longer than telomeres in human cells (Kipling and Cooke 1990). Additionally, telomeric DNA exhibits considerable diversity across species. Invertebrates, like *Caenorhabditis elegans* and *Ascaris lumbricoides* have repeat sequence (TTAGGC) while certain insects such as *Bombyx mori* (silk moth), and *Apis mellifiera* (honeybee), exhibit (TTAGG). Plant species like *Arabidopsis thaliana* possess (TTTAGGG), and *Lycopersicon esculentum* (tomato) harbour (TT(T/A)AGGG). Moreover, certain yeast species like *Saccharomyces cerevisiae* exhibit the repeat sequence of $(TG_{2-3}(TG)_{1-6})$ (Cohn 2008).

Beyond the basic repetitive DNA sequences, telomeres exhibit complex secondary DNA structures within the telomere region, including t-loops and G-quadruplexes (Figure 1.1). T-loops (telomeric loops) are formed when a 3' single-stranded DNA overhang (discussed in detail in Section 1.2.2) invades the double-stranded DNA upstream (Giardini et al. 2014). In certain circumstances, t-loops can transform into or generate extrachromosomal circular DNA structure called T-circles. T-circles are frequently associated with alternative lengthening of telomere (ALT), a mechanism for elongating telomeres without relying on telomerase (Cesare and Griffith 2004). Another intriguing telomeric DNA structure is the G-quadruplex, also known as G4. G-quadruplex consists of two or more G-quartets stacked on top of each other. G-quartets are square planar arrays of four guanines held together by Hoogsteen base pairing (Nandakumar and Cech 2013).

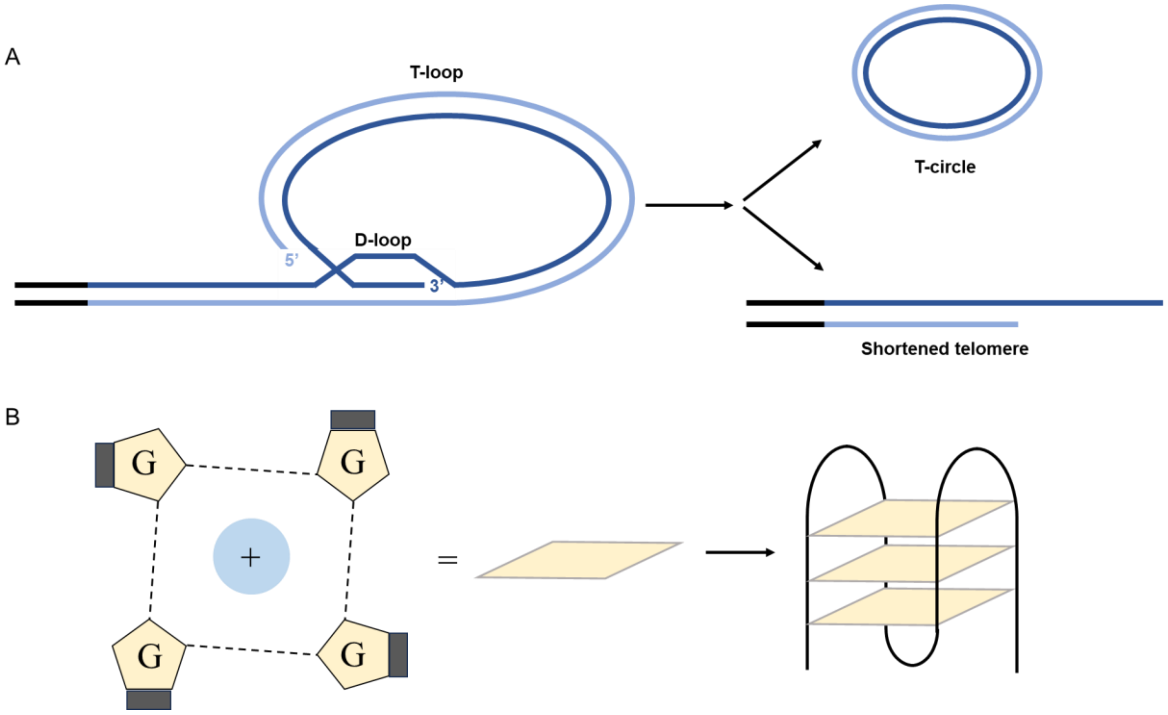

Figure 1.1 T-loops and G-quadruplexes are complex secondary DNA structures within telomere region

A) The structure of a t-loop. In certain circumstances, a t-loop can be deleted. The products are a shortened telomere and a relaxed telomeric circle (t-circle). This figure is modified from Wang, Smogorzewska, and De Lange 2004. B) The structure of a G-quadruplex. Four guanines are connected by Hoogsteen base pairing (black dotted line) to form a square planar plane, G-quartet (yellow parallelogram). Univalent metal cations (Na^+ or K^+) locate in the central channel of the G-quartet to stabilise the structure (blue circle with "+"). A G-quadruplex consists of three G-quartets stacked on top of each other (only one of the topologies is shown). This figure is modified from Zhang et al. 2023.

1.1.2 Telomere ssDNA overhang

The telomeric DNA terminus is not a simple blunt end. Instead, it typically ends with a G-rich strand that extends beyond the opposite C-rich strand, forming a G-tail or G-overhang (Verdun and Karlseder 2007). The conservation of the G-overhang across eukaryotic species suggests its vital role in telomeric function (Henderson and Blackburn, 1989).

The formation of telomeric DNA overhang can occur through various processes: 1) during semiconservative DNA replication, the RNA primer from the 5' end of the newly synthesized strand is degraded. 2) telomerase, an enzyme responsible for telomere elongation, extends the 3' end of the telomeric DNA, followed by fill-in synthesis of the C-rich strand. 3) both chromosome ends are resected by nucleolytic processing, contributing to the formation of the overhang (Wu, Takai, and De Lange 2012).

Several enzymes are involved in the regulation of telomeric DNA overhangs. For example, Apollo, a nuclease plays a role in initiating the formation of the 3’ overhang at the leading end telomere. Exonuclease 1 (Exo1), which processes 5' to 3' exonuclease activity and RNase activity, is also involved in overhang processing. The Ctc1/Stn1/Ten1 (CST) complex, a DNA Polα/primase accessory factor, participates in shortening the extended overhangs. Importantly, all these enzymes are associated with a protein complex called shelterin which consists of six components (discussed in detail in Section 1.3) (Wu, Takai, and De Lange 2012).

1.2 Telomere shortening and telomere maintenance

1.2.1 Telomere shortening

Hayflick and Moorhead in 1961 observed that human diploid fibroblasts have finite proliferation potential. Cells will stop dividing after a determined number of duplications in culture (Hayflick and Moorhead 1961). This number of replications is termed the Hayflick limit. This phenomenon is called replicative senescence.

Telomere shortening occurs with each cell division as a consequence of incomplete replication of chromosome ends by DNA polymerases, particularly at the lagging strand (Olovnikov 1973). The attrition of telomere results in the loss of approximately 200 nucleotides per cell cycle. This process involves restricting interactions between telomeric DNA and its binding proteins or the inactivation of telomerase (D’Adda Di Fagagna et al. 2003). When the length of a telomere reaches a critical limit, short telomeres will be detected as double-strand DNA breaks. DNA double-strand breaks induce the DNA damage response (DDR) through the ATM kinase which directly activates p53 and its downstream transcriptional target p21 (Lossaint et al. 2011). Then DNA damage checkpoint kinases are activated, preventing the transcription of genes associated with cell proliferation. At this stage, cells enter replicative senescence, leading to a stable cell cycle arrest which defines cellular senescence (cellular senescence can also be triggered by non-replicative senescence pathways) (Shay, Pereira-Smith, and Wright 1991; Beauséjour et al. 2003). This leads to cellular dysfunction and contributes to aging (Campisi and d’Adda di Fagagna 2007).

Moreover, the presence of extremely short telomeres rather than the average length or longest telomere triggers checkpoint activation even though the length of the telomeres varies across different chromosomes. Short telomeres contribute to recruiting checkpoint proteins like

Cdc13 (cell division cycle 13) and replication protein A (RPA), and DNA repair proteins like Rad52 (Khadaroo et al. 2009). These proteins further lead to replicative senescence.

The re-introduction of telomerase could (partially) rescue the cellular senescence resulting from telomere shortening. Introducing telomerase into normal human cells results in the elongation of telomeres, vigorous cell division, and a reduction in cell senescence (Bodnar et al. 1998). In mice, the telomerase-deficient cells displayed chromosome ends with undetectable telomere repeats, aneuploidy, and chromosomal abnormalities, including end-to-end fusions (Blasco et al. 1997). Telomerase reintroduction in these cells leads to telomere extension, decreased DNA damage signalling and associated cellular checkpoint responses, resumption of proliferation in quiescent cultures, and elimination of degenerative phenotypes across multiple organs, including the testes, spleens and intestines (Jaskelioff et al. 2011).

Saccharomyces cerevisiae also acts as a model to study replicative senescence triggered by telomere shortening (Teixeira 2013). Similarly to mammals, short telomeres in yeast activate the DNA damage checkpoints (IJpma and Greider 2003). In addition to that, eroded telomeres could face replication stress. Loss of telomere capping and loss of telomere sequences can both provoke senescence (Grandin, Bailly, and Charbonneau 2005).

1.2.2 Telomere maintenance

Telomere Maintenance Mechanisms (TMMs) are critical to preserve genomic stability, chromosome integrity, and the survival of proliferating cells. Cell senescence or cell apoptosis is not the fate of all cell types when telomeres shorten. Certain cells such as germinal cells, stem cells, and cancer cells are able to bypass telomere shortening mechanisms and maintain telomere length via TMMs. (De Vitis, Berardinelli, and Sgura 2018).

Two main TMMs are telomerase-mediated telomere maintenance and the alternative lengthening of telomere (ALT) pathway (De Vitis, Berardinelli, and Sgura 2018).

Telomerase is a ribonucleoprotein polymerase that adds DNA repeats to the 3’ ends of telomeres, thereby maintaining their length (Hou et al. 2022). In human cells, the core components of telomerase are the telomerase reverse transcriptase (hTERT) catalytic subunit, dyskerin (DKC1) and the non-coding RNA templates (hTR) (Cohen et al. 2007). Telomerase was first purified and identified from *Tetrahymena thermophila* by Greider and Blackburn in

1985, revealing its function as a terminal transferase adding telomeric repeat sequences (Greider and Blackburn 1985).

In the absence of telomerase, species employ different ALT mechanisms for telomere elongation. For instance, the budding yeast and certain dipteran insects utilize homologous recombination (HR) while *Drosophila* use retrotransposons (Cicconi et al. 2017; Biessmann and Mason 1997).

Drosophila telomeres use arrays of retrotransposons, which consist of telomere-specific non-long terminal repeat (LTR) retrotransposons (HeT-A, TART and TAHRE, abbreviated here as HTT elements), to maintain chromosome length (Abad et al. 2004; Casacuberta and Pardue 2005). The elongation is performed via a targeted transposition of HTT elements followed by homologous recombination between these elements (Melnikova, Biessmann, and Georgiev 2005; Pardue and DeBaryshe 2003; Mason and Biessmann 1995). *Drosophila* telomeres function similarly to those from eukaryotes that utilize telomerase to extend chromosome ends (Mikhailovsky, Belenkaya, and Georgiev 1999; Biessmann et al. 1992).

Budding yeast and certain dipteran insects use TMM, an alternative mechanism that instead relies on homologous recombination, rather than telomerase (Episkopou et al. 2014). This mechanism involves HR-dependent exchange or HR-dependent telomeric DNA synthesis (Londoño-Vallejo et al. 2004). In the HR-mediated synthesis, the DNA from other telomeres are employed as templates (Sobinoff et al. 2017). In yeast, ALT survivors can be categorized into two types: type I survivors stabilise chromosome ends by multiplying Y' elements which are the subtelomere regions protecting chromosome ends and maintain short terminal telomere repeats, relying on recombination proteins such as Rad52 and Rad51 (Teng and Zakian 1999; Chen, Ijpma, and Greider 2001; Le et al. 1999; Lundblad and Blackburn 1993); type II survivors display very long and heterogeneous terminal telomere repeats and depend on the recombination proteins such as Rad52 and Rad59 (Le et al. 1999; Teng et al. 2000; Teng and Zakian 1999; Chen, Ijpma, and Greider 2001; Lundblad and Blackburn 1993)**.** Recombination at telomeres can lead to substantially longer telomeres or the maintenance of very short telomeres in cells with weak telomerase activity (Basenko, Topcu, and Mceachern 2011). The existence of a unified ALT pathway, involving both Rad51-dependent and Rad51-independent steps, has been observed in both ALT survivor types yeast and may also occur in other species (Kockler, Comeron, and Malkova 2021).

Several unique observations have been made in ALT cells, such as C-circles, ALT-associated PML bodies (APBs), and a high frequency of telomere sister chromatid exchange (T-SCE).

C-circles are similar to C-rich overhangs and are formed due to replication fork collapsing at the telomere strand break. The collapsed fork can induce the fork regression mechanism, where newly synthesised strands anneal to one another, accompanied by parental strand re-annealing, which leads to telomeric HR (Meng and Zhao 2017; Zhang et al. 2019). C-circles serve as specific biomarkers for ALT. In some ALT+ cell lines which do not have APBs or other biomarkers, C-circles still show the quantitative and responsive correlation of ALT activity levels (Henson et al. 2009a). G-circles derived from the G-rich region, are less specific due to their lower quantity compared to C-circles (100 times) (Klebanov-Akopyan et al. 2018).

Promyelocytic leukemia (PML) bodies (also known as nuclear domain-10, ND10) are dynamic nuclear structures that take part in various cellular processes. ALT-associated PML bodies (APBs) are PML bodies that are found exclusively in telomerase-negative tumours. APBs usually are large donut-shape nuclear structure containing PML proteins, telomeric DNA, and telomere binding proteins such as human telomere repeat binding factors 1 and 2 (hTRF1 and hTRF2), and proteins essential for DNA synthesis and HR, such as replication factor A, RAD 51, and RAD 52 (Draskovic et al. 2009; Chung et al. 2012; Yeager et al. 1999). It is worth noticing that there is no PML protein ortholog encoded in the *C. elegans* genome. *C. elegans* does have orthologs of SUMO proteins, which localise to PML bodies in vertebrates (Pham et al. 2021).

Telomere sister chromatid exchange (T-SCE) is characteristic of ALT-positive cells and contributes to telomere elongation (Bechter et al. 2004; Londoño-Vallejo et al. 2004). However, T-SCEs have not been found in human telomerase-positive cells. Inhibition of telomerase will lead to the presence of T-SCE in human cancer cells while reactivation of telomerase completely abolishes the T-SCE pathway in these cells (Bechter et al. 2004). Increased T-SCE level has also been observed in telomere reverse transcriptase-deficient murine embryonic stem cells (Wang et al. 2005). However, no T-SCE has been observed in *C. elegans.*

Generally, the length of telomere is a symbol of lifespan and is a crucial biomarker of senescence. However, in *C. elegans*, there is no significant variation in lifespan between strains with very long telomeres (in the range of 16 kb) and standard wildtype N2 worms, suggesting that telomere length is not fully linked to lifespan in *C. elegans* (Raices et al. 2005).

1.2.3 Telomere inheritance

Telomere length inheritance and dynamics have been extensively researched, particularly concerning human aging and epidemiology. Research findings have uncovered strong correlations between telomere length and various factors such as environmental conditions, age, parental influences, cancer, and mortality.

Parental effects on the telomere length inheritance may vary between species. In humans, with homogametic (XX) sex for females and heterogametic sex (XY) for males, both paternal and maternal telomere inheritance were observed. Maternal inheritance was strongly supported by the research involving 19713 people participating (Broer et al. 2013). Early studies also suggested an X-linked mechanism for telomere length inheritance (Nawrot et al. 2004). Conversely, paternal inheritance has been observed in various cell types, including peripheral mononuclear cells, blood cells, and leukocytes. These results indicate that fathers contribute more to telomere length than mothers in some cells, with a stronger positive correlation between fathers and daughters (Nordfjäll et al. 2010; 2005; Njajou et al. 2007).

In birds, with homogametic (ZZ) sex for males and heterogametic sex (ZW) for females, maternal telomere length inheritance has been extensively observed. Telomeres in males tend to be longer than those in females (Reichert et al. 2015; Horn et al. 2011; Asghar et al. 2015). However, the association with maternal inheritance is significant only in offspring at early ages and diminishes as they age, suggesting a significant influence of environmental factors on telomere length (Reichert et al. 2015; Asghar et al. 2015).

Other factors influencing telomere inheritance include epigenetic inheritance and allele-specific inheritance. Epigenetic inheritance components are observed both in human and birds such as paternal age and maternal age (De Meyer et al. 2014; Bauch et al. 2019). In humans, paternal age is an important determinant for telomere length, whereas in birds, a stronger correlation is observed between mothers' age and offspring's telomere length (Asghar et al. 2015; De Meyer et al. 2007). The relative telomere lengths between children's chromosomes and genetically identical parental chromosomes show a high and significant correlation, suggesting allele-specific inheritance in humans (Graakjaer et al. 2006).

Telomere length in *C. elegans* is clonal and inherited within strains. The telomere length of clonal populations remains constant across generations. However, strong heterogeneity in

telomere length exists in different clones from the same strain and in different strains (Raices et al. 2005). However, the mechanisms underlying telomere length inheritance in *C. elegans* were poorly studied.

1.3 Shelterin

Telomeres can also be protected by proteins located at the telomere region. Shelterin is a vital protein complex located at telomeres, the protective caps found at the ends of chromosomes. It consists of six components: telomeric repeat-binding factor 1 (TRF1), telomeric repeat-binding factor 2 (TRF2), TRF1-interacting nuclear factor 2 (TIN2), repressor/activator protein 1 (RAP1), adrenocortical dysplasia protein homologue (ACD, also known as TPP1, PI1, PTOP and TINT1) and protection of telomeres 1 (POT1). These proteins, interacting with telomeric DNA and other telomeric proteins, contribute to the prevention of the DNA damage response and control telomerase activity to ensure proper regulation of telomere length (Giardini et al. 2014).

1.3.1 Components of shelterin

Telomeric Repeat-Binding Factor 1 (TRF1) was first identified by Zhong et al. in 1992 and later confirmed by Chong et al. in 1995 using specific DNA affinity ion-exchange chromatography (Zhong et al. 1992; Chong et al. 1995). TRF1 comprises a Myb-type DNA-binding domain and an amino-terminal acidic domain. It binds to the double-strand DNA sequence 5'-YTAGGGTTR-3' and primarily promotes the semi-conservative replication of telomeres (Sfeir et al. 2009). Deletion of TRF1 can lead to telomere dysfunction, including DNA replication problems by activating ATR kinase in the S phase and generating "fragile telomeres" during metaphase (Sfeir et al. 2009; Kibe et al. 2010; Schmutz and de Lange 2016).

Telomeric Repeat-Binding Factor 2 (TRF2) was first identified by Bilaud et al. in 1997 (Bilaud et al. 1997). Similar to TRF1, TRF2 can also bind to the double-strand DNA sequence 5'-YTAGGGTTR-3'. TRF2 contributes to T-loop formation by facilitating the invasion of ssDNA overhang into the end of dsDNA region. Deletion of TRF2 can activate the ATM-dependent DNA damage signalling pathway and the non-homologous DNA end joining (NHEJ) pathway, leading to a higher rate of telomere end fusions, primarily occurring during the G1

phase (Kibe et al. 2010; Schmutz and de Lange 2016; Celli and de Lange 2005; Konishi and De Lange 2008).

TRF1-interacting nuclear factor 2 (TIN2) was first identified by Kim et al. in 1999 (S. Kim, Kaminker, and Campisi 1999). TIN2 directly interacts with TRF1, TRF2 and ACD. Deletion of TIN2 can trigger DNA damage responses at telomeres, destabilise shelterin, and increase the rate of cell apoptosis (Denchi and De Lange 2007; Kim et al. 2008; Takai et al. 2011).

Protection of Telomeres 1 (POT1) was first identified by Baumann and Cech in 2001, both in fission yeast and humans (Baumann and Cech 2001). In humans, POT1 binds to ssDNA overhangs with two N-terminal oligonucleotide/oligosaccharide binding (OB) folds, OB1 and OB2. It is conserved among eukaryotic organisms (with different protein numbers and functions) and is typically considered a negative regulator of telomere length. POT1 will be discussed in detail in Section 1.5.2.

Adrenocortical Dysplasia Protein Homolog (ACD), first identified in 2004, was referred to as TINT1 (Depeursinge et al. 2004), PTOP (Liu et al. 2004), and PIP1(Ye and De Lange 2004). TPP1 is a combination of the first letters of each name. TPP1, along with TIN2, forms a bridge connecting POT1 with both TRF1 and TRF2. In mice, cells lacking TPP1 fail to localise POT1 to telomeres, exhibiting similar phenotypes to POT1a/b double knockout cells with no other telomere dysfunction (Kibe et al. 2010). TPP1 is also the only component in shelterin that interacts with telomerase, recruiting it to telomere (Nandakumar et al. 2012; Abreu et al. 2010).

Repressor/activator protein 1 (RAP1) was identified in 2000 by Li et al. in humans (Li, Oestreich, and De Lange 2000). RAP1 specifically interacts with TRF2 within shelterin and serves as an adaptor with other genes (Schmutz and De Lange 2016). Loss of RAP1 results in telomere recombination but does not affect telomere protection or maintenance regarding DNA damage response, non-homologous end joining (NHEJ), or telomere length (Sfeir et al. 2010; Kabir, Hockemeyer, and de Lange 2014).

1.3.2 Shelterin structure

Shelterin exhibits the ability to bind to both dsDNA and ssDNA within the telomeric region, sufficiently covering the entire length of telomeric DNA (Takai et al. 2010b; de Lange

2018). However, the shelterin complex binds to telomeric DNA as independent functional units rather than as a single entity. The binding of one complex does not change the binding of neighbouring complexes (Erdel et al. 2017).

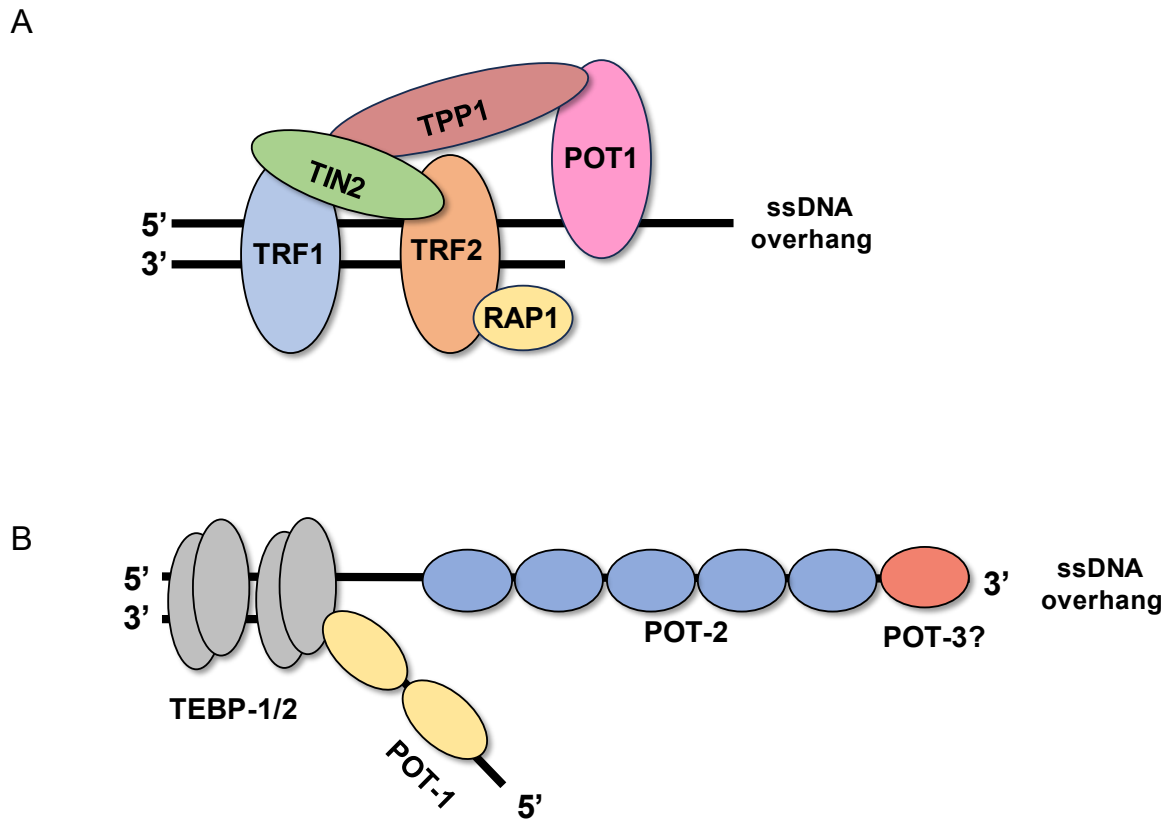

Figure 1.2 Shelterin is a vital protein complex located at the telomeres

A) The depiction of the six-subunit human shelterin complex, including telomeric repeat-binding factor 1 (TRF1), telomeric repeat-binding factor 2 (TRF2), TRF1-interacting nuclear factor 2 (TIN2), repressor/activator protein 1 (RAP1), adrenocortical dysplasia protein homologue (ACD, also known as TPP1, PI1, PTOP and TINT1) and protection of telomeres 1 (POT1). B) The depiction of shelterin-related proteins in *C. elegans*, including double-stranded DNA binding proteins, TEBP-1 and TEBP-2, single-stranded DNA binding proteins, POT-1, POT-2, and POT-3.

As depicted in Figure 1.2, TRF1 and TRF2 utilize Myb/SANT domains to bind to dsDNA while TIN2 bridges them through distinct interaction surfaces. Additionally, TIN2 binds to TPP1 through the TRFH domain, similar to its binding with TRF2. POT1 interacts with ssDNA overhangs using two N-terminal oligonucleotide/oligosaccharide binding (OB) folds and binds to TPP1 through the HJRL domain. The final connection is made when RAP1 binds to TRF2 (de Lange 2018).

TRF1, TRF2, TIN2, and RAP1 are considered the core components of the shelterin complex, as they are ten times more abundant compared to TPP1 and POT1 (Takai et al. 2010b).

The stoichiometry between TRF2 and RAP1, as well as TPP1 and POT1, is 1:1 (Takai et al. 2010b; de Lange 2018). Interestingly, there is no significant correlation between telomere length and the abundance of shelterin complex (Erdel et al. 2017).

In *C. elegans*, shelterin-related proteins or possibly a protein complex may exist, including double-stranded DNA binding proteins, TEBP-1 and TEBP-2, single-stranded DNA binding proteins, POT-1, POT-2, and POT-3 (Figure 1.2). TEBP-1 and TEBP-2 directly interact with POT-1 and interact with POT-2 in a POT-1-dependent manner (Dietz et al. 2021).

1.4 The Protection of Telomere (POT) protein

1.4.1 POT1 in humans

In humans, Protection of Telomeres 1 (POT1) is a crucial protein consisting of 634 amino acids. It features two oligonucleotide/oligosaccharide binding (OB) folds, known as OB1 and OB2, in its N-terminus, along with an additional OB fold (OB3) and a Holliday junction resolvase-like domain (HJRL) in its C-terminus.

The OB1 and OB2 domains in the N-terminus of POT1 play essential roles in binding to the ssDNA overhangs at telomeres. Specifically, OB1 recognises the first six nucleotides, while OB2 binds to the 3' end of the ssDNA, offering protection to this region (Lei, Podell, and Cech 2004). Each hPOT1 protein occupies two telomeric DNA repeats, and longer telomeric ssDNA substrates can be covered with multiple heterodimers assembled by POT1-TPP1 (Chen et al. 2017) .

In the C-terminus, OB3 is separated by the HJRL domain, which initially posed challenges for its identification. While neither of these domains directly binds to ssDNA, specific mutants within the C-terminus, such as P446Q, P475L, C591W, and Q623H mutants, have been found to decrease the DNA binding affinity of hPOT1. The C-terminus end is essential for binding to TPP1, and the POT1-TPP complex is crucial for preventing genome instability (Rice et al. 2017; Chen et al. 2017).

hPOT1 also plays a significant role in inhibiting the DNA damage response (DDR). By binding to the 3' ssDNA overhang, hPOT1 inhibits the ataxia telangiectasia and Rad3-related (ATR) signalling pathway and prevents the binding of replication protein A (RPA), essential for ATR recruitment. hPOT1 displaces RPA with the help of heterogeneous nuclear ribonucleoprotein A1 (hnRNPA1) and telomeric repeat-containing RNA (TERRA), effectively

blocking DDR activation (Denchi and De Lange 2007; Churikov and Price 2008; Gong and de Lange 2010; Flynn et al. 2011).

Another important function of hPOT1 is its involvement in the generation of 3' ssDNA overhangs. In mice, after the replication of the telomeric DNA, mPOT1b, a homolog of hPOT1, recruits the Ctc1/Stn1/Ten1 (CST) complex, which mediates Polα/primase-dependent fill-in after resection by Apollo and Exonuclease 1 (Exo1) proteins, facilitating the formation of telomeric overhangs (Wu, Takai, and De Lange 2012). The CST complex has also been shown to interact with hPOT1-TPP1 in humans, suggesting a similar function in regulating telomeric overhang generation (Takai et al. 2016; Kim et al. 2017).

hPOT1 also plays a role in regulating telomere length through its interaction with telomerase, exerting both positive and negative effects. When forming the hPOT1-TPP1 complex, TPP1 interacts with telomerase through its OB fold, enhancing its binding affinity to telomeric ssDNA compared to hPOT1 alone. Additionally, the recruitment of the CST complex by hPOT1-TPP1 further reduces telomerase access to telomeric ssDNA by competing for binding. However, the hPOT1-TPP1 complex can also act as a processivity factor for telomerase by recruiting it to the telomeres (Wang et al. 2007; Xin et al. 2007).

Furthermore, hPOT1 contributes to the stabilisation of telomeric ssDNA. As mentioned in Section 1.1.1, the G-rich telomeric DNA can form G-quadruplex (G4) structures, with the ssDNA region containing multiple G4 units. hPOT-1 can unfold various telomeric G-quadruplex structures, including antiparallel, hybrid, parallel monomers, or a 48 nt sequence with two contiguous quadruplexes, ensuring the stability of the telomeric region (Chaires et al. 2020).

1.4.2 POT1 homologs in other species

Due to the conservation of POT1 proteins across eukaryotes, homologs of human POT1 exist in different organisms. The quantity of POT1 proteins in these organisms may also vary due to gene duplication events. However, these proteins exhibit varied structures and functions, which may have resulted from divergence.

In budding yeast, *Saccharomyces cerevisiae*, the POT1 homolog known as Cdc13 was first identified in 1995 by Garvik et al. It was the first protein recognised to play a crucial role in chromosomal protection (Garvik, Carson, and Hartwell 1995). Cdc13 comprises 924 amino

acids and possesses a DNA binding domain structurally similar to the OB fold, which specifically binds to the single-stranded G-rich telomeric DNA. Cdc13 interacts with yKu70 for a positive effect or with Stn1 for a negative effect, along with Est1 as a comediator. This interaction regulates the recruitment of telomerase to chromosome ends, impacting telomere length regulation and stability (Grandin, Damon, and Charbonneau 2000; Evans and Lundblad 1999).

In fission yeast, *Schizosaccharomyces pombe*, the homolog known as SpPOT1, plays a vital role in maintaining chromosome stability. Deletion of SpPOT1 results in chromosome instability, such as the rapid loss of telomeric DNA and chromosome circularisation (Baumann and Cech 2001).

In *Tetrahymena thermophila*, two homologs of POT1, POT1a and POT1b (or POT1 and POT2), are present, both containing two OB folds. Two *Tetrahymena* POT1 genes have arisen from a gene duplication event. These two POT proteins are only 44% identical and exhibit distinct functions. tPOT1 is associated with cell aberrant phenotypes, growth arrest, and elongation of telomeres without altering the G-overhang. On the other hand, tPOT2 localises to regions of chromosome breakage rather than with telomeres (Jacob et al. 2007; Cranert et al. 2014).

In *Drosophila*, which lacks telomerase, as mentioned in Section 1.2.2, the telomeres are elongated by retrotransposons. The OB fold-containing protein, Verrocchio (Ver), is enriched at the telomere and binds to ssDNA without sequence preference. Deletion of Ver results in an increased frequency of telomere fusions and DNA damage responses such as the formation of RPA and γH2AX foci, similar to human cells lacking hPOT1 (Cicconi et al. 2017).

In vertebrates, such as the African clawed frog, *Xenopus tropicalis* and *Xenopus laevis*, the homologs xtPOT1 and xlPOT1, consisting of 621 amino acids, share 84% identity with each other. They exhibit 50% and 67% similarity with human POT1, respectively (Vizlin-Hodzic et al. 2009).

In mammals such as mice, *Mus musculus*, two homologs of POT1, POT1a and POT1b, share 72% sequence identity with human POT1. mPOT1a, a protein consisting of 641 amino acids with two OB folds, plays an indispensable role in maintaining telomere integrity and overall genomic stability. Deletion of mPOT1a results in telomere elongation and the 3’ ssDNA overhang, as well as increased incidence of T-circles and T-SCEs, important indicators of telomeric homologous recombination (Wu et al. 2006; Hockemeyer et al. 2006). Conversely,

mPOT1b, a protein consisting of 640 amino acids with two OB folds, exhibits similarities to mPOT1a but does not lead to lethality or sterility in mice upon deletion. Interestingly, overexpression of mPOT1b induces a DNA damage response at telomeres, reduction of the 3' ssDNA overhang, and increases chromosomal fusion and HR (Hockemeyer et al. 2006; He et al. 2006). Both mPOT1a and mPOT1b contribute redundantly to cell proliferation, as demonstrated by the ability of immortalized cells to proliferate normally without either mPOT1a or mPOT1b or when the total mPOT1 level is lowered two- to three-fold but not in the complete absence of both mPOT1a and mPOT1b (Hockemeyer et al. 2006). Specifically, mPOT1a is required to repress the DNA damage response by preventing ATR activation, while mPOT1b possesses the unique ability to prevent C-strand resection due to its specific domain. These distinct roles highlight the functional specialization of mPOT1a and mPOT1b in safeguarding telomere integrity, despite changes in the 3' ssDNA overhang length observed in both *pot1a* and *pot1b* mutants (Kratz and de Lange 2018). The study of POT1 genes in various rodents displays families containing two POT1 proteins, Muridae (rats, mice) and Cricetidae (hamsters), and other families containing only one POT1 protein. The study shows that the POT1 gene duplication occurred less than 75 Ma ago, when Muridae and Cricetidae branched off from Spalacidae (mole rats) and Dipodidae (jerboas) (Myler et al. 2021).

In swine (*Sus scrofa*), the SsPOT1 homolog is a 507-amino acid protein expressed to different levels in various tissues including muscle, heart, liver, fat, kidney, lung, pancreas, and spleen. (Yong et al. 2012).

Plant POT1s display some gene duplications which may or may not be accompanied functional divergence (Baumann and Price 2010). As shown in Figure 1.3 B, two *POT1* gene duplication events were detected which occurred independently in different lineages of the Angiosperms.

In *Physcomitrella patens*, there is only a single copy of the *pot1* gene. PpPOT1 deletion leads to shortened telomeres, elongated G-overhangs, increased chromosome fusion and severe developmental defects. Sterility can also be observed in PpPOT1 deleted plants (Shakirov et al. 2010).

One of the POT1 gene duplication events is a Panicoideae-specific event in grasses, such as maize (*Zea mays*). This duplication event occurred approximately 75 Ma ago, less than 30 Ma after the divergence of this lineage from the last common ancestor with rice (*Oryza sativa*). The overall amino acid sequence conservation is approximately 70-75%, similar to the

conservation observed in mouse mPOT1a and mPOT1b (Kellogg 1998; Paterson, Bowers, and Chapman 2004; Arora, Beilstein, and Shippen 2016).

The other gene duplication event occurred in the Brassicaceae (order Brassicales) of eudicots. In *Arabidopsis thaliana*, which is a member of Brassicaceae, three POT1 homologs, POT1a, POT1b and POT1c, exist. AtPOT1a exhibits specific telomerase interaction among all the paralogs via the highly conserved Phenylalanine residue (F65). AtPOT1a interacts with the canonical telomerase RNA (TER1), stimulating the repeat addition processivity. On the other hand, AtPOT1b specifically binds to a protein named TRB1, a Myb-containing telomere component which interacts with telomerase catalytic subunits (Jaiswal and Lakshmi 2015; Shakirov, McKnight, and Shippen 2009). The functional diversification between AtPOT1a and AtPOT1b occurred after the second POT1 duplication event, which happened sometime prior to the emergence of Brassicaceae (the family that includes *Arabidopsis thaliana*) (Beilstein et al. 2015). AtPOT1c is thought to have arisen through a recent duplication of the N-terminal region of AtPOT1a (Kobayashi et al. 2019; Rossignol et al. 2007). However, AtPOT1c is not actively transcribed, but forced expression of AtPOT1c results in reduced telomerase activity and shortened telomeres (Kobayashi et al. 2019).

In papaya (*Carica papaya,* family Caricaceae, order Brassicales), a single full-length POT1 homolog, CpPOT1, shares 58% similarity to both AtPOT1a and AtPOT1b in *A. thaliana*. This indicates that the duplication of *POT1* gene may have occurred in the Brassicaceae after its divergence from the last common ancestor with papaya approximately 100 Ma (Beilstein et al. 2015; 2010; Shakirov et al. 2008).

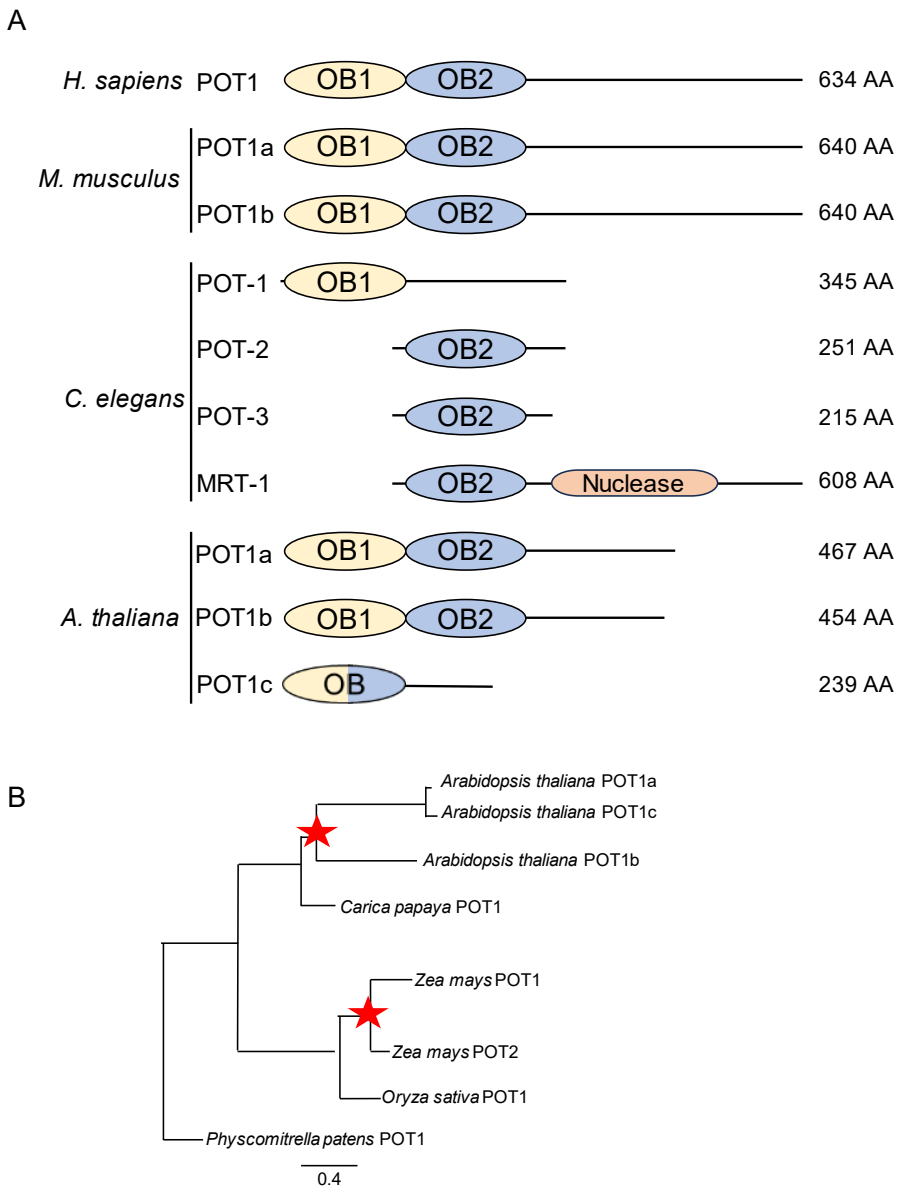

Figure 1.3 The POT1 protein is conserved across eukaryotes

A) Schematic of POT1 proteins in human (*Homo sapiens*), mouse (*Mus musculus*), *Caenorhabditis elegans*, and *Arabidopsis thaliana.* B) Phylogenetic tree of plant POT1 proteins. Red stars at nodes indicate duplication events. This phylogenetic tree is modified from Beilstein et al. 2015.

1.5 The POT1 homologs in *Caenorhabditis elegans*

In this work, we mainly focus on *Caenorhabditis elegans*, a model organism for investigating development, behaviours, and genetic analysis. We take advantage of its rapid (3-day) life cycle, small size (1.5-mm-long adult), and ease of laboratory cultivation (Riddle et al. 1997). The Bristol (or N2) strain has been used in many laboratories and became the

canonical wild-type strain since 1974 (Brenner 1974). In this study, we also use the N2 strain as wildtype.

C. elegans has two sexes: males with a single X chromosome (XO) and hermaphrodites with two X chromosomes (XX). Males are easily distinguished from hermaphrodites by the shape of their tails and their behaviour. Naturally, *C. elegans* perform self-fertilisation making the maintenance of homozygous strains in the lab very easy. Meanwhile, *C. elegans* hermaphrodites still retain the ability to mate with males, which simplifies the process of generating mutant strains (see Section 2.1.3) (Meneely, Dahlberg, and Rose 2019). These features make *C. elegans* a good model to study genetics.

C. elegans also has advantages when studying telomeres, longevity, and aging. The average lifespan for *C. elegans* under laboratory conditions is 14 to 21 days. The life cycle from fertilised egg to adult is approximately 3 days at 20°C. These characteristics make both inter-generational and trans-generational study relatively easy. Moreover, genes responsible for longevity in *C. elegans* are evolutionary conserved across animals (Meneely, Dahlberg, and Rose 2019).

As mentioned in Section 1.1.1, *C. elegans* have the telomeric repeat (TTAGGC), which shares similarity with most vertebrates, including humans. This similarity makes it beneficial to study telomere biology in *C. elegans*. Furthermore, the shelterin-related proteins in *C. elegans* bear resemblance to the shelterin complex in human, which provides us with a convenient tool to study the characteristics of these proteins and their roles in telomere regulation. In *C. elegans*, double-strand DNA binding proteins, TEBP-1 and TEBP-2, are part of a telomeric complex (Dietz et al. 2020). This telomeric complex also contains four homologs of human POT1, named POT-1, POT-2, POT-3, and MRT-1. However, each gene shares homology with only one of the two vertebrate OB-fold domains that make up the DNA binding domain (Figure 1.3).

1.5.1 MRT-1

MRT-1 protein is a unique and multifunctional component. MRT-1 is not only a POT1 homolog (with one OB fold at the N-terminus) but also a SNM1 nuclease homolog (with the SNM1 nuclease domain at the C-terminus). SNM1 proteins function in DNA repair, checkpoint response, and telomere protection. *In vitro* studies have shown that MRT-1 acts as a 3’ to 5’ exonuclease due to its SNM1 nuclease domain. This nuclease activity is independent of the

POT1 OB fold and remains unaffected by mutations in this domain. MRT-1 prefers single-stranded DNA as its substrate, and its activity is dependent on the configuration of the substrate (Meier et al. 2009). However, the precise nucleolytic processing function of MRT-1 *in vivo* has not yet been fully revealed.

Among all the POT1 homologous OB fold containing proteins in *C. elegans*, MRT-1 is the sole player essential for telomerase-dependent telomere maintenance. *mrt-1* mutants display reduced viability and ultimately sterility, similar to *trt-1* mutants, which lack the catalytic subunit of telomerase. The OB fold domain of MRT-1 allows it to bind various single-stranded oligonucleotides, including the telomeric G-strand oligonucleotide $(GGCTTA)_4$, C-strand, inverse C-strand from *C. elegans* and G-strand from humans, without any apparent binding preference *in vitro*. Mutations in the OB fold domain result in the loss of telomerase activity *in vivo*, underlining its crucial role in telomerase interaction (Meier et al. 2009).

MRT-1 is dispensable for DNA double-strand break (DSB) repair or the non-homologous DNA end joining (NHEJ) pathway but contributes to the interstrand cross-link (ICL) repair along with the 9-1-1 (Rad9-Rad1-Hus1) complex. This is based on results showing that MRT-1 deleted worms displayed hypersensitivity to trimethylpsoralen photoactivated by UVA radiation (Meier et al. 2009). Trimethylpsoralen photoactivated by UVA radiation is a commonly used method to introduce DNA damage to understand the cellular response to DNA damage and repair mechanisms in the organism.

1.5.2 POT-1

POT-1, also referred to as CeOB2, is a protein in *C. elegans*, consisting of 345 amino acids and featuring a single OB fold known as OB1. Interestingly, *C. elegans* harbours both G- and C-rich overhangs at its telomeres. However, POT-1 specifically exhibits affinity towards the single-stranded telomeric C-strand and can stably bind to a single GCCTAA repeat (Raices et al. 2008).

POT-1 plays a key role in repressing the activity of telomerase. Loss of POT-1 results in greater initial telomere heterogeneity in telomere length, leading to elevated levels of circular telomeric DNA while the overhang remains unchanged. Deficiency of POT-1 in *trt-1* mutant worms, which lack of telomerase reverse transcriptase, displayed accelerated telomere erosion rates and extended lifespan (Shtessel et al. 2013). Beyond its involvement in telomere

maintenance, POT-1 also participates in anchoring chromatin to nuclear envelope along with SUN-1 (Ferreira et al. 2013).

1.5.3 POT-2

POT-2, also known as CeOB1, is a protein consisting of 251 amino acids and featuring a single OB fold, known as OB2. POT-2 shows specific affinity towards the single-stranded telomeric G-strand (Raices et al. 2008). Research from our lab further revealed that POT-2 binds to a minimal six nucleotide GCTTAG motif, offering new insights into its binding preferences and specificity (Yu, Gray, and Ferreira 2023).

POT-2 functions as a negative regulator of telomerase, like POT-1, albeit with non-redundant roles. Loss of POT-2 results in progressively elongated telomeres, increased levels of circular telomeric DNA, and notably elongated overhangs, particularly for shorter telomeres. Interestingly, when POT-2 is deleted in *trt-1* mutant worms, the telomere erosion rate remains largely unchanged, unlike the accelerated telomere erosion rate in *pot-1;trt-1* strain. However, the *trt-1; pot-2; pot-1* triple mutant worms displayed delayed senescence comparing to *trt-1* mutant worms or *trt-1; pot-1* double mutant worms, with some survivors in the absence of telomerase (Shtessel et al. 2013).

1.5.4 POT-3

POT-3 is a protein 215 amino acids in length, containing a single OB fold, known as OB2. POT-3 shares various similarities with POT-2, including very high gene sequence similarity, approximately 60% amino acid identity, and identical minimal binding motif, GCTTAG. However, recent research from our laboratory has shed light on an important distinction that POT-3 exhibits a preference for binding at the 3’ end of telomeric ssDNA compared to POT-2 (Yu, Gray, and Ferreira 2023).

The functional role of POT-3 at telomeres remains enigmatic. Studies involving the *pot-3(ok1530)* allele have shown no impacts on telomere length. Consequently, POT-3 is considered a dispensable protein in the context of telomere maintenance (Shtessel et al. 2013).

1.6 Significance and aims of the thesis

In summary, telomeres play crucial roles in maintaining genomic stability and regulating cellular lifespan. POT1 protein participates in single-strand DNA binding and telomere regulation, including generating ssDNA overhangs, safeguarding telomere integrity, and interacting with telomerase. *C. elegans* serves as a powerful model for telomere biology study. However, some key questions regarding some specific proteins remain unanswered in *C. elegans*.

POT-3, the least understood telomeric ssDNA binding protein in *C. elegans*, is the focus of this study. Through the investigation of the POT-3 protein, we aim to elucidate the roles of POT-3 in telomere regulation and investigate telomere inheritance in *C. elegans*. This work contributes to our understanding of telomere biology, genome stability, and cellular aging.

The aims of the thesis include:

1. Determine the telomeric roles of POT-3 in *C. elegans*.
2. Identify the role of POT-3 in telomere maintenance and fertility.
3. Investigate telomere inheritance in *C. elegans*.

Chapter 3 focuses on the existence and telomeric roles of POT-3, as well as its relationship with other POT1 homologs in *C. elegans*. It shows that POT-3 behaves as a paralog of POT-2 and *pot-3* acts epistatically with *pot-2* in a POT-1-dependent manner. In chapter 4, the telomere inheritance process is investigated. It reveals that telomere length inheritance in *C. elegans* is a stochastic process rather than being exclusively parental. Chapter 5 aims to elucidate the effects of POT-2 and POT-3 on telomere maintenance and fertility. It demonstrates that telomere replication deficient strains, *mrt-1* and *trt-1*, display differential responses in fertility span and telomere length shortening to the loss of POT-2 or/and POT-3.

Chapter 2 : Materials and Methods

2.1 *C. elegans* maintenance and manipulation

2.1.1 *C. elegans* strains and maintenance

The *C. elegans* strains used in this study are listed as follows: the N2 (Bristol isolated, wildtype), *pot-2(tm1400), pot-1(tm1620), pot-3(syb2415)* (Sunybiotech Corporation, Fuzhou City, Fu Jian Province, China), *pot-3(ok1530), mrt-1(tm1354), trt-1(ok410)* (donated by Susan M. Gasser, Friedrich Miescher Institute), *trt-1(ok410);unc-29(e193), exo-1(tm1842). pot-2(tm1400), pot-3(ok1530), mrt-1(tm1354), trt-1(ok410), trt-1(ok410);unc-29(e193), exo-1(tm1842)* were obtained from *Caenorhabditis* Genetics Center (CGC) which is funded by NIH Office of Research Infrastructure Programs (P40 OD010440). All the strains are the N2 background.

These *C. elegans* strains were cultured on Nematode Growth Medium (NGM) agar (1.8% (w/v) agar, 0.3 (w/v) NaCl, 0.25% (w/v) Peptone, 25 mM potassium phosphate buffer (108.3 g/L KH_2PO_4, 35.6 g/L K_2HPO_4 in H_2O, pH6.0), 1mM $MgSO_4$, 1mM $CaCl_2$, 5 µg/mL cholesterol (in 100% ethanol)) in 60 mm or 90 mm Petri dish at 20°C. The worms were fed with the saturated culture of OP50, the *Escherichia coli* strain for *C. elegans* feeding chosen by Sydney Brenner (Brenner 1974). The OP50 was grown in Miller's LB broth (Foremedium) at 37°C overnight and set bacterial lawns growing on NGM agar plates before use.

2.1.2 Long-term *C. elegans* storage

The *C. elegans* strains were cultured on 90 mm NGM agar plates until the OP50 had just been consumed. Worms were collected in sterile freezing buffer (1:1 (v/v) mixture of: 1) 30% (v/v) glycerol, 50 mM potassium phosphate buffer (108.3 g/L KH_2PO_4, 35.6 g/L K_2HPO_4 in H_2O, pH6.0), 0.57% (w/v) NaCl, and 2) M9 buffer (0.3% (w/v) KH_2PO_4, 0.6% (w/v) Na_2HPO_4, 0.5% (w/v) NaCl, 1 mM $MgSO_4$ in H_2O, pH=7.5)). The suspension was used directly to store worms in 1.8 mL liquid freezing buffer or adding 0.5 mL freezing buffer supplemented with 0.4% (w/v) agarose to 1 mL suspension to store in soft agar freezing buffer. The freezing buffer or soft agar freezing buffer was gradually cooled down to -80°C in a Cryo 1°C Freezing Container (Nalgene). Another suspension in 0.4 mL liquid freezing buffer was used as a sample to test the viability of frozen worms after at least 14 days.

2.1.3 *C. elegans* crossing

C. elegans males were obtained by heat-shocking L4 hermaphrodites at 32°C for 5-6 hours. Crosses were performed on 32 mm NGM agar plates (honeymoon plates) seeded with very small amounts of the *E. coli* OP50. The crosses were performed by mating 3-5 males (depending on the number of males obtained) with two L4 hermaphrodites overnight at 20°C. P_0 hermaphrodites were singled onto 60 mm plates the following day and kept at 20°C until F_1 progeny appeared. A 50:50 male to hermaphrodite ratio indicated successful mating. A few (4-10) F_1 hermaphrodites were singled on to new 60 mm plates and left to self-fertilise at 20°C. The F_2 progeny could be identified visually or screened for desired strains by PCR genotyping (Section 2.1.5). F_2 progeny was singled onto new 60 mm plates and left them to self-fertilise at 20°C. After producing embryos, the matured F_2 adults were singled out for lysis (Section 2.1.4) and the lysates were further used to perform genotyping PCR (Section 2.1.5). Once the desired genotypes were identified among the F_2 adults, the plates contained F_3 progeny could be selected. The population on these plates were maintained for further use or stored for long-term use (Section 2.1.2).

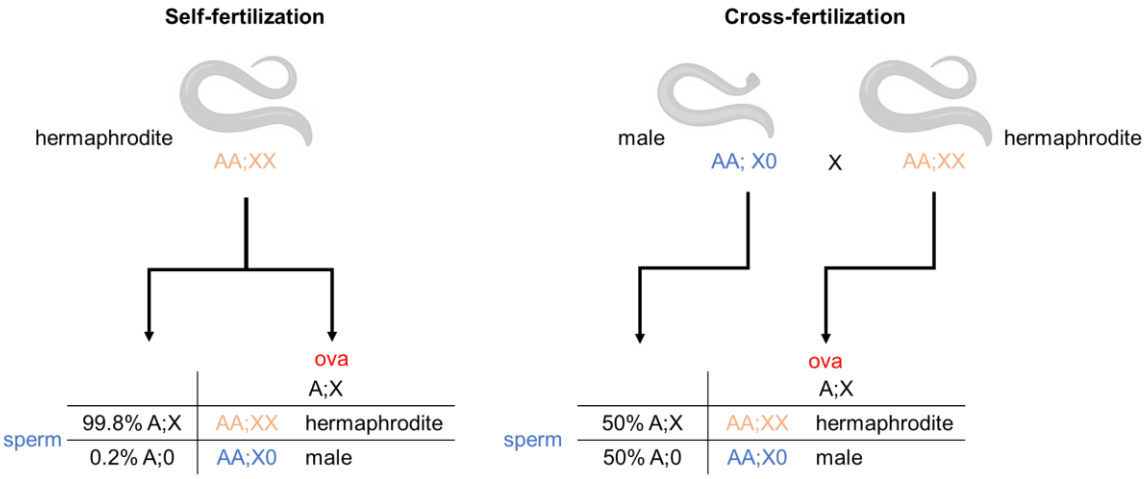

Figure 2.1 Schematic diagrams of self- and cross-fertilisation in *C. elegans*

In self-fertilisation, sperm and ova from the same animal produce zygotes. Hermaphrodites are genetically identical (or nearly) to the parent animal. Only 0.2% of offspring are males naturally. In cross-fertilisation, zygotes will be split between XX (hermaphrodites) and XO (males). 50% of offspring are hermaphrodites while the other 50% are males. This figure is modified from Meneely, Dahlberg, and Rose 2019.

2.1.4 *C. elegans* single-worm lysis

As described in Section 2.1.3, the F_2 adult worms were transferred into PCR tubes containing 20 µL single-worm lysis buffer (30 mM Tris-HCl (pH 8.0), 100 mM NaCl, 8 mM EDTA, 0.7% Tween-20, 0.7% NP-40) supplemented with 100 µg/mL Proteinase K (Invitrogen). The worms were lysed by incubation at 60°C for 90 minutes, then 90°C for 15 minutes (for heat-inactivation of Proteinase K). The lysates were stored at 4°C for short-term storage or -20°C for long-term storage.

2.1.5 Genotyping by PCR

The genotyping PCRs were performed in 20 µL total volume containing 10 µL 2× MyTaq™ Red Mix, 1 µL single-worm lysate from Section 2.1.4, 1 µL 10 nM forward primer, 1 µL 10 nM reverse primer and 7 µL sterile double-distilled H_2O. The single-strand DNA oligos for different genotyping PCRs are gathered in Table 2.1. The PCR conditions are shown in Table 2.2. The PCR products were resolved on a 1% agarose gel supplemented with 1% (v/v) ethidium bromide (Sigma). PCR products were screened for bands according to the pattern of primer combinations (Table 2.3).

Table 2.1: Single-stranded DNA primers used for Genotyping (5' to 3' direction)

allele	forward	reverse 1	reverse 2
tm1400	CGC GCA GTC AGT GTT GAA TAC AAC	CGC TTG AAG GAA TCC TGC GTA AC	CAC GTT GAT ATG ATG CTC CGC CA
tm1620	GAA TCC GAA ATG CAG CGT GG	CACATTCAGGATTTGGT ACCG	AGAATTGTTCTATCACC GGC
syb2415	AGG TGA AAA TGT TTT CAC CGC TCG	TTGTGGAAGATCACTCG GCAAAGG	CTGCGTGCACATTTTGA ATAGCC
tm1354	TAAGTCCGGCTGCATCG AAAAG	CTTGAAGAGTGGTCGG AATATGG	AATTTGTGAGGGACGTT CTCCTC
ok410	CCAGTAGATAATGGTTTC ATCATCTG	TGATACATTTGTTGCAT GCTCCA	TTG ATG ACA CGC ATA AAG CTT TG

Table 2.2: PCR conditions for genotyping

allele	initial denaturation	denaturation	annealing	extension	cycling	final extension	cooling
tm1400	95°C 3 min.	95°C 20 sec.	55°C 20 sec.	72°C 1 min.	35×	72°C 2 min.	4°C forever

tm1620	95°C 3 min.	95°C 20 sec.	55°C 20 sec.	72°C 70 sec.	35×	72°C 2 min.	4°C forever
syb2415	95°C 3 min.	95°C 20 sec.	55°C 20 sec.	72°C 45 sec.	35×	72°C 2 min.	4°C forever
tm1354	95°C 3 min.	95°C 20 sec.	55°C 20 sec.	72°C 1 min.	35×	72°C 2 min.	4°C forever
ok410	95°C 3 min.	95°Cs 20 sec.	50°C 20 sec.	72°C 2 min.	35×	72°C 2 min.	4°C forever

Table 2.3: PCR bands according to specific genotypes

allele	forward + reverse 1	forward + reverse 2
tm1400	wildtype: 520bp *tm1400*: no product	wildtype:780bp *tm1400*: 450 bp
tm1620	wildtype: 1100 bp *tm1620*: 350 bp	wildtype: 390 bp *tm1620*: no product
syb2415	wildtype: 700 bp *syb2415*: 200 bp	wildtype: 200 bp syb2415: no product
tm1354	wildtype: 1000 bp *tm1354*: 450 bp	wildtype: 300 bp *tm1354*: no product
ok410	wildtype: 2000 bp *ok410*: 500 bp	wildtype: 400 bp *ok410*: no product

.

2.1.6 Sequencing for strain determination

The sequencing was conducted by Eurofins Genomics Europe. The samples were consisted of 5 µl of the purified template DNA (at the concentration of 10 ng/µl) and 5 µl of primer with a concentration of 5 pmol/µl (5 µM). The template DNA we used was genomic DNA (detailed method for genomic DNA preparation in Section 2.2). The primers we used are gathered in Table 2.4.

Table 2.4 Single-stranded DNA primers used for sequencing (5' to 3' direction)

	forward	reverse
~1kb upstream/ downstream	TGCAAATGCGCTCTACTGATAA	GGTCGCCCACCACTCCTT
CDS	ATG TTT TCA CCG CTC GAG TGT CG	CATCACCTTCACCCTCTCC
syb2415	AATTGCAAACGGGTCTCGCT	CTACCATGATTACTGGCACG

2.2 Preparation of *C. elegans* genomic DNA

2.2.1 Genomic DNA extraction following bead-beating

The *C. elegans* populations were cultured on four to six 90 mm NGM agar plates at 20°C until not starved. Worms were collected in M9 buffer on ice and washed once with M9 buffer to remove contamination. The worms were pelleted by centrifugation at 1000 ×g, 4°C and frozen in 2 mL screw cap tubes with 1mL M9 buffer at -80°C until further usage.

Before extraction, the worms were re-centrifuged at 1000 ×g, 4°C. The worm pellets were lysed in a Fast Prep FP120 cell homogenizer (Thermo Fisher Scientific) after adding 500 µL M9 buffer, 400 µL 0.5 mm glass beads (Thistle Scientific), 73 µg/mL RNaseA (Thermo Fisher Scientific), 9 mM ethylenediaminetetraacetic acid (EDTA) and 270 mM NaCl. The homogenisation was repeated 3 times at 6 m/s for 20 s with cooling on ice for 2 minutes between each time. After puncturing the bottom of the screw cap tubes with 26 G needles, lysates were collected in 14 mL tubes by performing centrifugation for 2 minutes at 400 ×g, 4°C. The samples were heated at 65°C for 10 minutes with 1% (w/v) sodium dodecyl sulphate (SDS). The SDS was precipitated by adding 1.3 M potassium acetate and cooling on ice for 2 minutes. The supernatant was transferred into clean tubes after centrifuging for 5 minutes at 16000 ×g, 4°C. The DNA was precipitated by adding twice the volume of chilled 100% ethanol to the supernatant and cooling on ice for 10 minutes. The DNA pellet was collected by centrifugation for 5 minutes at 16000 ×g, 4°C and was resuspended in 10 mM Tris (pH 7.5) supplemented with 25 µg/mL RNase A (Thermo Fisher Scientific) incubating at 37°C for 30 minutes to remove RNA. The DNA was purified by adding one volume of phenol:chloroform:isoamyl alcohol (25:24:1), pH 6.7. The aqueous phase which contained DNA was collected by centrifugation for 1 minute at 16000 ×g, 4°C. One (up to three if needed) chloroform back-extraction was performed for better DNA quality. The DNA was precipitated by adding 0.3 M sodium acetate (pH 5.2) and twice the volume of chilled 100% ethanol and cooling on ice for at least 10 minutes. The DNA pellet was collected by centrifugation for 5 minutes at 16000 ×g, 4°C and washed with chilled 70% ethanol. The DNA pellet was resuspended in 50 to 100 µL of TE buffer. DNA concentration and quality were assessed by measuring absorbance at 260 nm using a NanoDrop™ 2000 microvolume spectrophotometer (Thermo Fisher Scientific). The DNA was stored at 4°C for usage within one week or -80°C for further usage.

2.2.2 Genomic DNA extraction following Proteinase K digestion

Worms were grown, collected and frozen as described in Section 2.2.1. The pellets were lysed in 1× NTE buffer (100 mM NaCl, 50 mM Tris pH 7.4, 20 mM EDTA) supplemented with 1% (w/v) SDS and 500 µg/mL Proteinase K (Invitrogen) overnight at 60°C under 180 rpm agitation. The lysis was centrifuged for 10 minutes at 1000 ×g and 4°C to remove debris. The following steps were performed as described in Section 2.2.1 after heating at 65°C with 1% SDS. The DNA was stored at 4°C for usage within one week or -80°C for further usage after being resuspended in 50 to 100 µL of TE buffer. DNA concentration and quality were assessed before storage.

2.2.3 Precise quantification of gDNA with Qubit™

To assess the accurate concentration of gDNA extracted in Section 2.2.1 and 2.2.2, the DNA was measured by Qubit™ 1× dsDNA Broad Range (BR) Assay Kits (Thermo Fisher Scientific). The DNA samples were diluted within the assay range of 0.2 to 2000 ng/µL and the diluted factor (DF) was recorded. 190 µL Qubit™ working solution (Qubit™ dsDNA BR Reagent 1:200 in Qubit™ dsDNA BR buffer) with 10 µL standard (0 ng/µL and 100 ng/µL in TE buffer) or diluted samples (between 0 to 100 ng/µL based on the concentration measured by NanoDrop™ in Section 2.2.1 and 2.2.2) was mixed vigorously and left at room temperature for 2 minutes. The samples and standards were read with a fluorometer. The concentration of DNA samples was assessed by the concentration obtained from the standard equation timing DF.

2.3 Molecular and biochemical assays

2.3.1 Immunofluorescence (IF)

Six to eight *C. elegans* worms were dissected in the M9 buffer (0.3% (w/v) KH_2PO_4, 0.6% (w/v) Na_2HPO_4, 0.5% (w/v) NaCl, 1mM $MgSO_4$ in H_2O, pH=7.5)) on poly-L-lysine (Sigma-Aldrich) coated slides. Following by mixing the same volume of 4% paraformaldehyde (PFA), the worms were incubated in 2% final concentration at room temperature for 5 minutes. After adding cover glasses on the worms, the slides were placed onto metal block sitting dry ice for 15 minutes. The slides were freeze-cracked followed by dehydrating in pre-chilled (-20°C) 100%

ethanol for 2 minutes. The slides were washed for 3 times in PBS-X100 (0.25%) at room temperature for 5 minutes. The slides were air-dried and loaded ProLong™ Diamond Antifade Mountant with DAPI (Molecular Probes™). The cover glasses were added and sealed with nail polish at four corners. Following leaving in the dark at room temperature overnight, the slides were ready to be observed under the microscope.

The slides were imaged under microscope (DeltaVision) with high-reservation objective lenses (60× and 100×) and DAPI filter. Following acquisition of cells from diakinesis, the number of chromosomes was counted with ImageJ (version 2.3.0) and Imaris Viewer for Windows (version 9.9.1).

2.3.2 C-circle assay

Genomic DNA of *C. elegans* was extracted following the procedures in Section 2.2.2, and the precise concentration was determined by procedures in Section 2.2.3. Rolling circle amplification (RCA) reactions were performed on 1000 ng of gDNA in a final reaction volume of 20 µL, containing 1× Φ29 reaction buffer (Thermo Fisher Scientific), 1 mM dNTP (Thermo Fisher Scientific), and 5 units of Φ29 DNA polymerase (Thermo Fisher Scientific) or replaced with water for blank reaction. The RCA reactions were incubated at 30°*C* for 8 hours followed by at 65°C for 20 minutes to denature Φ29 DNA polymerase.

The RCA reaction products were blotted onto Amersham Hybond-NX nylon membrane (GE Healthcare) followed by air-drying. The membranes were crosslinked with 1200 J/m^2 ultraviolet (UV) light in SpectroLinker™ XL-1000. Membranes were equilibrated with around 20 mL of DIG Easy Hyb™ hybridisation buffer (Roche) at room temperature for 1 hour, followed by being hybridised DIG Easy Hyb™ hybridisation buffer supplemented with 1 µg/mL in single-strand DNA probe (24-mer of *C. elegans* C-rich telomeric repeat sequence, $(GCCTAA)_4$) at 37°C overnight in a hybridisation oven.

After hybridisation, membranes were washed twice with 25 mL MS buffer (100 mM maleic acid, 150 mM NaCl, pH 7.5) supplemented with 0.3% (v/v) Tween-20 at room temperature for 5 minutes. Membranes were blocked with 50 mL MS buffer supplemented with 1% (w/v) Bovine serum albumin (BSA, Merck), 1% (w/v) milk and 0.1% (v/v) Tween-20 at room temperature for 30 minutes. After blocking, the membranes were incubated with blocking buffer supplemented 0.005% (v/v) AP-conjugated anti-digoxigenin Fab fragments (Roche) followed by being washed for 3 times in 50 mL of MS buffer supplemented with 0.3%

(v/v) Tween-20 at room temperature for 15 minutes. The membranes were equilibrated with AP buffer (100 mM Tris-HCl, pH 9.5, 100 mM NaCl) and incubated with 20 µL of CDP-Star® (Roche) per cm^2 in the dark for 2 minutes. The chemiluminescent signal was detected by using a Chemidoc™ XRS + (Biorad) CCD camera.

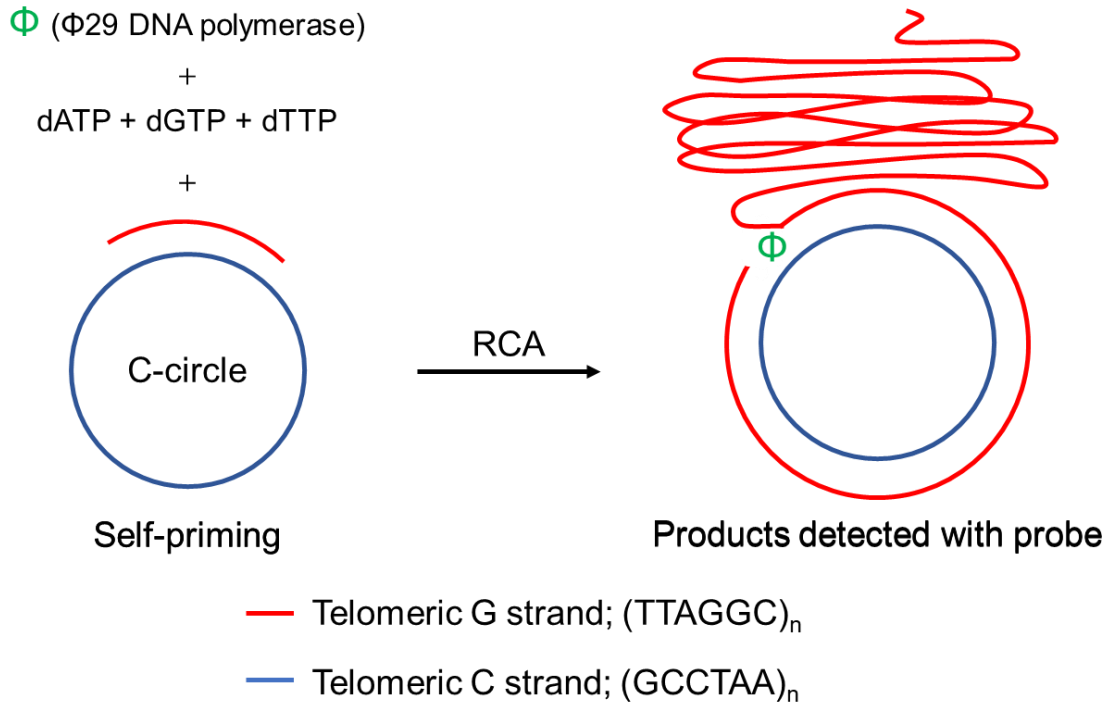

Figure 2.2 Schematic of C-circle assay

Genomic DNA contains C-circles which are self-priming. Rolling circle amplification (RCA) are conducted with Φ29 DNA polymerase. RCA products are detected by a single-strand DNA probe (24-mer of *C. elegans* C-rich telomeric repeat sequence, $(GCCTAA)_4$). This figure is modified from Henson et al. 2009a.

2.3.3 Terminal restriction fragment (TRF) analysis

TRF analysis was performed on gDNA extracted from *C. elegans* populations following the procedure described in Section 2.2.2. 5 µg gDNA was digested with 25 units of *HinfI* (NEB) and *HaeIII* (NEB) in 1× CutSmart® buffer (NEB) at 37°C overnight. The digests were resolved on a 1% (w/v) agarose gel containing 1× Invitrogen™ UltraPure™ ethidium bromide with addition of 1× purple gel loading dye (NEB) at 45 V for around 24 hours (longer if better differentiation between bands is needed). 10 µL GeneRuler 1 kb DNA Ladder (Thermo

Scientific™) and 20 µL DIG-labelled DNA Molecular Weight Marker II (Roche) were resolved on the same gel.

The gel was depurinated in 250 mM hydrochloric acid at room temperature for 20 minutes followed by washing twice in denaturing buffer (1.5 M NaCl, 0.5 M NaOH) and neutralising buffer (1.5 M NaCl, 0.5 M Tris-HCl, pH = 8), at room temperature for 15 minutes each time. The DNA was blotted onto Amersham Hybond-NX nylon membrane (GE Healthcare) by overnight capillary transfer in 10× SSC buffer (1.5 M NaCl, 150 mM sodium citrate, pH = 7) at room temperature.

The membranes were rinsed in 2× SSC buffer (300 mM NaCl, 30 mM sodium citrate, pH = 7) briefly followed by being crosslinked with 1200 J/m^2 ultraviolet (UV) light in SpectroLinker™ XL-1000. Membranes were equilibrated with around 20 mL of DIG Easy Hyb™ hybridisation buffer (Roche) at room temperature for 20 minutes followed by being hybridised DIG Easy Hyb™ hybridisation buffer supplemented with 1 µg/mL in single-strand DNA probe (24-mer of *C. elegans* C-rich telomeric repeat sequence, $(GCCTAA)_4$) at 37°C for at least 2 hours.

Following hybridisation, membranes were washed twice in 25 ml of 2× HW buffer (2× SSC buffer (300 mM NaCl, 30 mM sodium citrate, pH = 7) supplemented with 0.1% (w/v) SDS) at room temperature for 5 minutes and twice in pre-warmed 0.5× HW buffer (0.5× SSC buffer (75 mM NaCl, 7.5 mM sodium citrate, pH = 7) supplemented with 0.1% (w/v) SDS) at 50°C for 15 minutes. Following washing in 50 mL of MS buffer supplemented with 0.3% (v/v) Tween-20 at room temperature for 5 minutes, the membranes were blocked with 50 mL MS buffer supplemented with 1% (w/v) bovine serum albumin (BSA, Merck), 1% (w/v) milk and 0.1% (v/v) Tween-20 at room temperature for 30 minutes. The membranes were then incubated with blocking buffer supplemented with 0.005% (v/v) AP-conjugated anti-digoxigenin Fab fragments (Roche) followed by being washed three times in 50 mL of MS buffer supplemented with 0.3% (v/v) Tween-20 at room temperature for 15 minutes. The membranes were equilibrated with AP buffer (100 mM Tris-HCl, pH 9.5, 100 mM NaCl) and incubated with 20 µL of CDP-Star® (Roche) per cm^2 in the dark for 2 minutes. The chemiluminescent signal was detected by Chemidoc™ XRS + (Biorad) CCD camera.

2.4 Brood size assay

2.4.1 Brood size assay on OP50 NGM plates

The *C. elegans* brood size assay was performed by singling hermaphrodites of the L4 stage onto 60 mm NGM plates seeded with *E. coli* OP50. The plates were kept at 20°C overnight to allow the worms to self-fertilise. The worms were transferred onto new plates each day and kept at 20°C until the worms reached reproductive senescence (usually 3 to 4 days). The brood size of each worm was determined by the sum of the progeny numbers of each day.

2.4.2 Assay of brood size drop on OP50 NGM plates

The *C. elegans* brood size drop assay was performed by singling six hermaphrodites of L1 stage onto 60 mm NGM plates seeded with *E. coli* OP50. The plates were kept in 20°C over-week to allow the worms to self-fertilise and reproduce. Six hermaphrodites were transferred onto new plates each week and kept at 20°C until the worms became sterile or stable. The progeny on each week was counted approximately and determined brood size level as follows: W, wildtype, around 250 progeny per animal; M, medium, around 80 progeny per animal; F, few, around 20 progeny per animal; VF, very few, about 3-5 progeny per animal; S, sterile.

2.5 Data analysis

2.5.1 Software used for data analysis

The following software was used for analysis of experimental data. ImageJ version 2.3.0 was used for graphical analyse. Image Lab™ version 6.0.1 by Bio-Rad (Bio-Rad Laboratories, Hercules, California, USA) was used for processing and exporting gel and blot images acquired on the ChemiDoc™ system. Microsoft® Excel version 2210 for Windows (Microsoft Corporation, Redmond, Washington, USA) was used for data collection, subsequent documentation and processing and manipulation of numerical data. GraphPad Prism version 8.0.2 for Windows (GraphPad Software, La Jolla, California, USA, www.graphpad.com) was used for scientific graphing and statistical analyses.

2.5.2 Quantification of C-circle

C-circles were quantified from blots by measuring the optical density (OD) of the chemiluminescent signal. For each RCA reaction on each blot, the raw integrated density was assessed for circular selection of 0.044 px^2 (square pixels) using the "measure" command under the "analyze" menu in ImageJ. The measurements were exported into Excel and normalised by subtracting the raw integrated density obtained for negative controls (samples lack of polymerase) from the respective values obtained for samples in the presence of Φ29 DNA polymerase. The values were then normalised to *pot-2(tm1400)* by dividing the mean values obtained for other samples by the mean values obtained for *pot-2(tm1400)* and multiplying by 100 to attain percentages. The normalised data were shown as a percentage of *pot-2(tm1400)*.

2.5.3 Quantification of TRF assay

For the lanes on the TRF Southern blot, the lane profiles were obtained by using the straight line selection tool to draw vertical selections from top to bottom of the gel and exporting the data to Excel using the "plot profile" command under "analyze" menu in ImageJ. For each position (i) along the line, pixel intensity values were plotted on the Y-axis. The maximum pixel intensity values were determined manually or using the column statistic function in GraphPad Prism. The lane profile generated for the molecular weight marker lane was used to estimate the position (i) of each marker. An equation describing the relationship between position (i) and molecular weight (Kb) was derived from the data collected by molecular weight marker lane profile using the power trendline function in Excel. This equation was used to convert the signal positions (i) into molecular weight (Kb) for samples on the same blot.

Using column statistic function in GraphPad Prism to determine the maximum pixel intensity values. The peaks of pixel values were defined using area under curve (AUC) function by setting the baseline to the pixel intensity values and ignoring peaks below T% of the distance from minimum to the maximum (T=15,30 or 50 depending on the threshold used). The beginning and the end of each peak were defined as position (i) on the X-axis and corresponded to the first and the last X-values obtained from AUC function. If multiple peaks were found, the positions (i) were defined with the first and the last X-values of every peak.

2.5.4 Statistical analysis

The statistical analyses in this thesis were conducted using GraphPad Prism and involved several methods:

1. One-way ANOVA

   This method was conducted for to analyse differences among multiple groups in various assays, including TRF quantifications, C-circle quantifications, brood size assays, and telomere shortening rate assays. Tukey's multiple comparisons test was subsequently conducted to identify specific differences between groups.

2. Chi-squared test

   This method was conducted to analyse differences in chromosome fusions among different strains.

3. Log-rank test

   This method was used to analyse the fertility differences between groups in the fertility span assay (survival curve).

Chapter 3 : Telomeric role of POT-3 in *C. elegans*

3.1 Introduction

POT-3 was found in previous research but its telomeric function was not fully understood. After comparing the protein database of *C. elegans* with the structural features of hPOT1 and TEBPα, four proteins were identified, namely B0280.10, F57C2.3, 3R5.1, and F39H2.5, which were designated as POT-1, POT-2, POT-3 and MRT-1, respectively (Raices et al. 2008; Meier et al. 2009; Dargahi, Baillie, and Pio 2013). Notably, the deletion mutant of 3R5.1 or the *pot-3(ok1530)* deletion strain did not display any telomeric phenotype (Shtessel et al. 2013). In the study by Cheng *et al.*, the *trt-1; pot-3* double mutants showed no significant difference in survival frequencies compared to the *trt-1* or *pot-3* single mutants (Cheng et al. 2012). However, there has been a limited investigation into the role of POT-3 in regulating telomere length in *C. elegans*, leading prior researchers to suggest that POT-3 might have a dispensable role in regulating telomere length (Barstead et al. 2012; Raices et al. 2008; Shtessel et al. 2013).

Due to its high sequence similarity to *pot-2*, *pot-3* functioned similarly in telomere binding. Nevertheless, the previous study in our lab yielded some *in vitro* evidence regarding the DNA-binding activity and unique characteristics of POT-3. Using the His-tagged POT-3 protein expressed in *E. coli* and electrophoretic mobility shift assays (EMSA), we found that POT-3 specifically binds to the G-strand of telomeric DNA. Subsequent testing with various telomeric substrates revealed that, like POT-2, the minimal binding motif of POT-3 is GCTTAG, not TTAGGC (Yu, Gray, and Ferreira 2023). However, POT-3 was shown to have some unique characteristics compared to POT-2. POT-3 displayed a preference for binding at the 3’ end of DNA over POT-2, as demonstrated by the assay showing the ability of different DNA templates to outcompete pre-bound POT-2 or POT-3 complexes (Yu, Gray, and Ferreira 2023). Interestingly, despite sharing the same binding site and minimal binding motif with POT-2, POT-3 exhibited stronger selectivity for binding to the terminal telomeric repeat of the 3’ G-overhang. POT-3, displaying structural similarity to POT-2 and binding uniqueness, may exhibit a similar role in telomere regulating function *in vivo*.

Considering the structural homology between POT-3 and POT-2, as well as their similar *in vitro* binding activity, we suspected that POT-3 might also play a role in telomere biology *in vivo*. Therefore, this study aimed to assess the phenotypes of a new null allele, *pot-3(syb2415)*, including brood size, telomere length, C-circle level and chromosome fusions, to understand the role of POT-3 in telomere maintenance and genome stability. Our data showed

that POT-3 does serve an important role in telomeric function *in vivo* and it does not act redundantly with POT-2.

3.2 Results

3.2.1 *pot-3(syb2415)* contains a deletion of OB fold

Characterising the phenotype of a null gene deletion is one of the classic ways of identifying protein function. However, it is crucial to use a validated deletion strain to be able to interpret the results. The *pot-3(ok1530)* strain has been available via the CGC for a number of years, yet the *ok1530* allele itself has remained uncharacterised. We therefore decided to sequence the *pot-3* gene, including a stretch 1 kb upstream and downstream of the coding sequence. Remarkably, no mutations were identified within this region compared to wildtype (Figure 3.1). We cannot exclude that a mutation outside of this region is influencing the function or expression of POT-3. However, this suggests that any phenotype in the *pot-3(ok1530)* strain might only be indirectly linked to the POT-3 protein. We therefore decided to create a new *pot-3* allele containing a known deletion that inactivated the POT-3 protein. All POT proteins use OB-folds to bind ssDNA (Shtessel et al. 2013). Indeed, the OB-fold is the only region that hPOT1 uses to bind DNA and inactivating point mutations in the OB fold abrogate hPOT1 function *in vivo* (Lei, Podell, and Cech 2004). POT-3 contains a single OB-fold domain, and we reasoned that if we removed the OB fold, we would generate a null allele. The new *pot-3(syb2415)* contains a 500 bp deletion that spans the entirety of the OB fold (Figure 3.1). We were therefore confident that we could use the *pot-3(syb2415)* strain to characterise its telomeric phenotypes and use this to infer the normal function of POT-3. Interestingly *pot-3(syb2415)* worms are viable and fertile, indicating that *pot-3* is not an essential gene. This emphasises the importance of well characterised mutations as the previous *pot-3* alleles described in WormBase have distinct phenotypes. The *pot-3(ok1530)* strain is viable but the *pot-3(tm3732)* strain is described as being essential (Barstead et al. 2012). The reason for this discrepancy is not clear, but it is notable that the *pot-3* gene is subtelomeric. So it is possible that large deletions in that region might impact telomere integrity and organismal viability.

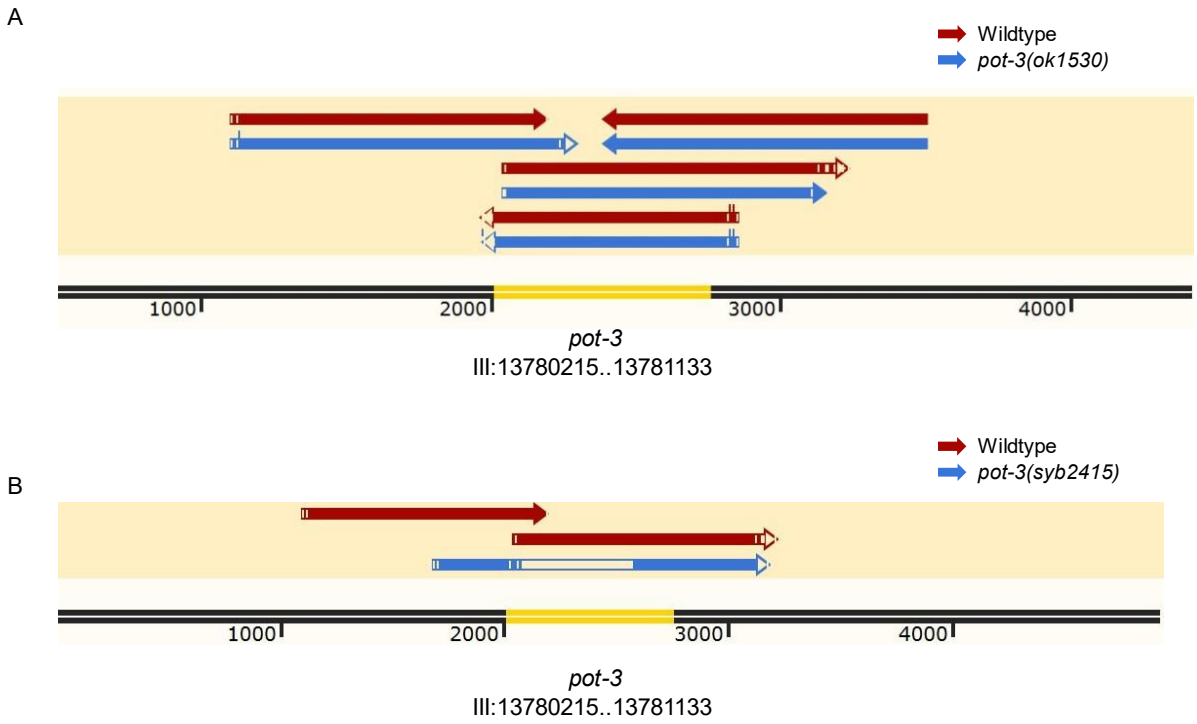

Figure 3.1 Gene deletion is observed in *pot-3(syb2415)* but not *pot-3(ok1530)*

POT-3 is a protein with 215 amino acids. A) *pot-3(ok1530)* contains no mutations observed within the regions of coding sequence or 1 kb region both upstream or downstream of the coding sequence. The blue arrows indicate the sequencing results of *pot-3(ok1530)*. The red arrows indicate the sequencing results of wildtype (N2). The yellow part indicates the coding sequence of *pot-3*. The difference in the sequencing results cannot be observed between wildtype and *pot-3(ok1530)*. B) *pot-3(syb2415)* contains a 500 bp deletion. The red arrows indicate the sequencing results of wildtype (N2). The blue arrow indicates the sequencing results of *pot-3(syb2415)*. The blank in the blue arrow indicates the 500 bp deletion.

3.2.2 Telomere length and C-circle levels are elevated in *pot-3*

Telomere length change is widely observed in worms lacking telomere binding proteins. It has been reported that POT-2, a single-stranded telomere-binding protein, negatively regulates telomerase-mediated telomere repeat addition in *C. elegans* (Raices et al. 2008; Shtessel et al. 2013). POT-3 shares approximately 60% amino acid identity with its homolog POT-2. Given this resemblance, we hypothesised that *pot-3(syb2415)* might also exhibit telomere lengthening phenotype. To investigate this hypothesis, we collected unsynchronised wildtype, *pot-3(syb2415)* and *pot-2(tm1400)* worms. The strains used in the tests were from early generations (newly isolated from crosses. Telomere lengths were not equilibrated). Genomic DNA was extracted from the collected worms by Proteinase K digestion, as described

in Section 2.2.2. The genomic DNA were assessed by terminal restriction fragment (TRF) analysis and TRF Southern blot. One-way ANOVA was conducted for analysing telomere length differences among multiple strains. Tukey's multiple comparisons test was subsequently conducted to identify specific differences between strains.

Our findings revealed that *pot-3(syb2415)* mutants displayed significantly longer telomeres compared to wildtype worms (12.5 ± 1.0 kbp versus 4.3 ± 0.2 kbp respectively, Mean ± SEM, P <0.0001) (Figure 3.2). However, it is worth noting that the elongated telomeres in *pot-3* was not as long as those observed in *pot-2* (17.6 ± 0.7 kbp, Mean ± SEM, P=0.0001) (Figure 3.2). These findings strongly suggest that, akin to *pot-2*, telomere length in *pot-3* mutant is elevated.

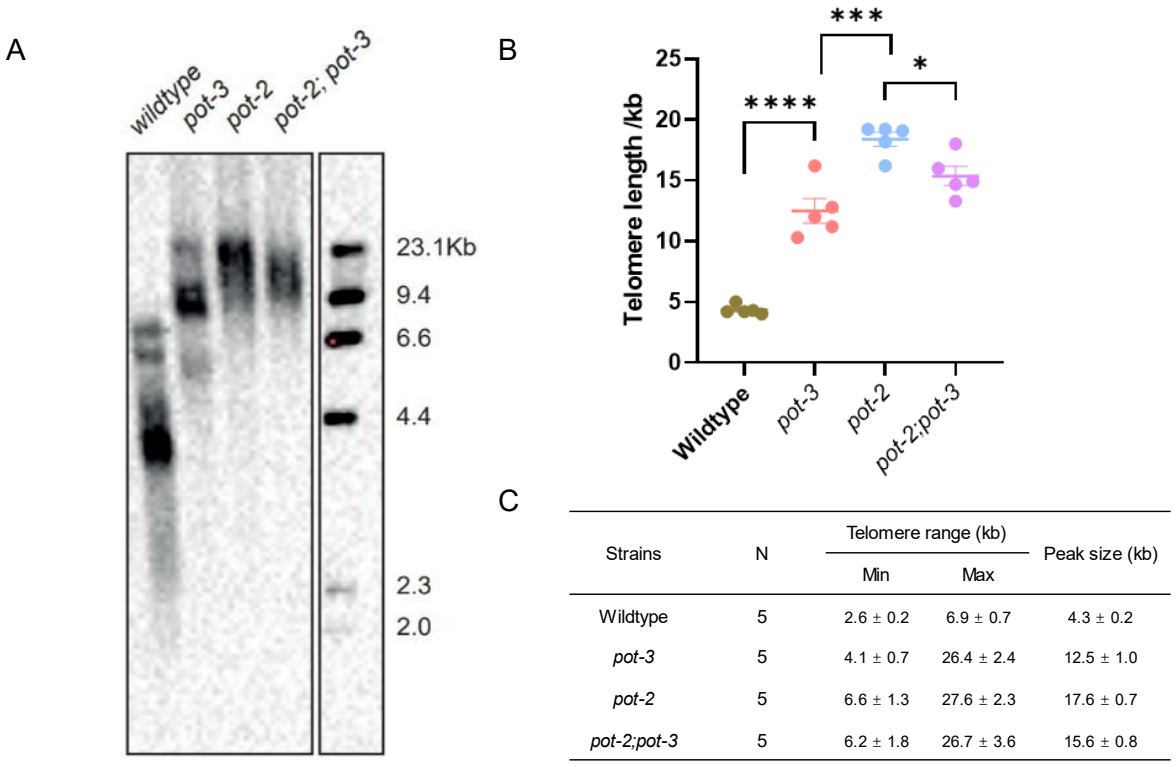

C

Strains	N	Telomere range (kb)		Peak size (kb)
		Min	Max	
Wildtype	5	2.6 ± 0.2	6.9 ± 0.7	4.3 ± 0.2
pot-3	5	4.1 ± 0.7	26.4 ± 2.4	12.5 ± 1.0
pot-2	5	6.6 ± 1.3	27.6 ± 2.3	17.6 ± 0.7
pot-2;pot-3	5	6.2 ± 1.8	26.7 ± 3.6	15.6 ± 0.8

Figure 3.2 *pot-3(syb2415)* mutants display long telomeres

A) Telomere Southern blots from genomic DNA of asynchronous populations of wildtype (N2), *pot-2(tm1400)*, *pot-3(syb2415),* and *pot-2;pot-3* double mutants animals grown at 20°C. Membrane was probed with DIG-labelled $(TTAGGC)_4$ oligos. The blots were from the same membrane and unrelated lanes were cut. B) TRF size quantification of the Southern blot was performed using ImageJ. The blot showed that telomere length *of pot-3* mutants increased compared to wildtype, and the *pot-2;pot-3* double mutants showed a centered length between *pot-3* mutants and *pot-2* mutants. * P < 0.05, *** P < 0.001, **** P < 0.0001 (One-way ANOVA, Tukey's multiple comparisons test). C) The descriptive table of TRF size quantification. Both telomere range and peak size are shown with Mean ± SEM. The blots showed that *pot-3* mutants have increased telomere levels compared to wildtype. The double mutant *pot-2;pot-3* shows an intermediate telomere length compared to *pot-2* and *pot-3*.

In addition to telomere lengthening, it is noteworthy that *pot-2* mutants also display higher levels of telomeric C-circles (Ferreira et al. 2013; Shtessel et al. 2013), a hallmark of the alternative lengthening of telomeres (ALT) pathway (Henson et al. 2009b). To investigate whether *pot-3(syb2415)* also displays elevated C-circle levels, we collected unsynchronised wildtype, *pot-3(syb2415)*, and *pot-2(tm1400)* worms. Genomic DNA was extracted from the collected animals using the bead-beating method, as described in Section 2.2.1. The C-circle assay was performed on the genomic DNA and the resulting data were quantified and analysed using ImageJ by measuring arbitrary units of signal intensity following chemiluminescent detection. The C-circle signals were normalised to the corresponding signal of *pot-2(tm1400)*, as a positive control, to compare signals in different blots. This normalisation allowed us to calculate the mean relative C-circle signal for each sample. One-way ANOVA was conducted to analyse C-circle level differences among multiple strains. Tukey's multiple comparisons test was subsequently conducted to identify specific differences between strains.

Our observations revealed a significant increase in C-circle levels in *pot-3* mutants compared to the wildtype strain, with an approximately 5-fold difference ($P < 0.0001$). However, it is important to note that the elevated C-circle levels in *pot-3* mutants was not as pronounced as those observed in *pot-2* mutants ($P < 0.0001$) (Figure 3.3). These results strongly suggest that akin to *pot-2*, C-circle levels in *pot-3* are elevated, further supporting the involvement of loss of POT-3 in the alternative lengthening of telomeres (ALT) pathway.

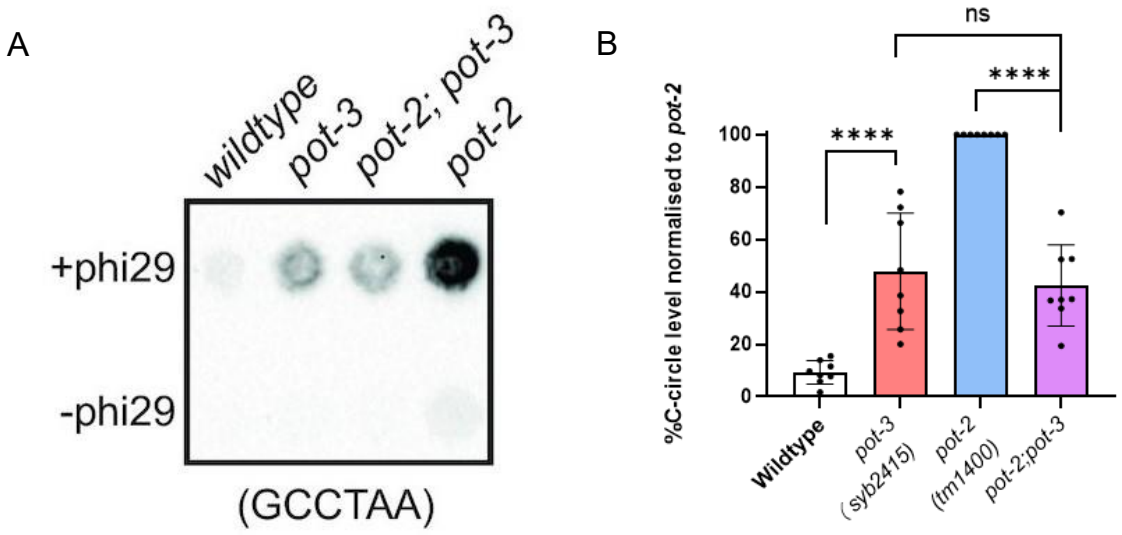

Figure 3.3 Loss of POT-3 partially suppresses the high C-circle levels of a *pot-2* mutant strain

Telomeric C-circle assays were carried out using phi29 polymerase from genomic DNA of asynchronous populations of wildtype (N2), *pot-2(tm1400)*, *pot-3(syb2415),* and *pot-2;pot-3* double mutants animals grown at 20°C, spotted onto a nitrocellulose membrane and probed with DIG-labelled $(TTAGGC)_4$ oligos. A) A representative dot blot of C-circle assays. B) Signal quantification using ImageJ. The signals were plotted relative to *pot-2* (set to 100%). The bar graph shows individual results displayed as dots (N=8). The *pot-3* mutants have an increased C-circle level than wildtype and supressed C-circle in *pot-2* background. ns = not significant, **** P < 0.0001 (One-way ANOVA, Tukey's multiple comparisons test). The partial suppression is consistent with *pot-2* and *pot-3* acting epistatically in the formation of C-circles.

3.2.3 Brood size of wildtype and *pot-3(syb2415)* are similar

Brood size, serving as an indicator of viability and fertility, represents the general fitness of *C. elegans*. Brood size was calculated by counting the total number of viable offspring produced by a single hermaphrodite over its entire lifetime. We compared the brood sizes of wildtype, *pot-2* and *pot-3*. Strikingly, wildtype and *pot-3* exhibited similar brood sizes (288.2 ± 14.37 and 288.4 ± 10.19 respectively, Mean ± SEM, P >0.9999). In contrast, *pot-2* displayed significantly smaller brood size (184.0 ± 9.07, Mean ± SEM, P <0.0001) (Figure 3.4). Taken together, these findings indicate that the POT-3 does not have a similar role to POT-2 in terms of viability and fertility in *C. elegans*. Loss of POT-3 exhibited no observable effects on the general fitness in *C. elegans*.

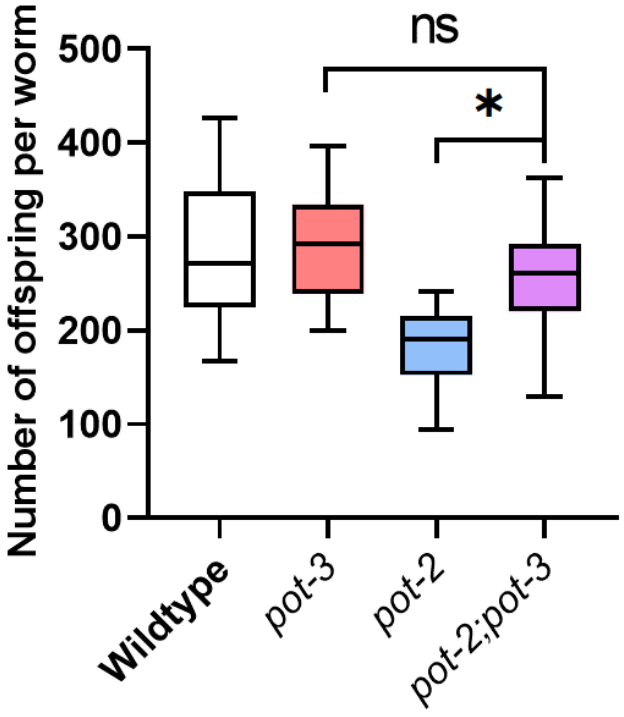

Figure 3.4 Loss of POT-3 partially suppresses the low brood size of a POT-2

mutant strain

The total number of viable offspring per adult worm (brood size) was measured for the wildtype (N2), *pot-3(syb2415)*, *pot-2(tm1400),* and *pot-2;pot-3* double mutants animals grown at 20°C. The box plot displays the mean, 25th and 75th percentile. N= 26, 28, 20, 20, respectively. Mutation of *pot-3* has no significant effect on brood size on its own but supresses the lower brood size of a *pot-2* mutant. ns = not significant, * P < 0.05 (One-way ANOVA, Tukey's multiple comparisons test). The partial suppression is consistent with *pot-2* and *pot-3* acting epistatically in normal animal development.

3.2.4 POT-3 does not act redundantly with POT-2 *in vivo*

It is worth noticing that the telomeric phenotypes in *pot-3* mutants are similar to those seen in *pot-2* mutants but weaker. This similarity raises the possibility that POT-2 and POT-3 might serve the same role in *C. elegans*, with POT-2 potentially being more important or abundant. If this hypothesis were accurate, we would expect that *pot-2;pot-3* double mutants would exhibit stronger telomeric defects and fertility defects compared to either *pot-2* or *pot-3* single mutants.

To test this hypothesis, we constructed *pot-2;pot-3* double mutants using the worm crossing method described in Section 2.1.3. After confirming the genotype through PCR, the *pot-2;pot-3* double mutants worms were collected for genomic DNA extraction, which was subsequently used in the TRF Southern blot assay. The strains used in the tests were from early generations (newly isolated from crosses. Telomere lengths were not equilibrated). Interestingly, we observed weaker telomeric phenotypes, including both the telomere length and C-circle level, in *pot-2;pot-3* double mutants when compared to *pot-2* single mutants. The loss of POT-3 supressed the telomere lengthening (from 17.6 ± 0.7 kbp to 15.6 ± 0.8 kbp, Mean ± SEM, P=0.0381) (Figure 3.2), and reduced the increase in C-circle level (from 10 times to 4.5 times, P <0.0001) (Figure 3.3) observed in *pot-2* mutants. These findings indicate that, rather than acting redundantly, *pot-2* and *pot-3* display an epistatic relationship in telomere length regulation and recombination.

To further assess whether the epistatic effect also has the same effect on worm fertility, we performed brood size assay on *pot-2;pot-3* double mutants. Strikingly, *pot-2; pot-3* double mutants displayed a significantly larger brood size (252.8 ± 14.17, Mean ± SEM) than those observed in *pot-2* single mutants (184.0 ± 9.07, Mean ± SEM) (P=0.0024) (Figure 3.4). This indicates that the epistatic relationship between *pot-2* and *pot-3* extends beyond telomeric phenotypes and influences fertility.

Taken together, these results displayed that *pot-3* acts in an epistatic manner with *pot-2* in terms of telomeric function and fertility rather than acting redundantly. The loss of POT-3 appears to have the ability to (partially) offset the effects caused by the absence of POT-2 in both general fitness and telomere regulation. These results differ from our initial hypothesis and strongly suggest that POT-3 and POT-2 do not perform the same function, but they work together within the same genetic pathway.

3.2.5 Loss of POT-3 does not change the telomeric phenotypes in *pot-1* mutants or *pot-1;pot-2* double mutants

Another important OB-containing protein in *C. elegans*, POT-1, plays an important role in telomere length regulation. POT-1, akin to POT-2, binds to ssDNA strands and negatively regulates telomerase-mediated telomere repeat addition in *C. elegans* (Raices et al. 2008; Shtessel et al. 2013). Given this, we speculated that *pot-3* might also have an epistatic relationship with *pot-1* regarding telomeric phenotypes. To investigate whether this relationship exists, we conducted crosses between *pot-1(tm1620)* and *pot-3(syb2415)* mutants to obtain the *pot-1;pot-3* double mutants.

We observed that the *pot-1;pot-3* double mutants displayed the similar telomeric phenotypes to those of *pot-1* single mutants, including telomere length and C-circle levels. The *pot-1;pot-3* double mutants displayed comparable telomere length compared to *pot-1* single mutant worms (20.9 ± 1.3 kbp versus 21.5 ± 0.9 kbp respectively, Mean ± SEM, P >0.9999) (Figure 3.5). Moreover, *pot-1;pot-3* double mutants displayed mild decrease in C-circle however this was not significantly different (P= 0.7909) (Figure 3.6). Additionally, we conducted G-circle assays on the same genetic DNA samples as C-circles and did not observe any significant changes in G-circle levels (data not shown).

To determine whether the epistatic effect also extended to worm fertility, we performed brood size assay on several strains, including *pot-1* single mutants, and *pot-1;pot-3* double mutants. Our findings revealed that the *pot-1;pot-3* double mutants exhibited the similar brood size to the *pot-1* single mutants (301.2 ± 14.50 and 325.0 ±12.45, Mean ± SEM), which is comparable with the brood size level of wildtype and *pot-3* mutants (P=0.9479) (Figure 3.7). *pot-1* single mutants displayed no defect on general fitness or fertility. Therefore, it is difficult to ascertain whether there is an epistatic effect on general fitness between *pot-3* and *pot-1*.

Taken together, these results confirm that the loss of POT-3 has no impact on the telomeric phenotypes in *pot-1(tm1620)*. Previous studies have revealed that POT-1 and POT-2 have independent roles in repressing a telomerase-independent telomere replication pathway (Shtessel et al. 2013; Cheng et al. 2012). All three POT proteins in *C. elegans* prevent telomere elongation. While POT-1 binds to C-overhangs, POT-2 and POT-3 bind to G-overhangs. POT-2 and POT-3 work together to antagonise telomerase via direct competition, whereas POT-1 likely acts via a different mechanism as it binds the opposite strand of DNA to telomerase. Therefore, the epistatic relationship observed between POT-3 and POT-2 does not extend to POT-1 in regulating telomere length and recombination.

A

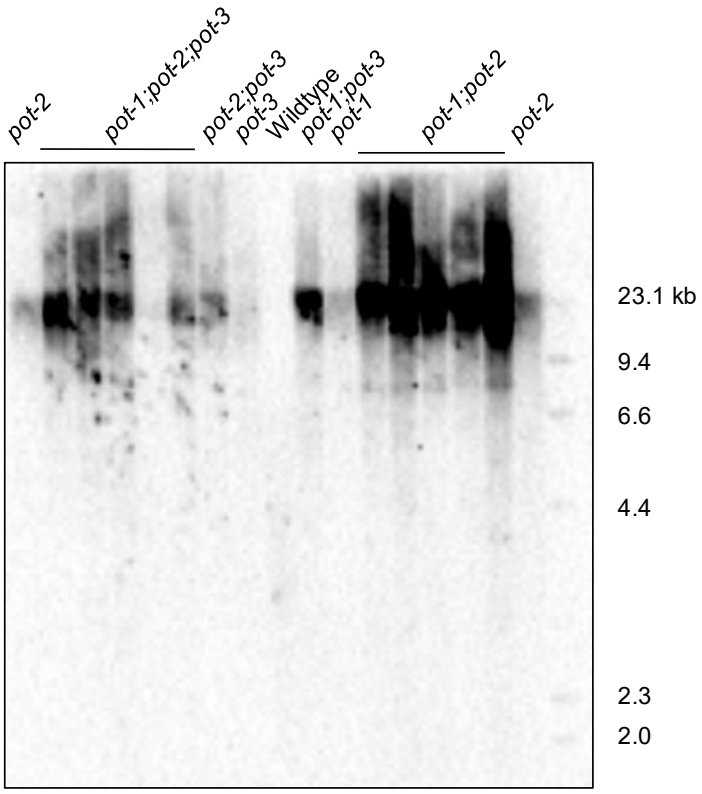

B

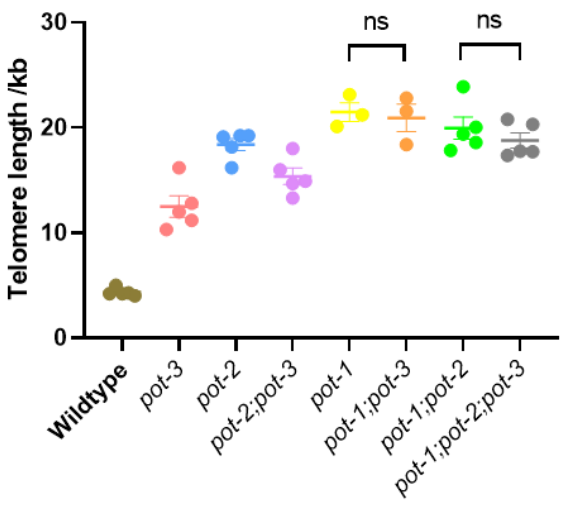

C

Strains	N	Telomere range (kb)		Peak size (kb)
		Min	Max	
Wildtype	5	2.6 ± 0.2	6.9 ± 0.7	4.3 ± 0.2
pot-3	5	4.1 ± 0.7	26.4 ± 2.4	12.5 ± 1.0
pot-2	5	6.6 ± 1.3	27.6 ± 2.3	18.4 ± 0.6
pot-2;pot-3	5	6.2 ± 1.8	26.7 ± 3.6	15.6 ± 0.8
pot-1	3	5.8 ± 1.1	28.6 ± 0.9	21.5 ± 0.9
pot-1;pot-3	3	6.3 ± 1.6	28.2 ± 1.4	20.9 ± 1.3
pot-1;pot-2	5	4.0 ± 0.5	28.0 ± 1.5	19.9 ± 1.1
pot-1;pot-2;pot-3	5	4.5 ± 0.5	26.8 ± 0.8	18.8 ± 0.7

Figure 3.5 Late passages of combinations of *pot-1*, *pot-2* or *pot-3* mutants show similar telomere lengths

A) Telomere Southern blots from genomic DNA of asynchronous populations of wildtype (N2), *pot-2(tm1400)*, *pot-3(syb2415)*, and *pot-2;pot-3* double mutants, *pot-1;pot-2* double mutants, *pot-1;pot-3* double mutants, and *pot-1;pot-2;pot-3* triple mutants animals grown at 20°C. Membrane was probed with DIG-labelled $(TTAGGC)_4$ oligos. B) TRF size quantification of Southern blot using ImageJ. The blot showed that no significant differences were observed between the telomere length of *pot-1;pot-2* double mutants, *pot-1;pot-3* double mutants or *pot-1;pot-2;pot-3* triple mutants with *pot-2* single mutants. ns= not significant (One-way ANOVA, Tukey's multiple comparisons test). C) The descriptive table of TRF size quantification. Both telomere range and peak size are shown with Mean ± SEM.

In a prior study by Shtessel *et al.*, it was observed that telomeres in *pot-1* and *pot-2* single mutants, as well as *pot-1;pot-2* double mutants exhibited functions in telomere elongation and telomerase repression (Shtessel et al. 2013). Given these findings, we sought to assess whether the loss of POT-3 would induce any changes in telomeric phenotype or fertility in *pot-1;pot-2* double mutants as it did in *pot-2* double mutants.

To investigate this, we conducted a cross to generate *pot-1;pot-2;pot-3* triple mutants. This involved crossing with *pot-2;pot-3* double mutants and *pot-1;pot-2* double mutants.

Our results revealed no significant changes in telomere length or C-circle level between *pot-1;pot-2* double mutants and *pot-1;pot-2;pot-3* triple mutants (19.9 ± 1.1 kbp versus 18.8 ± 0.7 kbp respectively, Mean ± SEM, P=0.9651) (Figure 3.5). The results suggest that the loss of POT-3 does not affect the telomeric phenotypes in *pot-1;pot-2* double mutants. We noticed that *pot-1;pot-2* double mutants and *pot-1;pot-2;pot-3* triple mutants had high levels of C-circle signal, which may be attributed to the loss of POT-2. However, *pot-1;pot-2;pot-3* triple mutants and *pot-1;pot-2* double mutants exhibited comparable C-circle levels (Figure 3.6). These results suggest that the loss of POT-3 cannot affect the telomere length or recombination level of *pot-1;pot-2* double mutants.

To further determine whether the epistatic effect exists in worm fertility, we performed brood size assays on several strains, including *pot-1;pot-2* double mutants and *pot-1;pot-2;pot-3* triple mutants. Our results revealed that the brood size of *pot-1;pot-2;pot-3* triple mutants (132.8 ± 15.41, Mean ± SEM) resembled that of *pot-1;pot-2* double mutants (175.5 ± 16.24, Mean ± SEM), without statistically significance (P=0.3098) (Figure 3.7). These results suggest that the loss of POT-3 cannot affect the fertility of *pot-1;pot-2* double mutants either.

Taken together, the results confirm that the loss of POT-3 does not affect the telomeric phenotypes or fertility in *pot-1;pot-2* double mutants. From our observations, *pot-3* acts epistatically with *pot-2* in a POT-1-dependent manner. Loss of POT-3 cannot affect the

telomere length or recombination level in *pot-1;pot-2* double mutants, and neither can it affect brood size, with even *pot-1;pot-2* double mutants displaying defective fertility. This suggests that POT-1 plays an important role in regulating the interaction between POT-3 and POT-2. Similar POT-1 requirements were observed in the interactions between dsDNA binder TEBP-1 and TEBP-2 with the ssDNA binders POT-2 and MRT-1 in *C. elegans* (Dietz et al. 2020; Yamamoto et al. 2021). The precise interplay between these telomeric factors needs to be further elucidated.

Besides these POT1-like proteins, which contain oligonucleotide/oligosaccharide-binding (OB) fold, there is another protein in *C. elegans*, MRT-1, that also features a similar OB fold. However, unlike POT-1 or POT-2, MRT-1 is required for telomerase activity (Meier et al. 2009). Moreover, the MRT-1 protein also contains an active nuclease domain, which indicates a distinct function (Meier et al. 2009). Detailed discussions regarding MRT-1 will be presented in chapter 5.

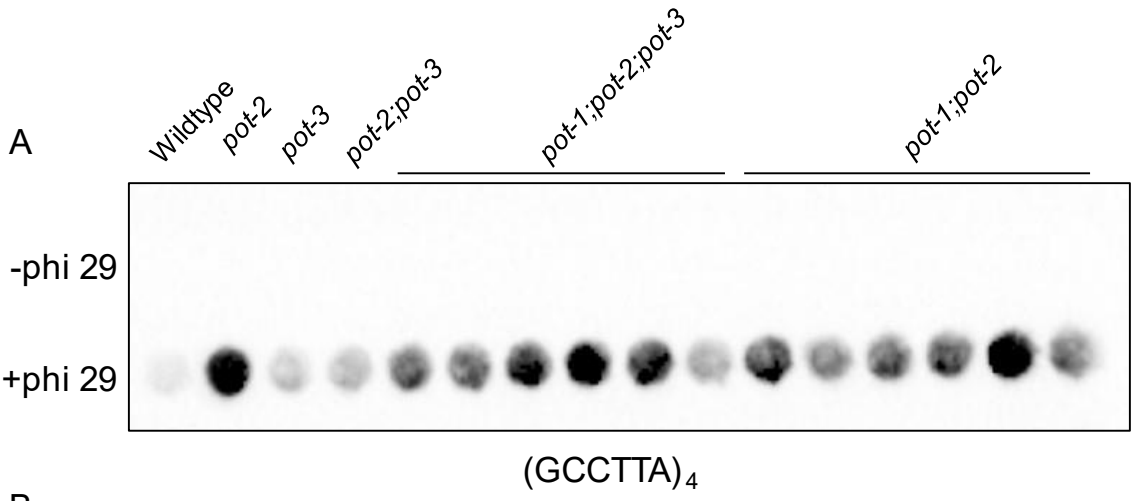
A
Wildtype
pot-2
pot-3
pot-2;pot-3
pot-1;pot-2;pot-3
pot-1;pot-2
-phi 29
+phi 29
(GCCTTA)4

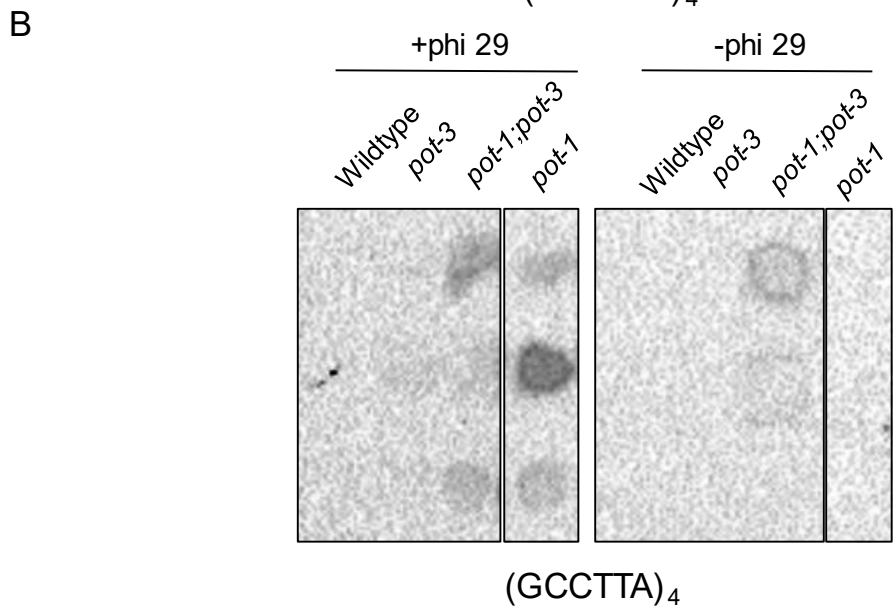
B
+phi 29
-phi 29
Wildtype
pot-3
pot-1;pot-3
pot-1
Wildtype
pot-3
pot-1;pot-3
pot-1
(GCCTTA)4

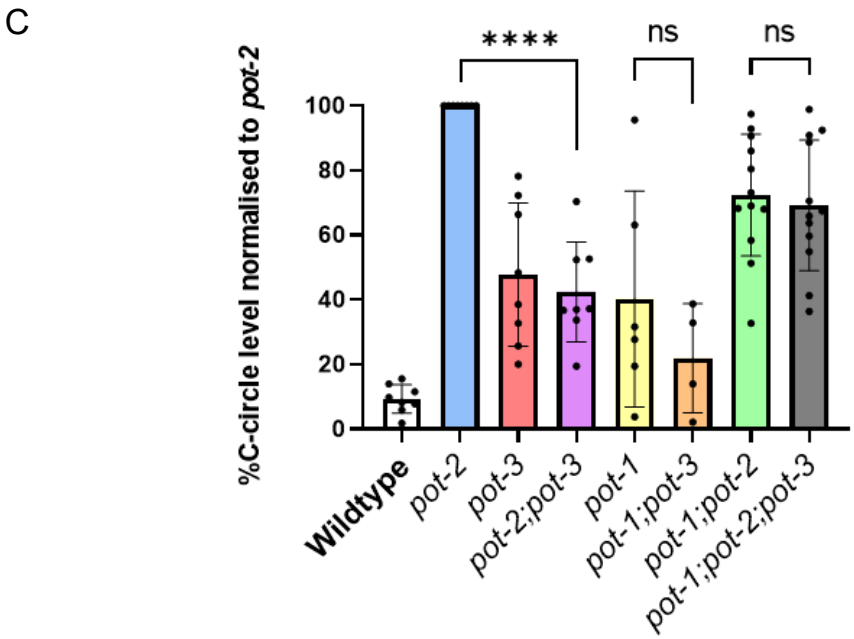
C
%C-circle level normalised to pot-2
****
ns
ns
100
80
60
40
20
0
Wildtype
pot-2
pot-3
pot-2;pot-3
pot-1
pot-1;pot-3
pot-1;pot-2
pot-1;pot-2;pot-3

Figure 3.6 The ability of *pot-3* to partially suppress *pot-2* C-circle levels is POT-1-dependent

Telomeric C-circle assays were carried out using phi29 polymerase from genomic DNA of asynchronous populations of wildtype (N2), *pot-2(tm1400)*, *pot-3(syb2415), pot-1(tm1620), pot-2;pot-3* double mutants, *pot-1;pot-3* double mutants, *pot-1;pot-2* double mutants and *pot-1;pot-2;pot-3* triple mutants animals grown at 20°C, spotted onto a nitrocellulose membrane and probed with DIG-labelled $(TTAGGC)_4$ oligos. A) A representative dot blot of C-circle assays of wildtype (N2), *pot-2(tm1400)*, *pot-3(syb2415), pot-1;pot-2* double mutants and *pot-1;pot-2;pot-3* triple mutants. B) A representative dot blot of C-circle assays of *pot-1(tm1620)*, and *pot-1;pot-3* double mutants. The blots were from the same membrane. Unrelated lanes were cut. C) Signal quantification using ImageJ. The signals were plotted relative to *pot-2* (set to 100%). The bar graph shows individual results displayed as dots (N= 8, 8, 8, 8, 6, 4, 12, 12, respectively). *pot-3* mutants have increased C-circle level than wildtype and supressed C-circle in *pot-2* background. ns = not significant. * P < 0.0001 (One-way ANOVA, Tukey's multiple comparisons test).

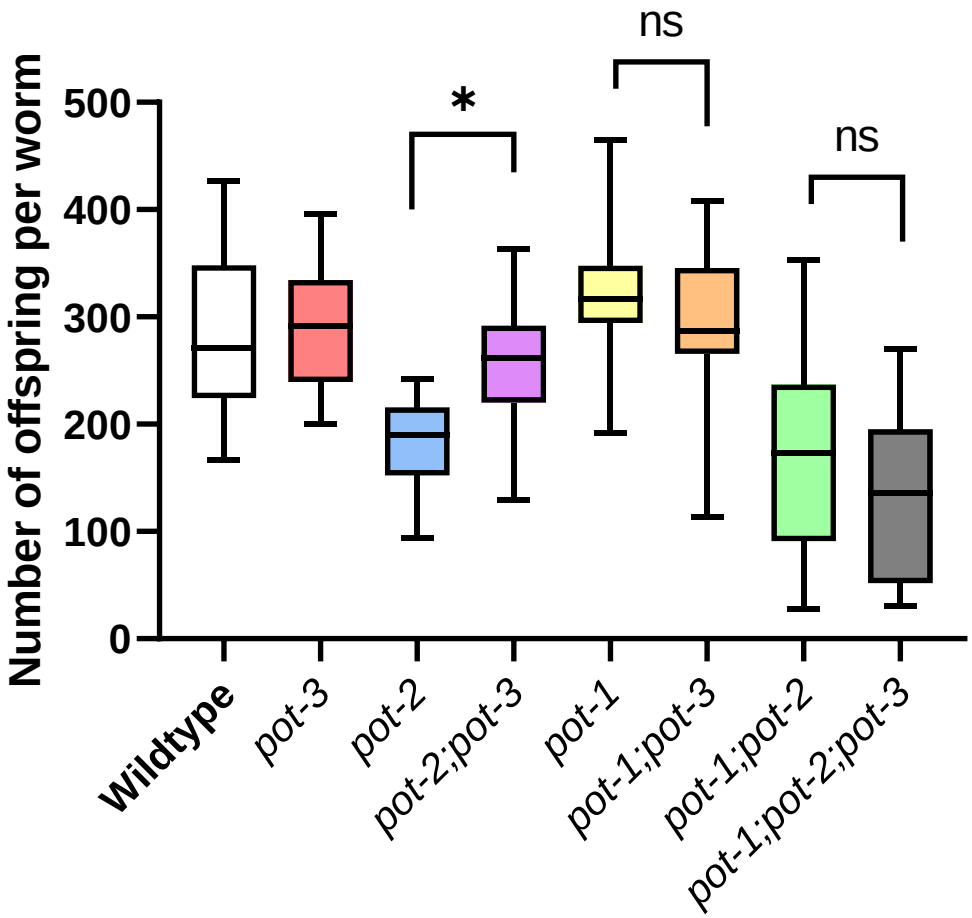

Figure 3.7 The ability of *pot-3* to partially suppress the low brood size of a *pot-2* mutant strain is POT-1-dependent

The total number of viable offspring per adult worm (brood size) was measured for the wildtype (N2), *pot-2(tm1400)*, *pot-3(syb2415), pot-1(tm1620), pot-2;pot-3* double mutants, *pot-1;pot-3* double mutants, *pot-1;pot-2* double mutants and *pot-1;pot-2;pot-3* triple mutants animals grown at 20°C. The box plot displays the mean, 25th and 75th percentile. N= 26, 28, 20, 20, 21, 21, 31, 23, respectively. Mutation of *pot-3* has no significant effect on brood size on its own but supresses the lower brood size of a *pot-2* mutant. Mutation of *pot-1* by itself also does not result in low brood size but, in contrast to *pot-3*, it does not supress the low brood size of *pot-2*. Interestingly, loss of POT-3 no longer suppresses the low brood size of *pot-2* mutant strain if *pot-*

1 is also mutated, compared to *pot-1; pot-2* with *pot-1; pot-2; pot-3*. ns = not significant. * P < 0.05 (One-way ANOVA, Tukey's multiple comparisons test).

3.2.6 Loss of POT-3 causes chromosome inhomogeneity

In yeast, loss of POT homologs leads to telomere uncapping, resulting in the loss of telomeric DNA and chromosome fusion (Garvik, Carson, and Hartwell 1995; Baumann and Cech 2001). Although chromosome fusion was not observed in *pot-2* single mutant worms (Cheng et al. 2012; Raices et al. 2008; Shtessel et al. 2013), we sought to determine whether the loss of POT-3 could induce chromosome fusion phenotypes.

To investigate this, we dissected several strains, including wildtype worms (N2), *trt-1(ok410);unc-29(e193)* (serving as positive control), *pot-2* single mutant, *pot-3* single mutant, and *pot-2;pot-3* double mutant worms. These dissected worms were fixed onto slides. After being stained with DAPI, the slides were observed under a microscope (DeltaVision) to acquire images of cells in diakinesis. The number of chromosomes was counted via ImageJ. The Chi square test was conducted to compare the chromosome counts among different strains.

Interestingly, in *pot-2*, *pot-3*, and *pot-2;pot-3* worms, we observed significantly inhomogeneous chromosome numbers compared to the homogeneous chromosome number observed in wildtype worms (P= 0.0012). However, chromosome fusions observed were not as large-scale as those observed in the positive control strain, *trt-1;unc-29* (P<0.0001). Furthermore, *pot-2*, *pot-3*, and *pot-2;pot-3* worms displayed comparable chromosome counts (P=0.4314) (Figure 3.8). These results suggest that POT-3 and POT-2 similarly participate in maintaining chromosome stability. Moreover, POT-3 is not involved in telomere uncapping, like POT homologs in yeast, because otherwise we would have seen a large-scale chromosome fusion (Wellinger 2010).

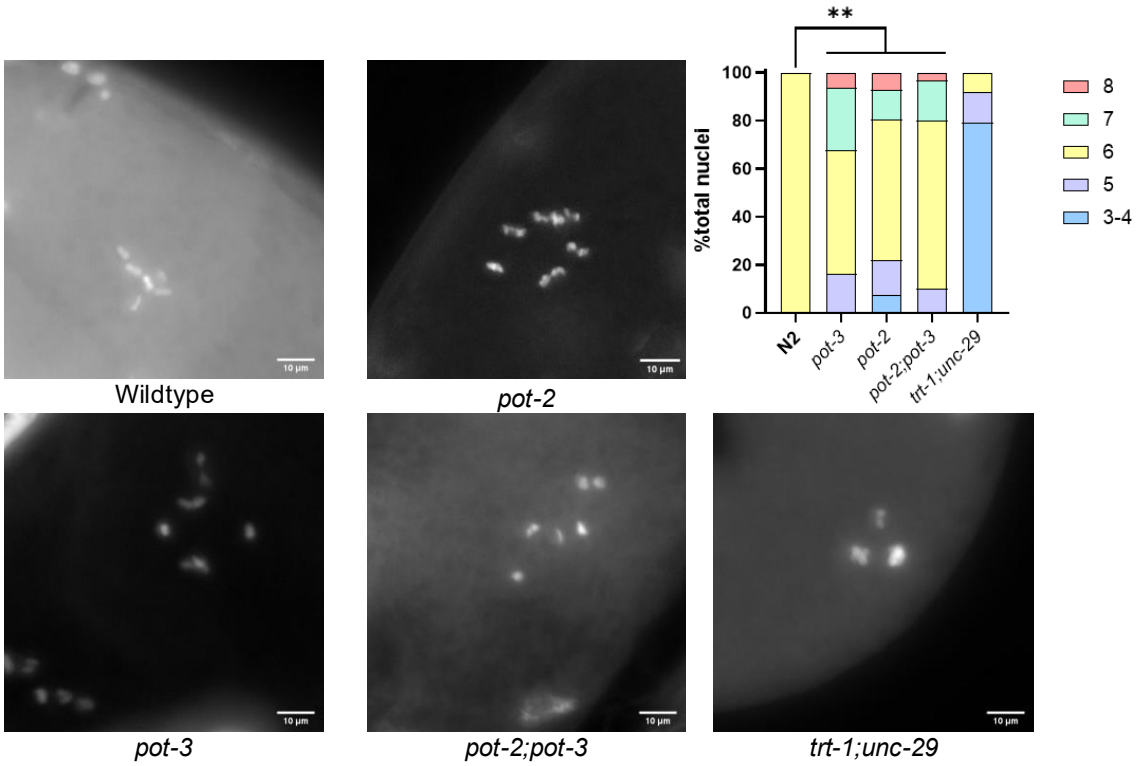

Figure 3.8 Inhomogeneous chromosome numbers are observed in *pot-2(tm1400)*, *pot-3(syb2415)*, and *pot-2;pot-3* double mutants

The total number of chromosomes per cell in in oocytes at diakinesis was measured for the wildtype (N2), *pot-3(syb2415), pot-2(tm1400)*, *pot-2;pot-3* double mutants, and *trt-1(ok410);unc-29(e193)* double mutants animals grown at 20°C. The *trt-1(ok410);unc-29(e193)* double mutants were used as a positive control. The bar indicates the percentage of worms contains different number of chromosomes. N= 30, 31, 41, 30, 24, respectively. Chi square test was conducted using ImageJ based on the chromosome counts. **P<0.01.

3.3 Discussion

3.3.1 POT-2 and POT-3 participate in telomere overhang protection

In our study, the elongated telomere lengths in both *pot-2* and *pot-3* mutants suggest that POT-2 and POT-3 participate in telomere length maintenance in *C. elegans*. It has been observed in our study and previous studies that POT-1 plays a key role in repressing the activity of telomerase, and its loss leads to elongated telomeres. However, POT-2 participates in regulating the overhang length while POT-1 does not (Shtessel et al. 2013).

There are also species in which POT proteins act differently in telomere length regulation, such as mice. In mice, POT1a-containing telomerase complex appears to positively regulate telomerase activity, while the POT1b-containing telomerase complex regulates telomerase.

Similar to POT-2 in *C. elegans*, POT1b also regulates overhang length in mice (Palm et al. 2009). On the contract, in simpler eukaryotes like yeast, loss of POT homologs leads to telomere shortening, rather than lengthening (Garvik, Carson, and Hartwell 1995; Nugent et al. 1996; Baumann and Cech 2001).

The evaluated C-circle levels in both *pot-2* and *pot-3* mutants suggest that POT-2 and POT-3 participate in preventing recombination in *C. elegans*. Similarly, POT-1 also plays a role in recombination repression, and loss of it leads to increased C-circle levels (Shtessel et al. 2013). The recombination-preventing function is widely observed in various species such as moss (Shakirov et al. 2010), mice (Palm et al. 2009), and humans (Kim et al. 2017). It suggests that upon POT1 loss, ALT is a feasible mechanism to regulate telomere length in various species.

In the aspect of POT protein telomere end protection functions, the complete loss of POT1 results in DNA damage activation and telomere lengthening but not telomere fusions in humans (Kim et al. 2017) and mice (Hockemeyer et al. 2006) cells. Interestingly, in simpler eukaryotes such as moss (Shakirov et al. 2010) and yeasts (Garvik, Carson, and Hartwell 1995; Baumann and Cech 2001), loss of POT1 homologs leads to increased chromosome fusions and telomere shortening, rather than lengthening. In *A. thaliana*, chromosome end protection appears to be achieved by the CST (Ctc1, Stn1, Ten1) complex rather than by POT1a or POT1b (Surovtseva et al. 2009).

Strikingly, the loss of either POT-2 or POT- 3 in *C. elegans* results in not only telomere elongation, but also a decrease in chromosome homogeneity. Unlike the large-scale chromosome fusion observed in *trt-1;unc-29* mutant, loss of either POT-2 or POT- 3 results in both increased and decreased chromosome numbers. This suggests that POT-2 and POT-3 play roles in maintaining chromosomal stability. Previous studies show that no massively end-to-end chromosome fusions are observed in *pot-2* mutants, unlike in the telomerase mutants (Cheng et al. 2012; Raices et al. 2008; Shtessel et al. 2013; Ahmed and Hodgkin 2000). As we have observed in Section 3.2.2, loss of POT-2 or POT-3 results in evaluated HR levels. However, tightly restricted activities of HR and NHEJ are needed for proper chromosome segregation (Lemmens and Tijsterman 2011). The increased HR level in *pot-2* and *pot-3* mutants might be the cause of chromosome inhomogeneity.

3.3.2 *pot-2* acts epistatically with *pot-3*

In our study, the high level of sequence identity between POT-2 and POT-3 suggests that these proteins may have arisen from a gene duplication event. Typically, gene duplication can lead to genetic redundancy. Duplicated genes that retain at least partially overlapping functions can provide robustness to mutation in the other copy (Lynch and Force 2000; Force et al. 1999). The similar telomeric phenotypes observed in *pot-2* and *pot-3* mutants are consistent with this theory. Additionally, gene duplications involving POT1 genes have been observed in various species, such as some ciliates, plants and some mammals (Shakirov et al. 2005; Jacob et al. 2007; Skopp, Wang, and Price 1996; Rossignol et al. 2007).

Functional divergence of the duplicated POT orthologs has been observed after duplication events. For example, *Tetrahymena* has two Pot1 proteins, Pot1a and Pot1b. Pot1a prevents checkpoint activation and participates in telomere maintenance, while Pot1b only plays a role in new telomere addition (Jacob et al. 2007; Cranert et al. 2014).

In plants, such as *Arabidopsis thaliana*, three POT proteins have been identified, namely POT1a, POT1b, and POT1c. POT1a and POT1b have turned out to be components of telomerase (Surovtseva et al. 2007; Rossignol et al. 2007) while POT1c displays no discernible molecular or developmental function in mutant plants; only forced expression of POT1c results in decreased telomerase enzyme activity and shortened telomeres (Kobayashi et al. 2019).

Interestingly, a similar phenomenon was observed in the mouse POT proteins, POT1a and POT1b. POT1a and POT1b are closely related in their sequence (72% sequence identity) and overlapping functions (preventing telomere recombination) (Palm et al. 2009). POT1a and POT1b exhibit similar *in vitro* binding affinity for G-strand DNA. However, POT1a is primarily responsible for preventing ATR activation, while POT1b prevents C-strand resection (Hockemeyer et al. 2006).

The term epistasis, a genetic interaction where one mutation masks or suppresses the effects of another allele at another locus, was first introduced by William Bateson in 1907 (Bateson 1907). Due to the sequence similarity and similar telomeric role of *pot-2* and *pot-3*, it is suggested that *pot-2* and *pot-3* come from a gene duplication event. Gene duplication and redundancy are likely to lead to epistasis (Tischler et al. 2006; Sanjuán and Elena 2006). However, the distinct binding preferences and telomere regulating functions between POT-2 and POT-3 suggest the fast diversification of their functions. It is believed that the telomeric proteins are undergoing rapid evolution across different species, such as flies, plants, and

mammals (Saint-Leandre and Levine 2020). The term “mixed epistasis” better describes the epistatic relationship between *pot-2* and *pot-3*, indicating that their functions are partially dependent on each other and are influenced by additional regulatory connections, including mutual repression (Van Wageningen et al. 2010). POT-2 and POT-3 exhibit partial overlapping roles in telomere length maintenance and the potential activation of ALT, whereas the loss of POT-3 is able to repress the fertility defect caused by the loss of POT-2.

The epistasis between *pot-2* and *pot-3* in telomere and C-circle formation is interesting. Based on findings in our lab that POT-3 has a preference for binding to the 3’ end of DNA compared to POT-2 (Yu, Gray, and Ferreira 2023), we speculate that part of the function of POT-2 is to coat the bulk of the G-overhang and restrict POT-3 to the terminal repeat. Therefore, the loss of POT-2 liberates POT-3 from the terminal telomeric repeat and may mislocalise to other regions. This mislocalisation may trigger G-strand displacement and subsequent T-loop formation. We propose that these T-loops are more unstable and more likely to aberrantly processed into C-circles with the presence of mislocalised POT-3. The instability allows the overhangs to participate in the elongation of telomere. Such a model would explain why a double *pot-2; pot-3* mutant displays lower C-circle levels and shorter telomere lengths than a *pot-2* single mutant.

3.3.3 The POT proteins prevent telomere elongation in different ways

The abundance of POT-2 in the worm embryo is approximately 100 times greater than that of POT-3 (Brenes et al. 2018). This abundance difference may explain why POT-2, but not POT-3, was detected via mass spectrometry in pulldowns using the telomere binding proteins TEBP-1 and TEBP-2 in *C. elegans* (Dietz et al. 2020). Moreover, the stronger phenotypes in telomere length regulation observed in *pot-2* mutants compared to *pot-3* mutants may also be attributed to these abundance distinctions.

We speculate that the loss of either POT-2 or POT-3 provides the G-overhang with opportunities to serve as the template in the formation of telomeres. In human, POT-1 participates in enhancing telomerase processivity through the POT1–TPP1 heterodimer (Wang et al. 2007). POT1–TPP1 achieves this by decreasing primer dissociation and increasing telomerase’s translocation efficiency (Latrick and Cech 2010). Despite the interaction between POT1–TPP1 and telomerase occurring in a TPP1-OB-fold-dependent manner (Xin et al. 2007), POT1 still interferes with the binding of telomerase to the 3′ end, further negatively regulating

telomerase activity at telomeres (Kelleher, Kurth, and Lingner 2005). This suggests that the POT1 regulates telomerase activity by controlling the access of telomerase to its templates.

On the other hand, telomeres in *C. elegans* are unique as they contain 5' C-strand overhangs (bound by POT-1) as well as 3' G-strand overhangs (bound by POT-2 and POT- 3), while telomeres in other species typically contain only one of these, canonically G-overhang (Raices et al. 2008). We have demonstrated that *pot-3* exhibits an epistatic relationship with *pot-2* but not *pot-1*. Therefore, POT-2 and POT-3 might antagonise telomerase via direct competition, whereas POT-1 likely employs a different mechanism due to its binding on the opposite DNA strand to telomerase.

Moreover, in a study involving two telomere double-strand DNA binding proteins, TEBP-1 and TEBP-2, it was shown that TEBP-1 and TEBP-2 are not able to interact with POT-2 and MRT-1 without the presence of POT-1. Their model suggests that POT-1 acts as a bridge between TEBP-1/-2 and POT-2/MRT-1 (Dietz et al. 2020). The involvement of dsDNA-binding proteins may help explain the mechanism of POT-1 in telomere length maintenance, potentially through mechanisms like bridging rather than direct competition.

Another theory, based on the model proposed by Raices *et al*., suggests that POT-1 plays a role in protecting specific telomeric single-stranded C-rich DNA from recombination of telomeric sequence and synthesis, while POT-2 serves as a transducer of telomere length to telomerase by regulating the telomere-specific reverse transcriptase at G-overhangs (Raices et al. 2008). The different roles of POT-1 and POT-2 in fertility in our study are consistent with the idea of POT-1 and POT-2 having different telomeric roles. POT-2 may antagonise telomerase directly, while POT-1 may protect overhangs from homologous recombination. Further research is needed to gain deeper insights into the mechanism of telomere length regulation by POT-1.

Chapter 4 : The inheritance of telomere length in *C. elegans*

4.1 Introduction

Telomeres, as part of the chromosome, are inherited by offspring from their parents. The famous example of Dolly the sheep has shown us the importance of organisms starting their life with the correct telomere length, as Dolly's premature senescence was thought to be due, in part, to the inheritance of short telomeres (Rakha 2015). Therefore, the study of telomere length inheritance became important.

The inheritance of telomere length is widely studied in various species, such as yeast, birds, and humans. Most telomere length inheritance studies mainly focus on various factors such as telomerase activity, paternal and maternal effects, and other factors like parental age, specific alleles, and environmental conditions. In this study, we keep parental age and environmental conditions constant, therefore we mainly focus on genetic factors like telomerase activity, and the paternal and maternal effect.

In simple, single-celled, eukaryotes like budding yeast (*Saccharomyces cerevisiae*), telomerase activity plays an important role in telomere length inheritance. Previous research showed that when a short telomere length (telomerase-negative) strain was mated with a wildtype telomere length (telomerase-positive) strain, the average telomere length of the resulting zygotes were of wildtype length (Teixeira et al. 2004). Later work showed that the activity of the Tel1 kinase directs budding yeast telomerase to preferentially bind to and elongate short telomeres (Phillips et al. 2015; Torrance and Lydall 2018). Thus, any telomere in the cell that is sensed as being too short becomes rapidly restored to wildtype length by telomerase. Indeed, mechanisms also exist in yeast to restore long telomeres to wildtype length. Over-elongated telomeres in yeast meiotic cells undergo a high rate of precise deletion to wild-type telomere size via the mechanism of telomere rapid deletion (TRD). These and other inspirational studies in yeast have defined many of the important players. However, the situation in multicellular organisms is likely to be more complex.

One of these complications is the extent to which telomere lengths from the father or the mother are treated equally or whether one dominates in deciding the average telomere length in the resulting offspring. Humans appear to show maternal inheritance. In other words, the telomere length of an individual is disproportionately influenced by the average telomere length of the mother compared to the father. The theory of maternal inheritance of telomere length is supported by compelling evidence and widely accepted (Broer et al. 2013; Eisenberg 2014; Asghar et al. 2015; Bhaumik et al. 2017). One particularly large study analysed six

independent cohorts, involving 19713 humans, and revealed very strong evidence of high and consistent heritability of maternal telomere length inheritance. The study showed heritability, which is used to describe the resemblance between parents and their offspring, was 0.70 (95% CI 0.64–0.76) for leukocyte telomere length with a stronger mother–offspring correlation ($r=0.42$; P-value=3.60×10^{-61}) than father–offspring correlation ($r=0.33$; P-value=7.01×10^{-5}) (Broer et al. 2013).

Furthermore, maternal telomere length inheritance has been widely observed in other animals, including various species of birds. For example, in the king penguin *Aptenodytes patagonicus*, offspring telomere length was positively associated with maternal telomere length early in life (at 10 days old) (Reichert et al. 2015). Similarly, in a songbird, the great reed warbler *Acrocephalus arundinaceus*, heritability of telomere length is linked to the maternal side but not paternal side (Asghar et al. 2015). In the case of the kakapo (*Strigops habroptilus*), maternally inherited telomere length and some sex-specific differences were also displayed (Horn et al. 2011). It is important to note that in these studies, not only maternal effect, but also the environmental conditions and mothers' age influence the telomere length inheritance.

Interestingly, there are some reports of paternal telomere length inheritance, although these tend to be associated with particular tissue types. A study looking at peripheral mononuclear cells from people form 49 unrelated families revealed highly significant father–offspring telomere length correlation, surpassing that of mother–offspring (Nordfjäll et al. 2005). Similarly, in blood cells from 962 individuals with a wide age range (0 to 102 years), fathers were found to contribute more to telomere length inheritance than mothers (Nordfjäll et al. 2010). Additionally, a study on leukocytes from large Amish families (356 men and 551 women, aged 18–92 years) exhibited a positive correlation and association between offspring telomere length and paternal telomere length, with an additive positive correlation and association between a daughter's telomere length and paternal lifespan (Njajou et al. 2007). Therefore, the paternal telomere length inheritance pattern might be cell type-dependent. However, the studies mentioned above, while providing valuable insights, were conducted on relatively limited sample sizes. The apparent contradiction between studies on paternal and maternal telomere length inheritance may also be attributed to variations in telomere measurement methods and sample types, which require further investigation and clarification.

Paternal age also plays an important role in telomere length determination. Analysis of telomere length and paternal age data from 2433 volunteers (1176 men and 1257 women) aged approximately 35–55 years old revealed a positive association between paternal age at birth

and offspring telomere length (De Meyer et al. 2007). Based on large-scale analysis of offspring telomere length, the paternal age association remained stably significant even when additionally adjusting for maternal age, while the maternal age association disappeared after additionally adjusting for paternal age (Broer et al. 2013). Correlation and association between paternal age and telomere inheritance of offspring has been observed not only in humans, but also in other species such as jackdaws (*Corvus monedula*). Interestingly, older jackdaws fathers produced offspring with shorter telomere lengths, as determined by long-term individual-based data from jackdaw families (Bauch et al. 2019).

Telomere lengths in *C. elegans* are stably maintained and genetically conserved within clonal populations while variable among populations. The telomere length of clonal populations remains constant intergenerationally due to its self-fertilisation. The telomere length was stably transmitted to the progeny within each clone. However, strong heterogeneity in telomere length exists within individual clones and different strains of *C. elegans* (Raices et al. 2005). Additionally, in another study, the non-transgenic progeny from the longer-telomere transgenic worms displayed significantly extended telomeres in early generations, but these lengths returned to normal telomere length in later generations (Joeng et al. 2004). This suggests that telomere length inheritance in *C. elegans* is genetically dependent over generations despite the initial telomere length. However, the mechanisms underlying telomere length inheritance in *C. elegans* still remain largely unknown.

C. elegans serves as an advantageous model organism for investigating telomere length inheritance due to its short lifespan and special sexual dimorphism. This includes considerations for age-related effects and sex-specific influences. To better understand the telomere length inheritance dynamics in *C. elegans* and ascertain whether there exists a bias towards maternal or paternal influence, we investigated the telomere length inheritance pattern through crosses from different strains and the reciprocal cross assays. The results highlight that telomere length inheritance in *C. elegans* depends on both male and hermaphrodite contributions, rather than favouring one over the other.

4.2 Results

4.2.1 The initial telomere length of the progeny from the cross is affected by both male and hermaphrodite

As mentioned above, in the study of humans or birds, parental telomere length has a significantly greater effect on offspring length than maternal telomere length. Here, we want to explore whether there is a maternal or paternal effect on telomere length inheritance regulations in *C. elegans*.

To analyse the parental effect on the initial telomere length after cross in *C. elegans*, we conducted crosses between the long telomere length strain, *pot-2(tm1400)*, and the wildtype strain (N2). We performed these crosses with switched male and hermaphrodite (Figure 4.1) and extracted genomic DNA from the progeny via Proteinase K digestion, as described in Section 2.2.2. The genomic DNA were assessed by terminal restriction fragment (TRF) analysis and TRF Southern blot. One-way ANOVA was conducted to determine whether there are any statistically significant differences between offspring strains (Tukey's multiple comparisons test). We used the strongest telomeric signal (mode) and average of the telomeric signal range (median) to show the telomere changes in offspring.

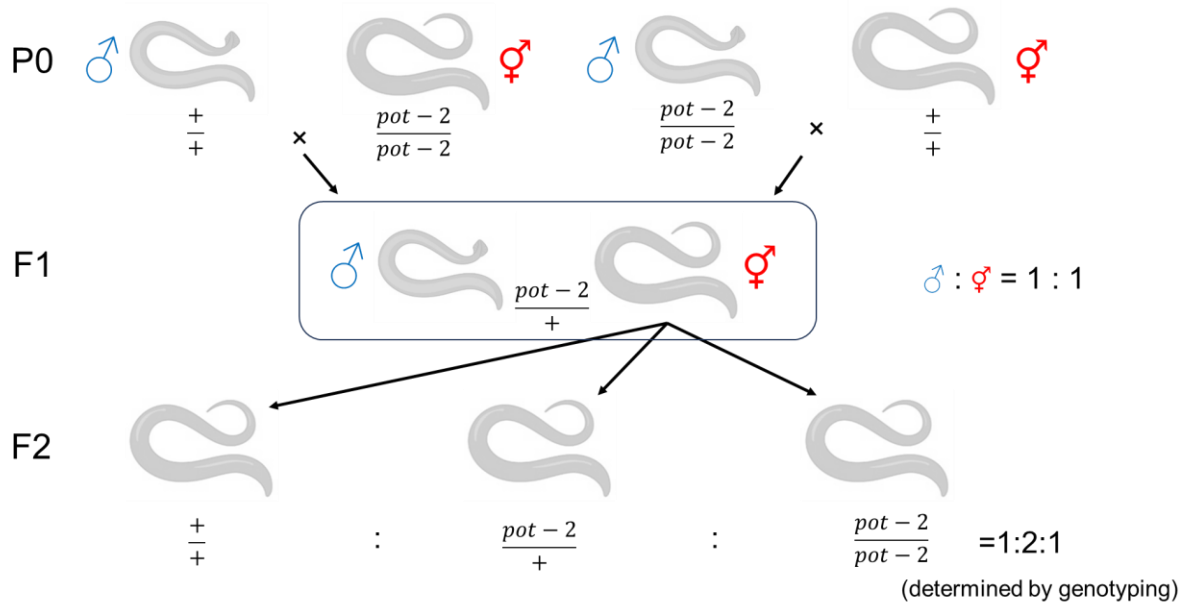

Figure 4.1 Schematic diagrams of cross-fertilisation with switched male and hermaphrodite

Crosses between long telomere length strain, *pot-2(tm1400)* (*pot-2* / *pot-2*), and wildtype strain (N2) (+ / +). All F1 worms are heterozygotes (*pot-2* / +). F1 hermaphrodites self-fertilise to generate homozygous and heterozygous F2 offspring ((+ / +): (*pot-2* / +): (*pot-2* / *pot-2*) = 1:2:1)). The strains were determined by genotyping.

We first investigated whether there were any differences between the telomere lengths of the offspring. Surprisingly, the results revealed that the wildtype and *pot-2* offspring from the different crosses exhibited similar initial telomere lengths, both in terms of strongest telomeric signal and telomere smear range (Figure 4.2). Comparing the strongest telomeric signal (mode) from the cross of wildtype males and *pot-2* hermaphrodites, the telomere lengths of wildtype and *pot-2* mutants are 19.1 ± 1.1 kbp and 17.1 ± 0.5 kbp (Mean ± SEM), respectively. On the other hand, comparing the strongest telomeric signal (mode) from the cross of *pot-2* males and wildtype hermaphrodites, the telomere length of wildtype and *pot-2* mutants are 13.6 ± 3.6 kbp and 14.9 ± 1.9 kbp (Mean ± SEM), respectively. No significant differences were observed in the telomere length of among these crosses (P=0.2364) (Figure 4.2). It suggests that the offspring inherited the longest telomere from their parents regardless of the combination of crosses involving *pot-2*.

However, the strongest telomeric signals can be misleading as they tend to over-emphasize long telomeres over short ones. Therefore, we also analysed the average of the telomeric signal range (the average telomere ranges were showed via the median). Similar results were observed with the average of the telomeric signal range from the crosses involving of *pot-2* and wildtype (P=0.6053) (Figure 4.2). From the cross of wildtype males and *pot-2* hermaphrodites, the telomere length of wildtype and *pot-2* mutants are 5.4 ± 0.6 kbp and 5.2 ± 0.2 kbp (Mean ± SEM), respectively. From the cross of *pot-2* males and wildtype hermaphrodites, the telomere length of N2 and *pot-2* mutants are 4.5 ± 0.4 kbp and 5.3 ± 0.5 kbp (Mean ± SEM), respectively (Figure 4.2). It suggests that the offspring inherited not only the long telomeres but also the short ones from their parents regardless of the combination of crosses. Therefore, our findings suggest that different combinations of male and hermaphrodite in the crosses display similar telomere lengths, regardless of whether the progeny are genetically wildtype or mutant for the POT-2 allele. Additionally, no rapid average telomere length resetting, as observed in yeast (Joseph, Jia, and Lustig 2005), was observed in *C. elegans*.

We sought to explore whether telomere length of offspring is biased paternally or maternally inherited in *C. elegans*. We found that the telomere length of progeny did not solely resemble that of either the male or hermaphrodite worms (Figure 4.2). The wildtype or *pot-2* mutant offspring from the cross displayed the strongest telomeric signals similar to *pot-2* mutants (17.7 ± 0.7 kbp, Mean ± SEM, P=0.4612), significantly longer than the telomere length in wildtype parents (4.7 ± 0.3 kbp, Mean ± SEM, P<0.0001). Importantly, not only the strongest

telomeric signals (mode) in the assay, but also the range of telomeric signal smear (median) differed between parents and offspring. The telomere signal ranges from the cross displayed similar telomere signal range to that of wildtype parents (5.8 ± 0.7 kbp, Mean ± SEM, P=0.4724), while the *pot-2* mutants parents showed significant concentrated signal range (14.6 ± 1.9 kbp, Mean ± SEM, P<0.0001). The results from crosses switched male and hermaphrodite pairs were consistent. Collectively, our results suggest that the different cross combinations of male and hermaphrodite do not exhibit an absolute paternal or maternal telomere length inheritance effect on offspring in *C. elegans*. Instead, the offspring displayed telomeres that incorporated aspects from both parental signals, featuring longer and stronger telomeric signals from *pot-2* mutants (approximately 20 kb) and with shorter and weaker signals from wildtype (approximately 2-5 kb). Due to the limited number of samples, we cannot fully exclude the possibility that the partial maternal inheritance exists (in Figure 4.2 B, the offspring resulting from crosses involving *pot-2* hermaphrodites displayed longer telomeres, yet not statistically significant).

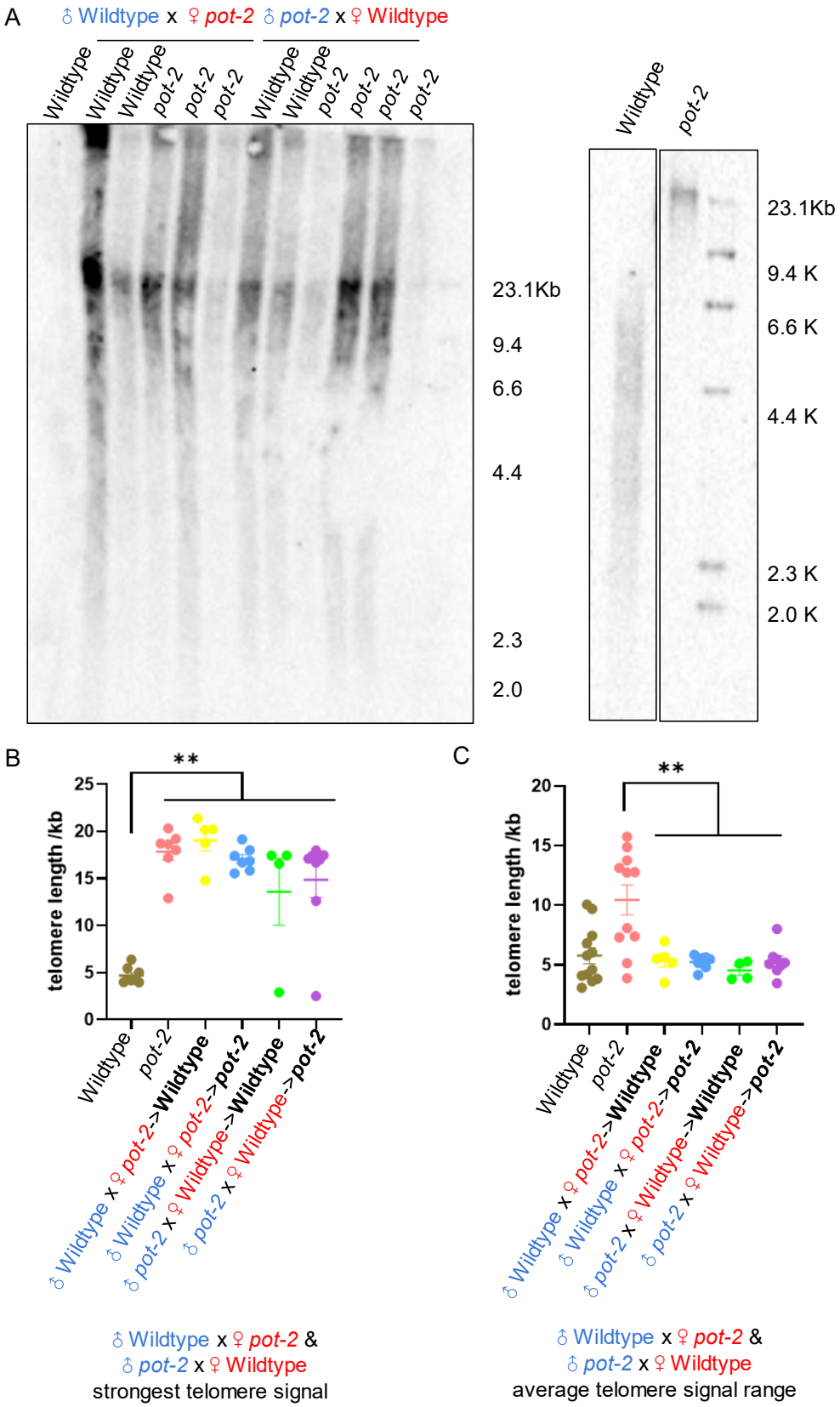

Figure 4.2 Telomere lengths of offspring resulting from crosses involving wildtype (N2) and *pot-2(tm1400)* do not show absolute paternal or maternal telomere length inheritance effect

A) Telomere Southern blots from genomic DNA of asynchronous populations of wildtype

(N2), *pot-2(tm1400)*, and offspring resulting from crosses involving wildtype (N2) and *pot-2(tm1400)* animals grown at 20°C. Membrane was probed with DIG-labelled $(TTAGGC)_4$ oligos. The right blots were from the same membrane. Unrelated lanes were cut. B) The quantification of telomere length summarising TRF size quantification of strongest telomeric signal (mode) using ImageJ. C) The quantification of telomere length summarising TRF size quantification of the average of the telomeric signal range (median) using ImageJ. The dots represent the independent strains from independent crosses. N= 8, 7, 5, 7, 4, 8, respectively. Error bars represent the SEM. ** P < 0.01 (One-way ANOVA, Tukey's multiple comparisons test).

.

To exclude the possibility that our observations drawn from crosses of wildtype and *pot-2* mutants were specific to *pot-2* and not representative of strains with long telomeres generally, we expanded our investigation to include other long telomere length strains, *pot-1(tm1620)*, with wildtype telomere length (N2). We conducted crosses with switched parents to assess our findings, following the same approach depicted in Figure 4.1. One-way ANOVA was also conducted to determine whether or not there were any statistically significant differences between offspring strains (Tukey's multiple comparisons test).

In our observations, the strongest telomeric signal (mode) of offspring in crosses of wildtype with *pot-1* mutants (with switched male and hermaphrodite parents) remained at a similar level across the strains, as we observed in crosses involving *pot-2* and wildtype (P=0.2905) (Figure 4.3). In the cross of wildtype males and *pot-1* hermaphrodites, the telomere length of wildtype and *pot-1*mutants was 22.6 ± 2.8 kbp and 18.9 ± 0.2 kbp (Mean ± SEM), respectively. Similarly, in the cross of *pot-1* males and wildtype hermaphrodites, the telomere length of wildtype and *pot-1* mutants was 19.0 ± 0.3 kbp and 18.8 ± 0.6 kbp (Mean ± SEM), respectively (Figure 4.3). This suggests that the offspring inherited the longest telomere from their parents regardless of the combination of crosses involving *pot-1*. This conclusion aligns with what we observed for POT-2. Our results revealed that the strongest telomeric signals exhibited no significant differences among the offspring from these crosses. These observations confirmed that the offspring strains, which should have wildtype telomere length, could inherit long telomeres from their parents without resetting to a wildtype telomere length during embryogenesis.

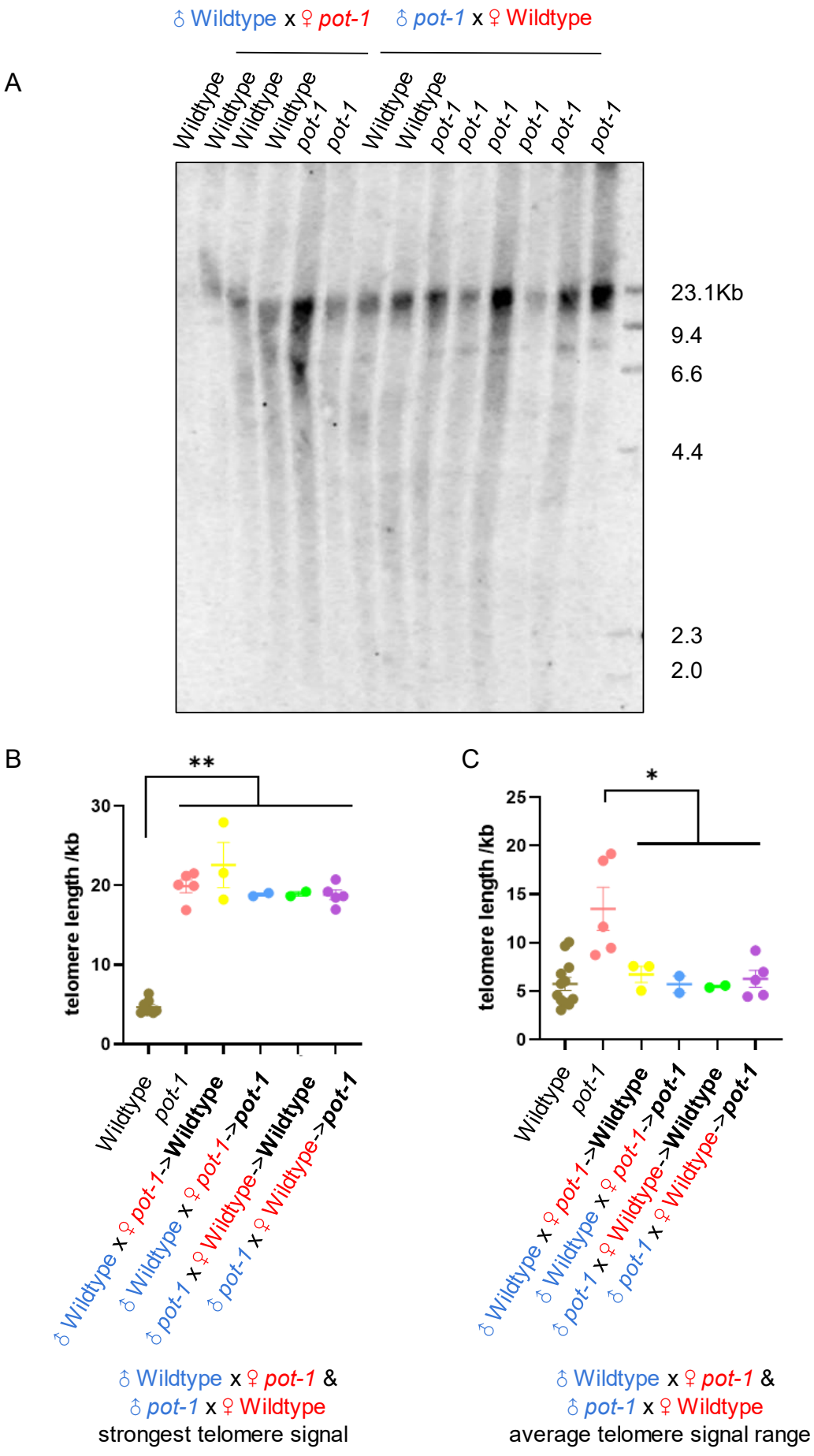
♂ Wildtype x ♀ pot-1
♂ pot-1 x ♀ Wildtype
A
Wildtype
Wildtype
Wildtype
Wildtype
pot-1
pot-1
Wildtype
Wildtype
pot-1
pot-1
pot-1
pot-1
pot-1
pot-1
23.1Kb
9.4
6.6
4.4
2.3
2.0
B
**
telomere length /kb
30
20
10
0
Wildtype
pot-1
♂ Wildtype x ♀ pot-1->Wildtype
♂ Wildtype x ♀ pot-1->pot-1
♂ pot-1 x ♀ Wildtype->Wildtype
♂ pot-1 x ♀ Wildtype->pot-1
♂ Wildtype x ♀ pot-1 &
♂ pot-1 x ♀ Wildtype
strongest telomere signal
C
*
telomere length /kb
25
20
15
10
5
0
Wildtype
pot-1
♂ Wildtype x ♀ pot-1->Wildtype
♂ Wildtype x ♀ pot-1->pot-1
♂ pot-1 x ♀ Wildtype->Wildtype
♂ pot-1 x ♀ Wildtype->pot-1
♂ Wildtype x ♀ pot-1 &
♂ pot-1 x ♀ Wildtype
average telomere signal range

Figure 4.3 Telomere lengths of offspring resulting from crosses involving wildtype (N2) and *pot-1(tm1620)* do not show absolute paternal or maternal telomere length inheritance effect

A) Telomere Southern blots from genomic DNA of asynchronous populations of wildtype (N2), *pot-1(tm1620)*, and offspring resulting from crosses involving wildtype (N2) and *pot-1(tm1620)* animals grown at 20°C. Membrane was probed with DIG-labelled $(TTAGGC)_4$ oligos. B) The quantification of telomere length summarising TRF size quantification of the strongest telomeric signal (mode) using ImageJ. C) The quantification of telomere length summarising TRF size quantification of the average of the telomeric signal range (median) using ImageJ. The dots represent the independent strains from the same cross. Error bars represent the SEM. * P < 0.05, ** P < 0.01 (One-way ANOVA, Tukey's multiple comparisons test).

Additionally, the median of telomere signal smear range showed no significant differences among the offspring strains resulting from the crosses involving *pot-1* (P=0.8242). In the cross of wildtype males and *pot-1* hermaphrodites, the telomere length of wildtype and *pot-1* mutant offspring was 6.7 ± 0.8 kbp and 5.7 ± 0.9 kbp (Mean ± SEM), respectively. In the cross of *pot-1* males and wildtype hermaphrodites, the telomere length of wildtype and *pot-1* mutant offspring was 5.5 ± 0.1 kbp and 6.3 ± 0.9 kbp (Mean ± SEM), respectively (Figure 4.3). The telomere signal smear ranges were at comparable levels in crosses involving *pot-1* and wildtype. Likewise, all these results collectively suggest that the specific male and hermaphrodite combinations we used in the crosses had no significant impact on the average telomere length range of the offspring. These observations confirmed that the offspring strains, which should have long telomere length such as *pot-2* or *pot-1*, could inherit short telomeres from their parents.

Moreover, similar to the observations in crosses involving wildtype and *pot-2* mutants, we also observed that the initial telomere length of the progeny did not solely reflect the telomere length of either male worms or hermaphrodite worms in *pot-1* mutants. The strongest signal (mode) of telomere length of wildtype or *pot-1* mutant offspring in from the crosses displayed significantly longer telomeres than those in wildtype parents (4.7 ± 0.3 kbp, Mean ± SEM, P<0.0001), similar to those observed in *pot-1* mutant parents (19.9 ± 0.8 kbp, Mean ± SEM, P=0.3075) (Figure 4.3).

Interestingly, the median of the average telomere signal smear range indicated that the wildtype or *pot-1* mutant offspring from the crosses were significantly lower than *pot-1* mutant parents (13.5 ± 2.2 kbp, Mean ± SEM, P=0.0321) but showed similar median of the telomere signal as observed in wildtype parents (5.8 ± 0.7 kbp, Mean ± SEM, P=0.9382) (Figure 4.3 C). These results suggest that the offspring, no matter from the crosses of wildtype and *pot-1*

mutants, appear to inherit telomere characteristics from both parents as observed in crosses of wildtype and *pot-2* mutants.

4.2.2 The long telomere length from the cross does not change genetically over generations

According to the observations discussed in Section 4.2.1, wildtype strains derived from long telomere parents exhibited notably longer telomere lengths compared to wildtype worms that were generated due to self-fertilisation. To determine whether this elongated telomere length phenotype persisted consistently across subsequent generations, we followed these worms for multiple generations (2^{nd}, 6^{th}, 12^{th}, 20^{th}, 28^{th}, and 38^{th} generations) to monitor how telomere lengths change over time. Surprisingly, no significant changes in the telomere length of the worms collocated from those generations were observed (P=0.2954), within a range of approximately 19.2 ± 1.9 kbp in the 2^{nd} generation to 16.7 ± 0.9 kbp in the 38^{th} generation (Figure 4.4). It is important to note, however, that the overall TRF size remained consistent (range from 2.5 ± 0.3 to 26.8 ± 0.8 kbp). These results suggest that the telomere length in offspring, which should display genetically wildtype telomere length, remained stably long and exhibited little variability across multiple generations we observed. However, we cannot exclude that the telomere length will eventually reset to wildtype level due to the limited generations we observed.

To investigate whether the observed stable telomere inheritance is specific to long telomere strains or extends to strains with wildtype telomere length, we focused on one *pot-2* progeny resulting from crosses, which inherited wildtype length telomeres. Surprisingly, the findings revealed that the telomere length of the worms reverted to the long telomere phenotype after a relatively short period of time, telomere lengths increased from approximately 3.2 kbp in the 2^{nd} generation to 17.4 kbp in the 6^{th} generation (Figure 4.4). Following this shift, the long telomere length remained stable, as we anticipated, with the overall TRF size consistently falling within the range of 2.4-28.1 kbp. These results suggest that the stability of telomere length inheritance in offspring is contingent on both the initial telomere length and the genetic background, implying the interplay between genetic factors and telomere dynamics. Moreover, these observations also suggest that telomeres undergo lengthening rapidly while the telomere shortening occurs slowly in *C. elegans*. However, among all the *pot-2* strains we isolated from the crosses (more than 25 independent strains tested with TRF), we only obtained one strain

with wildtype-length telomeres. This strain may not be representative for the studies conducted. The potential reasons for the existence of this strain will be discussed in Section 4.3.3.

A

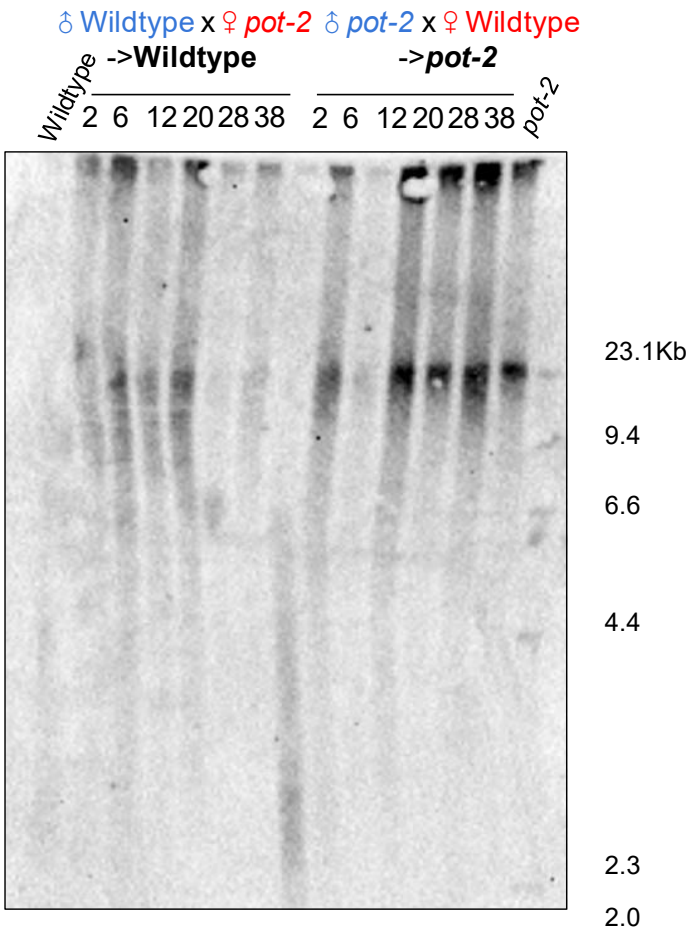

B ♂Wildtype x ♀*pot-2*->**Wildtype**

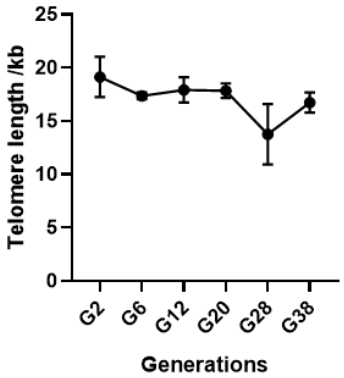

Generations	N	Telomere range (kb)		Peak size (kb)
		Min	Max	
G2	3	5.2 ± 2.2	24.9 ± 2.9	19.2 ± 1.9
G6	3	4.4 ± 1.0	25.0 ± 2.0	17.4 ± 0.3
G12	3	4.3 ± 1.1	26.8 ± 0.8	17.9 ± 1.2
G20	3	3.5 ± 1.2	26.4 ± 1.0	17.9 ± 0.7
G28	3	2.7 ± 0.2	24.4 ± 1.5	13.76 ± 2.8
G38	3	2.5 ± 0.3	22.4 ± 0.9	16.7 ± 0.9

C ♂*pot-2* x ♀Wildtype->***pot-2***

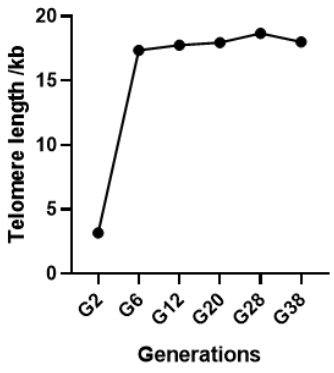

Generations	N	Telomere range (kb)		Peak size (kb)
		Min	Max	
G2	1	2.4	8.1	3.2
G6	1	2.6	25.3	17.4
G12	1	4.9	26.1	17.8
G20	1	2.5	24.6	18.0
G28	1	5.3	26.9	18.7
G38	1	4.8	28.1	18.0

Figure 4.4 Telomeres undergo lengthening rapidly while the telomere shortening occurs slowly in offspring resulting from crosses involving wildtype (N2) and *pot-2(tm1400)*

A) Telomere Southern blots from genomic DNA of asynchronous populations of wildtype (N2), offspring resulting from crosses involving *pot-2(tm1400)* and wildtype (N2) animals from successive generations grown at 20°C. The membrane was probed with DIG-labelled $(TTAGGC)_4$ oligos. B) The quantification of telomere length of N2 offspring resulting from crosses wildtype (N2) male and *pot-2(tm1400)* hermaphrodites from successive generations. The tables summarise the TRF size quantification, including the telomeric signal ranges and the strongest telomeric signals (peak size) (Mean ± SEM) using ImageJ (N=3). C) The quantification of telomere length of *pot-2* offspring resulting from crosses between *pot-2(tm1400)* male and wildtype (N2) hermaphrodites from successive generations. The tables summarising TRF size quantification of telomeric signal range and strongest telomeric signal (peak size) using ImageJ (N=1).

To further validate our findings and eliminate any potential influence from wildtype parents, we collected the samples of the wildtype strain resulting from the cross of *pot-2* and *trt-1*, and the cross of *pot-3* and *mrt-1*. The wildtype offspring from the cross of *pot-2* and *trt-1* displayed a telomere length range from 2.8 ± 0.3 to 27.1 ± 2.5 kbp, with the strongest signals concentrated between 15.5 ± 0.4 and 16.6 ± 0.4 kbp (Figure 4.5). Similarly, the wildtype offspring from cross of *pot-3* and *mrt-1* displayed a telomere length range from 3.1 ± 1.2 to 22.8 ± 1.5 kbp with the strongest signals clustered between 14.0 ± 0.5 and 15.2 ± 0.8 kbp (Figure 4.5). No significant change in telomere length was observed (P=0.6853 and 0.6753, respectively). These results provide further support for the fact that the long telomere length in genetically wildtype offspring remains stable across multiple generations, regardless of the specific combination of the crosses.

A

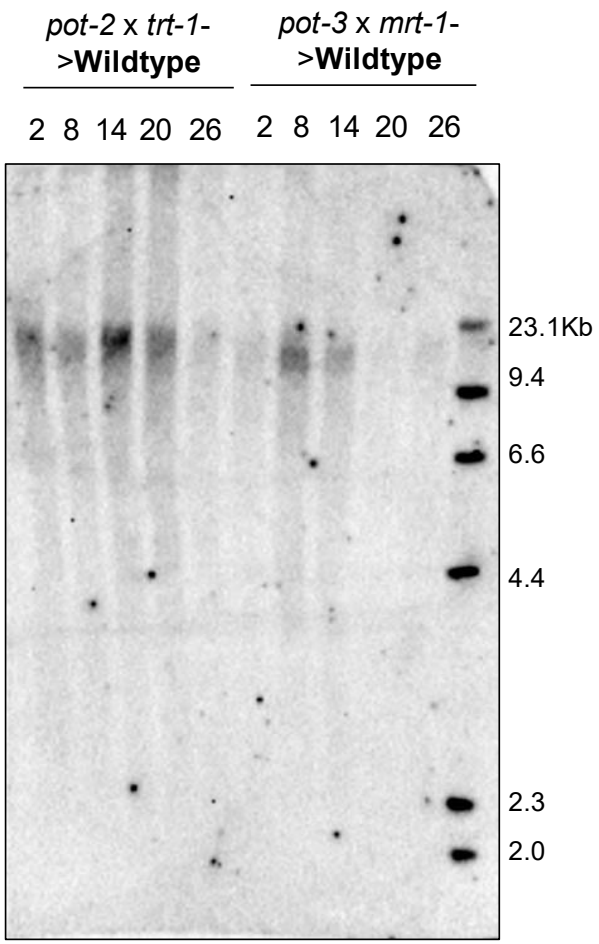

B *pot-2* x *trt-1*->**Wildtype**

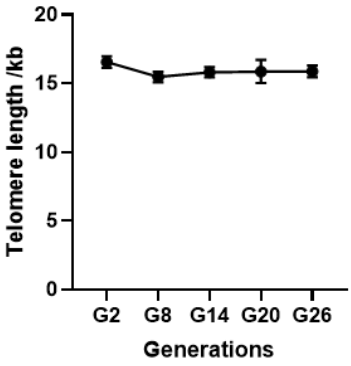

Generations	N	Telomere range (kb)		Peak size (kb)
		Min	Max	
G2	3	4.0 ± 1.1	22.0 ± 1.9	16.6 ± 0.4
G8	3	3.7 ± 0.9	27.1 ± 2.5	15.5 ± 0.4
G14	3	2.8 ± 0.3	25.0 ± 2.4	15.8 ± 0.4
G20	3	3.1 ± 0.5	21.9 ± 1.6	15.9 ± 0.8
G26	3	4.6 ± 2.1	21.6 ± 1.4	15.9 ± 0.4

C *pot-3* x *mrt-1*->**Wildtype**

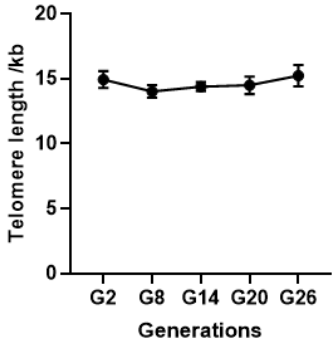

Generations	N	Telomere range (kb)		Peak size (kb)
		Min	Max	
G2	3	6.5 ± 1.7	22.8 ± 1.5	14.9 ± 0.7
G8	3	3.1 ± 1.2	21.0 ± 0.8	14.0 ± 0.5
G14	3	4.0 ± 0.9	21.7 ± 1.4	14.4 ± 0.3
G20	3	6.8 ± 2.4	19.1 ± 0.3	14.5 ± 0.7
G26	3	6.4 ± 2.0	22.1 ± 0.6	15.2 ± 0.8

Figure 4.5 The telomere length of offspring remains stable regardless of the specific combination of the crosses

A) Telomere Southern blots from genomic DNA of asynchronous populations of wildtype offspring resulting from crosses involving *pot-2(tm1400)* and *trt-1(ok410)*, *pot-3(syb2415)* and *mrt-1(tm1354)* animals from successive generations grown at 20°C. The membrane was probed with DIG-labelled $(TTAGGC)_4$ oligos. B) The quantification of telomere length of N2 offspring resulting from crosses *pot-2(tm1400)* and *trt-1(ok410)* from successive generations. C) The quantification of telomere length of wildtype offspring resulting from crosses involving *pot-3(syb2415)* and *mrt-1(tm1354)* from successive generations. The tables summarise TRF size quantification of telomeric signal range and strongest telomeric signal (peak size) (Mean ± SEM) using ImageJ (N=3).

4.2.3 The telomere length of offspring shows heterozygosity

The results of Section 4.2.1 strongly imply that the initial telomere length of offspring is not solely dependent on either male or hermaphrodite but appears to be influenced by both parental contributions. For example, the telomere length pattern resulting from the cross between wildtype and *pot-2* mutants is characterised by longer, stronger signals akin to *pot-2* mutants and as well as shorter, weaker signals akin to wildtype. This observation suggests that offspring inherit their telomere length from both parental sources.

Considering that telomere length inheritance in *C. elegans* is not absolutely paternally or maternally determined, we propose that starting telomere length is inherited from both male and hermaphrodite. However, an additional challenge emerged during our investigation: the presence of long telomeres often results in stronger signals, potentially overshadowing signals from shorter telomeres. Moreover, the telomere signals tend to exhibit a smeary pattern in the TRF assay, making precise quantification more challenging. The smeary pattern of telomere lengths likely derived from heterogeneity in the lengths of the 24 telomeres in each *C. elegans* cell and between the different cell types in the animal. At the molecular length, telomere length is ultimately decided by the opposing action of telomerase and exonucleases. We therefore thought that we could reduce this heterogeneity if we used strains that lacked telomerase activity and that had reduced exonuclease activity. To this end, we conducted crosses involving two exonuclease mutant strains *exo-1(tm1842)* and *mrt-1(tm1354)*. Notably, MRT-1 processes 3’ to 5’ exonuclease activity and is also required for telomerase activity *in vivo* (Meier et al. 2009). The TRF assay of *mrt-1* mutants displayed a distinct pattern characterised by sharp bands instead of the typical smeary ones. This characteristic permits more accurate quantification of telomere length in the worms compared to the smeary pattern in other strains.

This approach helped bypass challenges related to signal strength and smearing, contributing to a more precise assessment of telomere inheritance patterns in *C. elegans*.

The *mrt-1* mutant parent exhibited a total of six signal bands at lengths of 2.6 kbp, 3.1 kbp, 5.3 kbp, 8.4 kbp, 12.3 kbp, and 14.5 kbp, respectively. On the other hand, *exo-1* mutant parents displayed a smear pattern ranging in length from 2.8 to 12.2 kbp, with a mild peak at length of 6.9 kbp (Figure 4.6). In the offspring strains resulting from the crosses, we observed varying numbers and sizes of telomere signal bands (details shown in Figure 4.6). Importantly, all observed signals fell within the range demonstrated by *exo-1* mutant and *mrt-1* mutant parents. Moreover, three independent *mrt-1; exo-1* double mutant offspring strains exhibited different telomere length pattern, on the aspects of number and size (Figure 4.6). It is worth noting that none of the offspring strains resulting from crosses involving *exo-1* and *mrt-1* displayed an identical number or size of telomere signal bands as either the *exo-1* mutant or *mrt-1* mutant parent alone. On the other hand, the offspring strains displayed telomere signal bands at the length of various bands from both of their parents. Using *exo-1* offspring strain as an example, the telomeres exhibiting lengths of 14.5 kbp and 2.5 kbp were consistent with those found in *mrt-1* parents while telomeres at other lengths observed in the offspring strain were potentially inherited from the *exo-1* parents. These observations suggest that the telomere length inheritance in *C. elegans* is a stochastic process. These results also provide strong confirmation that the offspring in *C. elegans* inherit random subsets of telomeres from both male and hermaphrodite parents, marking a departure from the solely paternal or maternal effects observed in humans and birds.

A

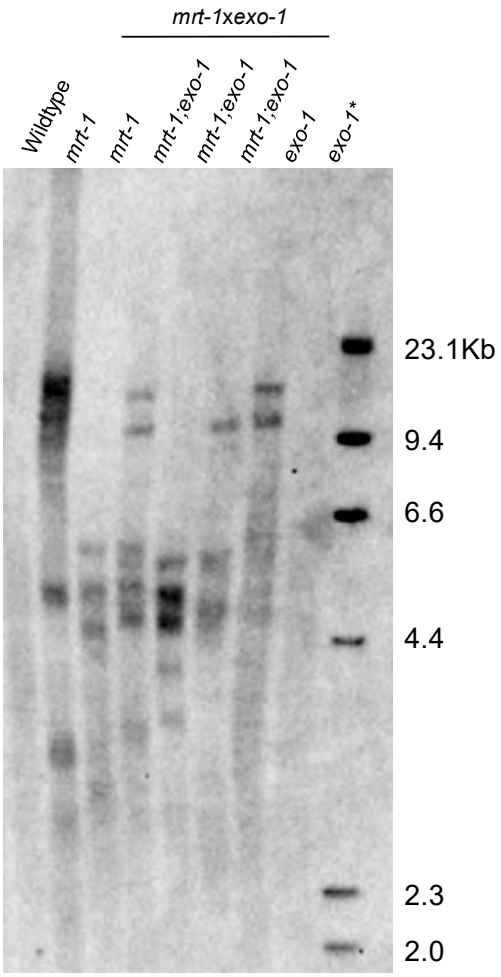

B

	mrt-1xexo-1					
mrt-1	*mrt-1*	*mrt-1;exo-1*	*mrt-1;exo-1*	*mrt-1;exo-1*	*exo-1*	*exo-1**
14.5		14.0			14.5	
12.3		11.3		11.5	11.9	12.2
8.4		8.4				↓
	6.3	6.2				6.9
			6.0	6.0	6.0	
5.3	5.4	5.4	5.2			
	4.6	4.8	4.8	5.0	4.9	
		3.4	3.4	3.7		
3.1	3.2	3.0		2..9		↑
	2.8		2.7			2.8
2.6					2.5	

Figure 4.6 The offspring inherit random subsets of telomeres from both male and hermaphrodite parents

A) Telomere Southern blots from genomic DNA of asynchronous populations of offspring resulting from crosses involving *exo-1(tm1842)* and *mrt-1(tm1354)* animals grown at 20°C. The membrane was probed with DIG-labelled $(TTAGGC)_4$ oligos. The *exo-1* with * is the parent strain. B) The quantification of telomere length of offspring resulting from crosses *exo-1(tm1842)* and *mrt-1(tm1354)*. The tables summarising TRF size quantification of the strongest telomeric signal (peak size, mode) using ImageJ. The numbers in the table indicate the size of the peaked signals (kb). The arrows in the table indicate the telomere signal smear range.

4.3 Discussion

4.3.1 The *mrt-1* mutants and alternative telomere measuring method contribute to the understanding of telomere inheritance

In this chapter, we have presented a comprehensive summary of our TRF analysis results and have put forward a hypothesis to explain how telomere lengths are inherited in *C. elegans* offspring. We discovered that the distinct telomeric signal pattern of *mrt-1* mutants, characterised by sharp bands from TRF assay, may bypass the limitation of the smear telomere signal pattern and overshadowing weak/short telomere signals by strong/long telomere signals. Our results strongly support the hypothesis that telomere length inheritance is a stochastic process in *C. elegans*, resulting from both males and hermaphrodites.

However, it is essential to acknowledge that our telomere measuring method are only limited to terminal restriction fragment (TRF) analysis and TRF Southern blot. While TRF Southern blotting offers several advantages, such as the ability to measure absolute length of telomere restriction fragments, high sensitivity of fragments detection, and good correlation and agreement (Kimura et al. 2010; Lai, Wright, and Shay 2018; Tarik et al. 2018; Behrens et al. 2017). Even though the TRF by Southern blot analysis is considered the gold standard in telomere length measurement (Behrens et al. 2017), certain drawbacks still remain. For instance, it is time-consuming, expensive, and requires large amounts of DNA. Importantly, there are limitations in measuring only the absolute average telomere length of the entire cell population, which may lead to overestimation of telomere lengths (Behrens et al. 2017; Tarik et al. 2018). Additionally, the TRF Southern blot technique may not be capable of visualising the very short telomeres and chromosome ends that lack telomeres (Lai, Wright, and Shay 2018), which poses limitations for our study of telomere length inheritance. Furthermore, the presence of long telomeres can result in higher signal levels during visualisation, potentially overshadowing signals from shorter telomeres. Given these considerations, TRF Southern

blotting may not be the optimal choice for investigating telomere length inheritance in *C. elegans*.

There are alternative methods or techniques available for telomere length measurement. (1) PCR-based techniques, including quantitative PCR (qPCR) (Aviv et al. 2011; Elbers et al. 2014; Cawthon 2002; O'Callaghan and Fenech 2011; Cawthon 2009; Lindrose et al. 2021; Lin et al. 2019), Single Telomere Length Analysis (STELA) (Bendix et al. 2010; A. J. Sfeir et al. 2005; Baird et al. 2003), and Telomere Shortest Length Assay (TeSLA) (Lai et al. 2017). (2) Techniques based on fluorescence *in situ* hybridization (FISH), including Quantitative fluorescence *in situ* hybridization (Q-FISH) and fluorescent *in situ* hybridization with flow cytometry (Flow-FISH) (Poon and Lansdorp 2001; Poon et al. 1999; Alter et al. 2007; Baerlocher and Lansdorp 2003; Lansdorp et al. 1996; Canela et al. 2007; Slijepcevic 2001; Rufer et al. 1998; Baerlocher et al. 2006; Baerlocher and Lansdorp 2004). (3) Sequencing-based techniques, including whole-genome sequencing (WGS) (Farmery et al. 2018; Lee et al. 2017; Nersisyan and Arakelyan 2015) and nanopore DNA sequencing (Smoom et al. 2023; Chalapati et al. 2021; Tan et al. 2022; Sholes et al. 2022; Tham et al. 2023). However, most of the methods display various disadvantages for appliance in both average and short telomere length measurement.

It is worth noting that nanopore DNA sequencing is most superior among all the methods. The MinION platform from Oxford Nanopore Technologies offers a unique approach to sequencing by passing single strands of DNA through a layer of biological nanopore sensors. This method can sequence short, single-strand oligonucleotides directly without amplification or second-strand synthesis, even though the protocol recommends using double strand DNA as templates. It is worth noting that oligo-nucleotides with a free 3'-OH can also be successfully sequenced using this method (Chalapati et al. 2021). Nanopore DNA sequencing technique is considered the most promising approach for quantitative, high-resolution telomere length measurement, including the measurement of ssDNA overhangs. Several studies have already demonstrated telomere length measurement using nanopore sequencing on samples from human blood (Arnqvist 2011), the yeast *S. cerevisiae* (Sholes et al. 2022), and mice (Smoom et al. 2023). For our study of telomere length inheritance in *C. elegans*, the observations we mentioned above may be further confirmed with the application of Nanopore DNA sequencing. The method makes the measurements possibly suitable for high throughput quantifications. It can also provide valuable insights into measuring the length of ssDNA overhangs to help identify the ssDNA-binding functions of POT proteins as we discussed in chapter 3. Future

studies in the lab may benefit from nanopore DNA sequencing with further optimisation and experimentation.

4.3.2 The telomere length inheritance of progeny is attributed to heterozygosity

In this chapter, we have explored the inheritance of telomere length in *C. elegans*, and our findings challenge the traditional maternal or paternal inheritance observed in humans and birds. Both male and hermaphrodite contribute to the telomere length of offspring. However, the precise inheritance mechanism remains elusive. Based on our results and observations, two plausible theories emerge: 1) offspring inherit telomere from both male and hermaphrodite, resulting in telomeres displaying both lengths. This theory aligns with our observations of offspring inheriting telomeres from both parents, as evidenced by the broad range of telomere signals in the crosses we conducted. 2) the offspring may reset and restore their telomere length based on genetic factors. This theory suggests that the offspring do not simply inherit telomere length from their parents but actively manage their telomeres during development.

Studies in humans point toward both maternal inheritance (Broer et al. 2013; Eisenberg 2014; Asghar et al. 2015) and paternal inheritance within a limited number of cases (Nordfjäll et al. 2005; 2010; Njajou et al. 2007). The paternal effect is also seen in other animals like the sand lizard (Olsson et al. 2011). On the contrary, in birds, maternal effects play a more important role in telomere length inheritance (Horn et al. 2011; Asghar et al. 2015; Reichert et al. 2015). These differences could be attributed to the sex chromosomes (XX/XY in humans and ZW/ZZ in birds). In *C. elegans*, with its XX/XO sex chromosome system for hermaphrodites and males, presents a unique scenario that could facilitate unbiased telomere inheritance, as observed in our study.

Heterozygosity, defined as both parents contribute to the offspring's cells, aligns with most of our observations. The broader range of telomere smear in the crosses involving *pot* strains suggests that offspring tends to inherit telomeres at a length similar to their wildtype parents. However, it is essential to acknowledge that the limitation of TRF for detecting short telomeres may not definitively confirm the theory. As discussed in Section 4.3.1, the application of nanopore sequencing method could provide a more accurate assessment. Further evidence supporting heterozygosity is seen in the cross of *mrt-1* and *exo-1*, where offspring showed telomere lengths representing both *exo-1* and *mrt-1*. A similar phenomenon, known as telomere

length dimorphism, has been observed in the Tasmanian devil (*Sarcophilus harrisii*). In that study, the X chromosome consistently had short telomeres while the Y chromosome had long telomeres, suggesting that telomere length was mixed at fertilisation and maintained through somatic development in offspring (Bender et al. 2012).

On the other hand, the concept of telomere resetting, observed in mice and cattle in previous research, indicates that telomeres undergo a reset during early embryogenesis, which is telomerase-dependent (Schaetzlein et al. 2004). The telomere length resetting was also observed in yeast. The average telomere length of the zygotes resulting from long telomere and wildtype telomere cross were of wildtype length (Teixeira et al. 2004). However, the offspring resulting from the cross of *pot-2* mutants and N2 shows homogenous telomere lengths. This may support that there is no telomere resetting in *C. elegans*. The lack of rapid telomere length resetting observed in *C. elegans*, compared to yeast, may be attributed to several factors. 1)The sample of yeast came from populations of late generations. For enough amount of Southern blot materials, yeast need to grow approximately 20 generations while worms only need approximately two generations. 2) The absolute telomere length is different between yeast (approximately 300 bp in wildtype strains and approximately 2000 bp in long telomere strains such as *rif2*) and *C. elegans* (approximately 2-9 kb in wildtype strains while >20 kb in long telomere strains like *pot-2*). The short absolute length in yeast and relatively more generations required for Southern blot sample magnify the telomere shortening or resetting in yeast. The limited generations we observed may be the reason why we did not observe shortening.

In conclusion, our study sheds light on the complex and unique nature of telomere length inheritance in *C. elegans*, where both male and hermaphrodite contributions play significant roles. While our findings strongly suggest an unbiased telomere inheritance theory, further research, particularly using nanopore sequencing or other advanced techniques, is needed to provide a more understanding of this theory. However, *C. elegans* may not be the perfect model for telomere inheritance study in nematodes. In the future study of telomere inheritance in nematodes, nematodes with different types of sex determination should be included, such as *Rhabditis* sp. SB347 who have males, females and hermaphrodites (Tischler et al. 2006).

4.3.3 The telomere length homeostasis fits in protein-counting model

In our study, we investigated the intriguing phenomenon of telomere length homeostasis in *C. elegans*, particularly in cases where the telomere length did not align with the genotype.

For instance, we observed wildtype strains with initially long telomeres (approximately 20 kbp) maintained their length, while one *pot-2* strain with initially short telomere (approximately 5 kbp) elongated to match the typical *pot-2* length within a short period time (by the 8th generation). This suggests that *C. elegans* possesses a mechanism that recognises and rectifies short telomeres but does not seem to apply the same mechanism to longer telomeres.

The presence of this *pot-2* strain with wildtype telomeres may be attributed to that offspring inherit telomeres randomly from the parents. It is possible that the *pot-2* parent possess wildtype length telomeres which were shadowed by the signals from other long telomeres in the TRF assay. Then, during cross-fertilisation, these wildtype length telomeres were the only telomeres inherited from the *pot-2* parent, while the other telomeres were inherited from the wildtype parent. Despite the low probability of this scenario, it remains a viable possibility. The low possibility is consistent with the occurrence of the only one *pot-2* strain with short telomere out of 25 *pot-2* strains tested.

Our findings strongly suggest that the telomere length homeostasis in *C. elegans* is genotype dependent. Previous studies have proposed models to explain how telomere length homeostasis is maintained. One of these models is the protein counting model. This model is originally based on the idea that a specific number of telomere-binding proteins is required to block telomerase access to telomeres in yeast. In this model, longer telomeres exhibit stronger repression of telomerase due to the higher number of telomere-binding proteins (Marcand, Gilson, and Shore 1997). This model was adopted in the studies of mammalian telomere regulation, especially focusing on telomere-binding proteins, such as TRF1, TRF2, POT1, and TIN2 (Ye and De Lange 2004; Takai et al. 2010a; Diotti and Loayza 2011; Steensel and Lange 1997; Loayza and De Lange 2003). In this model, telomerase has preference for elongating shorter telomeres over longer ones, which is consistent with our results. In our study, the wildtype length telomeres in *pot-2* mutants were recognised as “shorter telomeres” and elongated in a short amount of time. However, it is important to note that our results differ from observations in yeast, where over-elongated telomeres experience a progressive and constant loss of telomeric DNA, approaching wildtype length (Marcand, Brevet, and Gilson 1999). This contrast is evident in the stable, long telomere length we observed in successive generations of wildtype worms. In the previous study, individual wildtype (N2) clones which have heterogenous telomere lengths remain relatively constant (Raices et al. 2005). The rapid telomere deletion is an event where elongated telomeres quickly return to wildtype length, found in yeast (Li and Lustig 1996). Similarly, short outlying telomeres were observed as a

product of rapid telomere deletion (Cheung et al. 2004). *trt-1*, a telomerase deficient strain, displays higher frequency of short outlying telomeres relative to wildtype, suggesting that telomerase is required to prevent or repair sporadic telomere truncations (Cheung et al. 2006b). In our study, the lack of rapid telomere deletions in long telomere wildtype strains may be attributed to the abundance of telomerase in wildtype worms.

Another model suggests that telomerase switches between extendible and non-extendible states to achieve telomere length homeostasis. In *S. cerevisiae*, telomerase does not activate in every cell cycle, and it displays a preference for shorter telomeres. Moreover, the number of nucleotides added to end of telomere varies between cell cycles, and the adding is telomere length-independent (Teixeira et al. 2004). Short telomeres are more likely to be extended, which may explain the observations that the short-telomere length *pot-2* mutants underwent rapid telomere elongation (from 2^{nd} to 8^{th}) back to the classic telomere length of *pot-2* mutant. Studies of cancer cells revealed that telomere length homeostasis may also be attributed to limiting amounts of telomerase, explaining the short telomeres in telomerase positive cancer (Cristofari and Lingner 2006). In our research, the maintenance of long telomere length in wildtype offspring resulting from crosses could be explained by the abundance of telomerase.

A more recent model, the replication fork model, was introduced, emphasising the role of origin firing or lagging strand synthesis in regulating telomere length. In this model, telomerase travels with the replication fork. The telomeres can only be elongated when telomerase is deposited at the telomere end. The existence of telomere-binding proteins increases the probability of telomerase dissociating from the traveling replication fork. This model explains both negative regulation of telomere elongation and preferential elongation of short telomeres (Greider 2016). The feedback mechanism in this model successfully explains the rapid telomere length recovery of short-telomere *pot-2* mutants, by the observation that telomere-proximal origin fires more efficiently at short telomeres (Bianchi and Shore 2007). However, this model still does not fully explain the maintenance of long telomere length observed in wildtype worms.

In summary, among all the models, the protein-counting model aligns with our findings the best. While existing models help us understand the regulation of telomere length homeostasis in various organisms, they may not entirely capture the unique features of telomere length homeostasis observed in *C. elegans*. Hopefully, the observations in our study may offer valuable insights into the regulation of telomere length in *C. elegans*.

Chapter 5 : The effects of POT-2 and POT-3 on fertility and telomere maintenance in a telomere replication deficient background

5.1 Introduction

Telomeres are employed to maintain chromosome integrity and genome stability. Therefore, telomere replication is required to compensate for the telomere shortening caused by the incomplete replication of chromosome ends via DNA polymerases. There are several proteins in *C. elegans* that have been found to be essential is this process.

Firstly, telomeres are replenished by telomerase, a ribonucleoprotein composed of the telomerase reverse transcriptase (TERT) and an RNA component (TR) (Greider and Blackburn 1989; Collins 2006). The reverse transcriptase component of telomerase in *C. elegans*, TRT-1, consists of 540 amino acids, which is one of the shortest TERT proteins known (Malik, Burke, and Eickbush 2000). The *trt-1* mutant strain exhibits several distinct phenotypes, including progressive decline in brood size, progressive telomere attrition (an average loss approximately 100 to 150 bp of telomeric DNA per generation), and a high frequency of extremely short telomeres (Cheung et al. 2006a). Interestingly, sterility in *trt-1* mutants is primarily attributed to defects in chromosome segregation rather than telomere erosion or uncapping. Despite the detrimental effects on fertility in later generations, the absence of *trt-1* does not seem to significantly impact the overall lifespan of *C. elegans*. Since approximately 90% of all cells at L1 stage are already post-mitotic, it suggests that *C. elegans* TRT-1 plays a role in proliferative rather than post-mitotic aging (Meier et al. 2006). These findings illustrate the important role of *trt-1* in telomere maintenance and fertility.

Similarly, MRT-1 is also required for telomerase activity and fertility in *C. elegans*. As we mentioned in previous chapters, MRT-1 is another protein binding to telomeric ssDNA besides POT proteins. MRT-1 is a multifaceted protein characterised by an N-terminal OB-fold domain, coupled with a C-terminal SNM1 family nuclease domain. The N-terminal OB-fold domain enables MRT-1 to bind to single-strand DNA, while the C-terminal SNM1 family nuclease domain grants it processive 3'-to-5' exonuclease activity. Similar to *trt-1* mutants, *mrt-1* mutants also display declining brood size and progressive telomere loss, indicating their roles in telomere maintenance. Notably, *mrt-1* mutants exhibit hypersensitivity to UV/TMP but not to ionizing radiation, suggesting a role in promoting DNA inter-strand cross-link (ICL) repair rather than DNA double-strand break repair (Meier et al. 2009).

Another identified *C. elegans* telomere replication protein is MRT-2, encoded by *mrt-2*. *mrt-2* is the *C. elegans* homologue of the *S. pombe rad1* $^{+}$ and *S. cerevisiae RAD17* checkpoint genes, which is conserved from yeast to mammals (Dean, Lian, and O'Donnell 1998; Freire et

al. 1998; Bluyssen et al. 1998). The *mrt-2* mutants have defects in the DNA damage response and double-strain break repair at telomeric regions leading to the accumulation of end-to-end chromosome fusions in later generations (Ahmed and Hodgkin 2000). Similar to *mrt-1* mutants, *mrt-2* mutants also exhibited normal brood sizes at generation F_2, but their brood size gradually declined to the point of sterility, suggesting its essential role in telomere maintenance in *C. elegans* (Ahmed and Hodgkin 2000).

As we presented in chapter 3, POT-2 and POT-3 negatively regulate telomerase activity and suppress the ALT pathway. Therefore, our investigation aimed to determine whether the absence of POT-2 and POT-3 could rescue the progressive telomere shortening and brood size decline associated with telomere replication deficiency. To better understand the role of POT-2 and POT-3 in telomerase-deficient background worms, we investigated the telomere function and fertility intergenerationally through the mutants of POT-2 and/or POT-3 in a *mrt-1* or *trt-1* mutant background. Our results reveal that POT-3 prevents excessive telomere lengthening. Furthermore, our findings highlight the non-identical functions of TRT-1 and MRT-1 in telomere maintenance and fertility.

5.2 Results

5.2.1 Loss of POT-2 or POT-3 increases the number of generations over which *mrt-1* mutant worms remain fertile

Brood size, serving as an indicator of viability and fertility, represents the general fitness of *C. elegans*. *mrt-1* mutants exhibit progressive reduction in progeny and eventual sterility. This is comparable to *trt-1* mutants, which undergo telomere erosion (Meier et al. 2006). Even though telomere erosion may not be the ultimate reason for eventual sterility, it still plays important roles in fertility through resulting in critically short telomeres. In theory, telomere elongation could recover the telomeres from being critically short, thereby rescuing the worms from eventual sterility. As we showed in chapter 3, loss of POT-2 and POT-3 leads to telomere elongation and activation of ALT pathway, suggesting POT-2/3 proteins seem to inhibit telomerase. On the contrary, MRT-1 seems to promote telomerase activity (Meier et al. 2009). We sought to determine whether MRT-1 promote telomerase through its inhibition of POT-2/3. If so, deleting POT-2 and POT-3 in an *mrt-1* background would rescue the telomere loss phenotypes, such as reduced fertility and eventually sterility. To investigate whether the

absence of POT-2 or POT-3 can mitigate the reduced fertility and eventually sterility observed in *mrt-1* mutants, we performed an assay of brood size drop involving *pot-2;mrt-1* and *pot-3;mrt-1* double mutants as well as *pot-2;pot-3;mrt-1* triple mutants. The mutant strains were constructed using standard methods and genotyped by PCR. For the assay of brood size drop, six L1 hermaphrodites were singled onto a 60 mm Petri dish containing *E. coli* OP50 bacteria lawn and kept at 20°C for one week. This is enough time for the worms to go through two generations as they self-fertilise. We kept record of the approximate brood size of every 2 generations and the maximum generation that worms stayed fertile of individual strains, thereby analysing the survival curves of the strains.

We first investigated whether the loss of POT-2 and POT-3 changes the fertility span of the *mrt-1* mutants. Here, we used the term fertility span to indicate the maximum generation that worms stayed fertile, to indicate the long-term fitness of the worms. Our observations revealed that the maximum fertility span of *pot-2;mrt-1* double mutants (60 generations), *pot-3;mrt-1* double mutants (64 generations), and *pot-2;pot-3;mrt-1* triple mutants (60 generations) significantly exceeded that of *mrt-1* mutants (32 generations) (Figure 5.1). Moreover, the progeny numbers indicated that *pot-2;mrt-1* double mutants, *pot-3;mrt-1* double mutants, and *pot-2;pot-3;mrt-1* triple mutants displayed sustained medium (M) or few (F) level of progeny production, while *mrt-1* mutants exhibited a rapid decline to very few (VF) level of progeny production (Figure 5.1). These observations suggest that the loss of POT-2 and POT-3 improve the long-term fitness of the *mrt-1* mutant worms.

To further analyse the differences among all the strains we tested, especially in a more quantifiable and statistical way, we conducted the log-rank test to compare the survival curves of the strains. On average, we find that *mrt-1* strains only remain fertile for 22 generations (Figure 5.1), similar to the results from a previous study (Meier et al. 2009). However, the medium survival generation for *mrt-1* is significantly shorter than *pot-2;mrt-1* double mutants (medium survival = 30, $P<0.0001$), *pot-3;mrt-1* double mutants (medium survival = 32, $P<0.0001$), and *pot-2;pot-3;mrt-1* triple mutants (medium survival = 28, $P = 0.0156$) (Figure 5.1). It suggests that the loss of POT-2 and POT-3 enhances the long-term fertility of the *mrt-1* mutants. Additionally, there were no differences among *pot-2;mrt-1* double mutants, *pot-3;mrt-1* double mutants, and *pot-2;pot-3;mrt-1* triple mutants. It suggests that POT-2 and POT-3 act similarly in regulating the fertility of the *mrt-1* mutants. Collectively, these results strongly suggest that the loss of POT-2 or/and POT-3 similarly extends the span of fertility in *mrt-1* mutants and enhances the general fitness of *mrt-1* mutant worms at a comparable level.

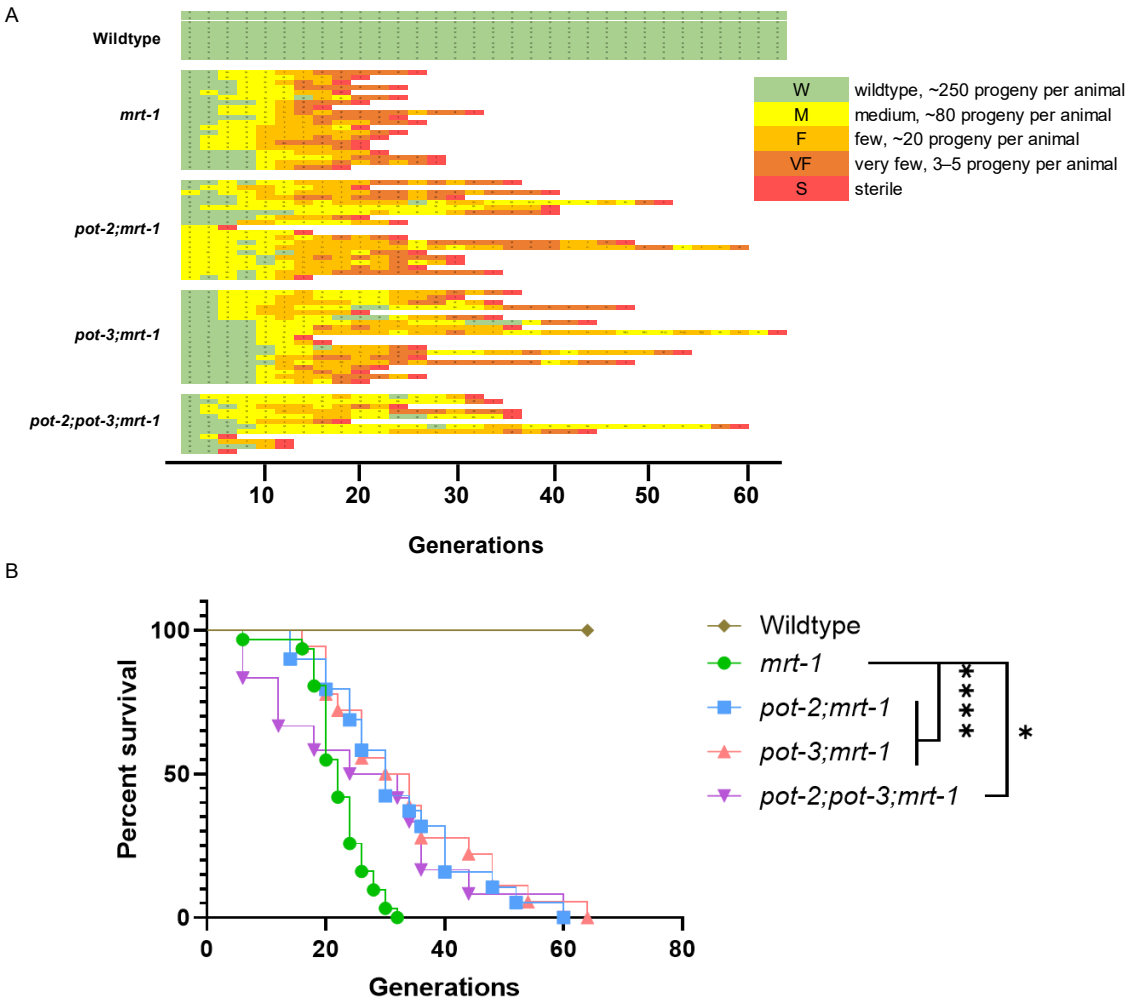

Figure 5.1 Loss of POT-2 and POT-3 improves the long-term fitness of the *mrt-1* mutant worms

Six L1 animals from 10 to 20 homozygous lines of the indicated genotypes were seeded onto plates, grown at 20°C. The brood size was scored after 7 days. A) The assay of brood size drop involving *mrt-1*, *pot-2;mrt-1* double mutants, *pot-3;mrt-1* double mutants, and *pot-2;pot-3;mrt-1* triple mutants. Brood size and sterility are indicated: W, wildtype, around 250 progeny per animal; M, medium, around 80 progeny per animal; F, few, around 20 progeny per animal; VF, very few, about 3–5 progeny per animal; S, sterile. B) The survival curves of *mrt-1*, *pot-2;mrt-1* double mutants, *pot-3;mrt-1* double mutants, and *pot-2;pot-3;mrt-1* triple mutants. * P < 0.05, **** P < 0.0001 (Log-rank test).

5.2.2 Loss of POT-3 causes decrease in telomere length shortening rate in *mrt-1* mutant worms

In *mrt-1* mutants, the rate of telomere shortening closely resembles that of telomerase deficient worms, *trt-1* mutants (Meier et al. 2009). Given that both *pot-3* mutants and *pot-2* mutants exhibit elongated telomere length, we sought to investigate whether the loss of POT-

2 or/and POT-3 could counteract the progressive telomere loss effects induced by the absence of MRT-1.

To elucidate the dynamics of telomere changes across generations resulting from the loss of POT-2 or/and POT-3 in *mrt-1* mutants, we collected samples from different generations and performed TRF Southern blot assays. Following genotype confirmation via PCR, the *pot-2;mrt-1* and *pot-3;mrt-1* double mutants and *pot-2;pot-3;mrt-1* triple mutants animals were collected for genomic DNA extraction, and TRF southern blot assay (Proteinase K digestion). For the *pot-2;mrt-1* and *pot-3;mrt-1* double mutants, samples were collected every 4 or 6 generations, starting from the 2nd generation and continuing until the 26th generation (at which point most of independent strains became sterile). In *S. cerevisiae* telomere replication defective strains, "survivors" typically emerge that maintain their telomeres using homologous recombination (Kironmai and Muniyappa 1997). In *C. elegans*, survivor stains can also be isolated and are defined as those that escape the eventual sterility from a telomerase mutant background (Lackner and Karlseder 2013). Survivor worm strains in our study, if present, were also collected at the 52nd and the 54th generations, which has already shown the delayed sterility. In the case of *pot-2;pot-3;mrt-1* triple mutants, samples were collected in every 4 generations, starting from the 2nd generation and continuing until the 22nd generation (at which point most of the tested strains became sterile). Survivor strains were likewise collected at the 52nd and 54th generations. The telomere signals from various generations were quantified, and telomere shortening rates were calculated based on the size of the telomere signals (telomeric signal peaks within the TRF range) from different generations. Telomere shortening rates were analysed by one-way ANOVA with multiple comparisons via Tukey's test.

In our investigation, we observed that *pot-3;mrt-1* double mutants displayed a small but significant reduced telomere shortening rate (123.8 ± 14.3 bp/generation) compared to that of *mrt-1* mutants (200.2 ± 23.6 bp/generation) (Mean ± SEM, P=0.0425) (Figure 5.2). We also examined the *pot-2;mrt-1* double mutants and *pot-2;pot-3;mrt-1* triple mutants. While both of these strains showed a mild decrease in telomere shortening rates, 172.2 ± 20.1 bp/generation and 156.7 ± 19.5 bp/generation respectively (Mean ± SEM), these reductions were not statistically significant compared to *mrt-1* mutants alone (P=0.7234 and 0.6169 respectively) (Figure 5.2). It suggests that loss of POT-3, but not POT-2, decelerates the telomere shortening in *mrt-1* mutants. However, we cannot exclude the possibility that POT-2 also plays a role in decelerating the telomere shortening in *mrt-1* mutants due to the limited number of samples.

Despite this, it is possible to say that POT-3 has a stronger effect on decelerating the telomere shortening in *mrt-1* mutants compared to POT-2.

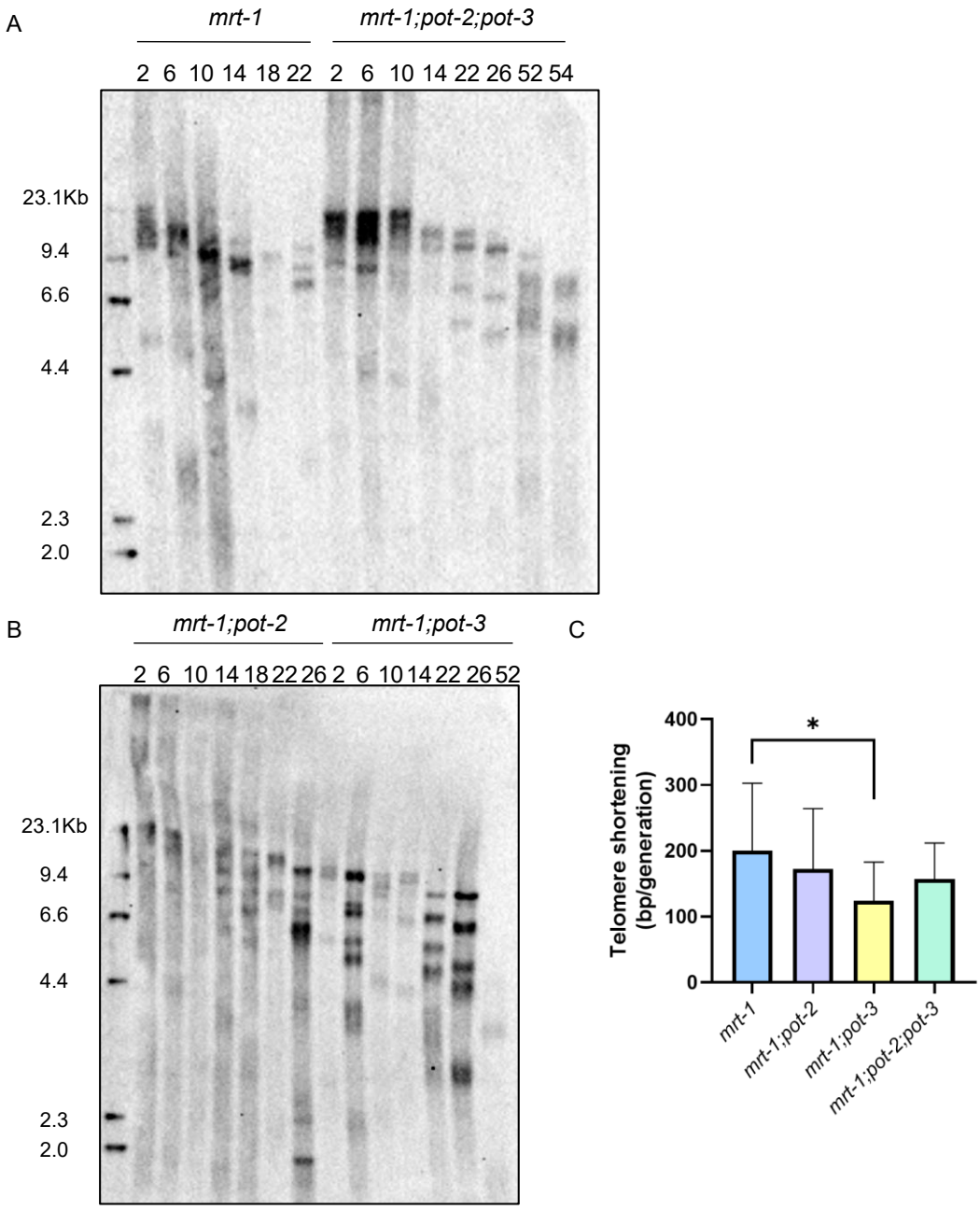

Figure 5.2 Loss of POT-3, but not POT-2, decelerates the telomere shortening in *mrt-1* mutants

A) Telomere Southern blots from genomic DNA of populations of *mrt-1* and *pot-2;pot-3;mrt-1* triple mutants animals grown at 20°C. *mrt-1* samples were collected from the 2nd, 6th, 10th,14th 18th,and 22nd generation. *pot-2;pot-3;mrt-1* triple mutants were collected from the 2nd, 6th, 10th,14th, 22nd, 26th, 52nd, and 54th generation. The membrane was probed with DIG-labelled $(TTAGGC)_4$ oligos. B) Telomere Southern blots from genomic DNA of populations of *pot-2;mrt-1* double mutants and *pot-3;mrt-1* double mutants animals grown at 20°C. *pot-2;mrt-1* double mutants samples were collected from the 2nd, 6th, 10th,14th 18th,22nd and 26th generation. *pot-2;mrt-1* double mutants were collected from the 2nd, 6th, 10th,14th, 22nd, 26th, and 52nd generation.

The membrane was probed with DIG-labelled $(TTAGGC)_4$ oligos. C) Statistical analysis of the telomere shortening rate in *mrt-1*, *pot-2;mrt-1* double mutants, *pot-3;mrt-1* double mutants, and *pot-2;pot-3;mrt-1* triple mutants. The telomere shortening rate indicates the mean of individual telomere shortening rate measurements over indicated generations. Error bars show SEM. *P<0.05 (One-way ANOVA, Tukey's multiple comparisons test).

At this point, we wanted to test the recombination level because, as we observed in chapter 3, loss of POT-2 or POT-3 leads to the activation of ALT. As the C-circle level represents the potential ALT activation level, we sought to determine whether the C-circle level changes resulting from the loss of POT-2 or/and POT-3 can be expanded to the *mrt-1* background strains. We conducted C-circle assays as described in Section 2.2.1 with genomic DNA obtained from the same generations as we did for Southern blot. However, the data was deemed not of good enough quality because the standard deviation of C-circle signals was considerable, and no discernible consistent pattern of change emerged (shown in appendix, Figure AP.2). These results suggest that the C-circle level lacks a stable, predictable changing pattern. Therefore, in the following study, we did not further test the C-circle level changes.

5.2.3 Loss of POT-2 or POT-3 does not promote the fertility of *trt-1* mutant worms

It has been established that MRT-1 plays an important role in telomerase activity *in vivo*, and functions in the same pathway as TRT-1 for telomere replication (Meier et al. 2009). Therefore, we wondered whether the loss of POT-2 and POT-3 would have a similar effect on a telomerase deficient strain, *trt-1(ok410)*. To assess this, we performed the assay of brood size drop with the *pot-2;trt-1* and *pot-3;trt-1* double mutants. It is worth noting that obtaining fertile *trt-1* mutant males is a challenging task due to their low occurrence after heat-shocking. Consequently, we constructed the cross using *pot-3* mutant and *pot-2* mutant male worms, which were obtained through heat-shocking at 32°C for 5-6 hours, along with *trt-1* mutant hermaphrodites L4 worms. Confirmation of the resulting *pot-2;trt-1* and *pot-3;trt-1* double mutants was achieved by PCR genotyping.

For the assay of brood size drop, we individually placed six L1 hermaphrodites onto a 60 mm Petri dish with *E. coli* OP50 bacteria lawn, maintaining them 20°C over the course of one week to allow the worms to self-fertilise and reproduce. We recorded the number of progenies each week and assessed brood size level as described in Section 2.4.2.

Our observations revealed a progressive reduction in progeny in *trt-1* mutants consistent with prior studies. However, we also noted the presence of a small number of survivors in our assay (6.25%, 1 in 16 strains observed, one of 2 surviving strains in Figure 5.3 became sterile at 76th generation, data not shown) (Figure 5.3). Long-term *trt-1* survivors are rare (Meier et al. 2006) but have been observed in previous studies (Lackner et al. 2012).

Additionally, comparable amounts of survivors were observed in *pot-2;trt-1* and *pot-3;trt-1* double mutants to *trt-1* mutant (5% and 5.3% respectively) (Figure 5.3). This indicates that the absence of POT-2 or POT-3 did not affect the longest generations in which the worms remained fertile in the *trt-1* mutants. However, the loss of POT-2 or POT-3 led to a better long-term health condition in the *trt-1* mutants (Figure 5.3). The progeny numbers indicated that *pot-2;trt-1* double mutants and *pot-3;trt-1* double mutants displayed sustained wildtype (W) level of progeny production, while *trt-1* mutants exhibited a rapid decline to medium (M) or very few (VF) progeny. Notably, *trt-1* mutants displayed a higher number (18.75% of observed strains) of sterile strains in early generations (those younger than the 10th generation) compared to the *pot-2;trt-1* and *pot-3;trt-1* double mutants (none observed) (Figure 5.3). These observations suggest that the loss of POT-2 or POT-3 improves the general fitness of the *trt-1* mutant worms but does not affect the maximum fertility span.

To further analyse the differences of fertility spans among all the *trt-1* background strains we tested, we conducted the log-rank test to compare the survival curves of the strains. Surprisingly, both *pot-2;trt-1* and *pot-3;trt-1* double mutants exhibited similar levels of progeny level and fertility span to *trt-1* mutant (Figure 5.3). The medium survival generation for *trt-1* is 24 generations, similar to the average survival generation in previous studies (20 to 26 generations) (Meier et al. 2009). Similarly, the medium survival generation for *trt-1* was comparable to those of *pot-2;trt-1* double mutants (medium survival = 26, P=0.8563), and *pot-3;trt-1* double mutants (medium survival = 26, P=0.9220) (Figure 5.3). These results suggest that loss of POT-2 or POT-3 does not alter the fertility span of *trt-1* mutant background worms. Taken together, these results indicate that the loss of POT-2 or POT-3 does not significantly alter the fertility span of *trt-1* mutant background worms, but it does strengthen the health condition of individual worms at early generations.

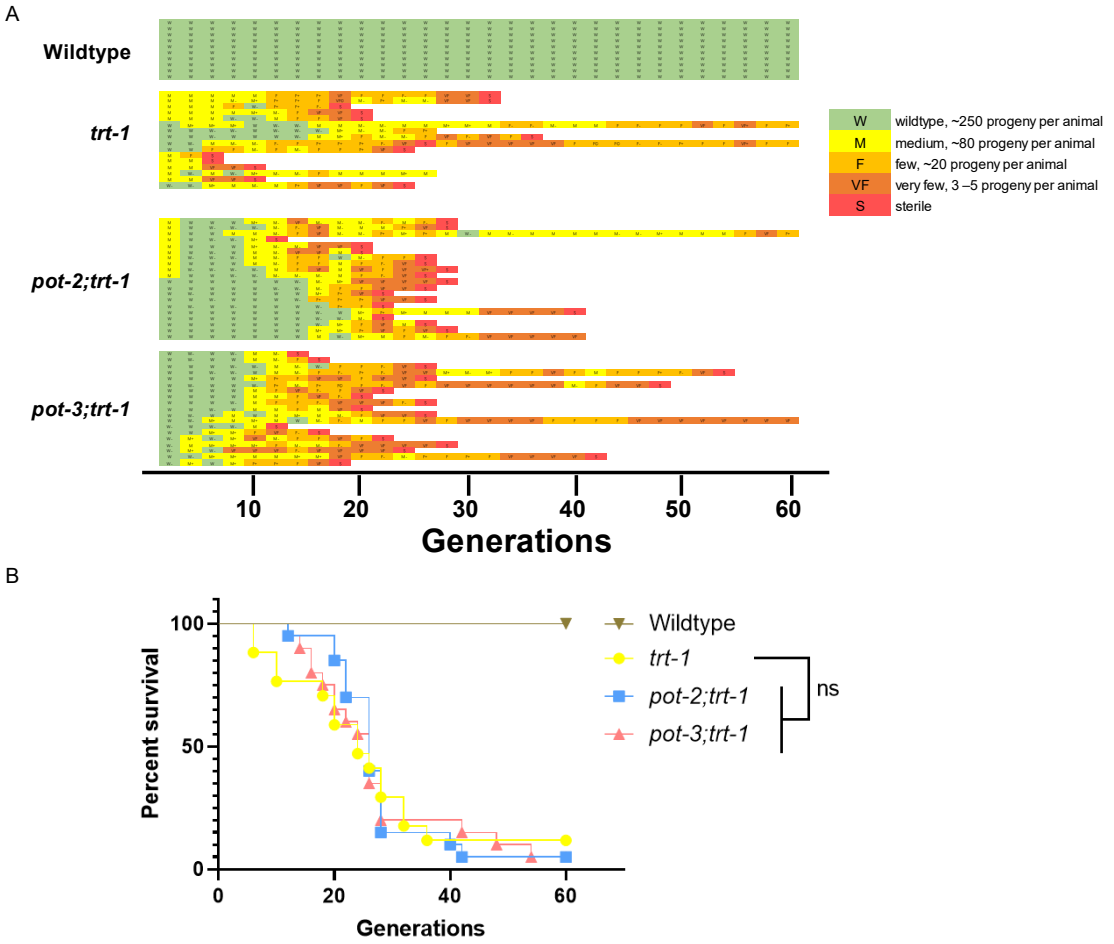

Figure 5.3 Loss of POT-2 and POT-3 does not improve the long-term fitness of the *trt-1* mutant worms

Six L1 animals from 10 to 20 homozygous lines of the indicated genotypes were seeded on to the plates, grown at 20°C. The brood size was scored after 7 days. A) The assay of brood size drop involving *trt-1*, *pot-2;trt-1* double mutants, and *pot-3;trt-1* double mutants. Brood size and sterility are indicated: W, wild-type, around 250 progeny per animal; M, medium, around 80 progeny per animal; F, few, around 20 progeny per animal; VF, very few, about 3–5 progeny per animal; S, sterile. B) The survival curves of *trt-1*, *pot-2;trt-1* double mutants, and *pot-3;trt-1* double mutants. ns= not significant (Log-rank test).

5.2.4 Loss of POT-2 or POT-3 causes a decrease in telomere length shortening rate in *trt-1* mutant worms

While the absence of POT-2 or POT-3 does not change the fertility span of *trt-1* mutant background worms, we sought to investigate whether the alterations in telomere length might be influencing these findings. To explore the telomere dynamics resulting from loss of POT-2 or POT-3 in *trt-1* mutants across generations, we conducted TRF Southern blot assay. After confirming the genotype with PCR, we collected genomic DNA samples from different generations of *pot-2;trt-1* and *pot-3;trt-1* double mutants. The *pot-2;trt-1* and *pot-3;trt-1*

double mutants population were collected in every 6 generations, spanning from the 2nd generation to the 26th generation (most of tested strains became sterile). We also collected survivors, if any, at the 52nd generation. The telomere signals from these various generations were quantified and the telomere shortening rates were calculated based on the sizes of the telomere signals from different generations. The telomere shortening rates were analysed using one-way ANOVA with multiple comparisons employing Tukey's test.

Interestingly, we found that the telomere shortening rate in *trt-1* mutants is 231.0 ± 46.7 bp/generation (Mean ± SEM), similar to what we observed *mrt-1* mutants (Figure 5.4). This telomere shortening rate is higher than that from previous study (125.6 ±17.5 bp/generation) (Meier et al. 2006). This higher telomere shortening rate in our study may attribute to the longer initial telomere length. Surprisingly, the *pot-2;trt-1* and *pot-3;trt-1* double mutants displayed a significant reduction in telomere shortening rates, 145.2 ± 16.2 and 134.6 ± 13.2 bp/generation respectively (Mean ± SEM, P=0.0384 and 0.0148 respectively) (Figure 5.4). These results suggest that loss of POT-2 and POT-3 decelerates telomere shortening in *trt-1* background worms.

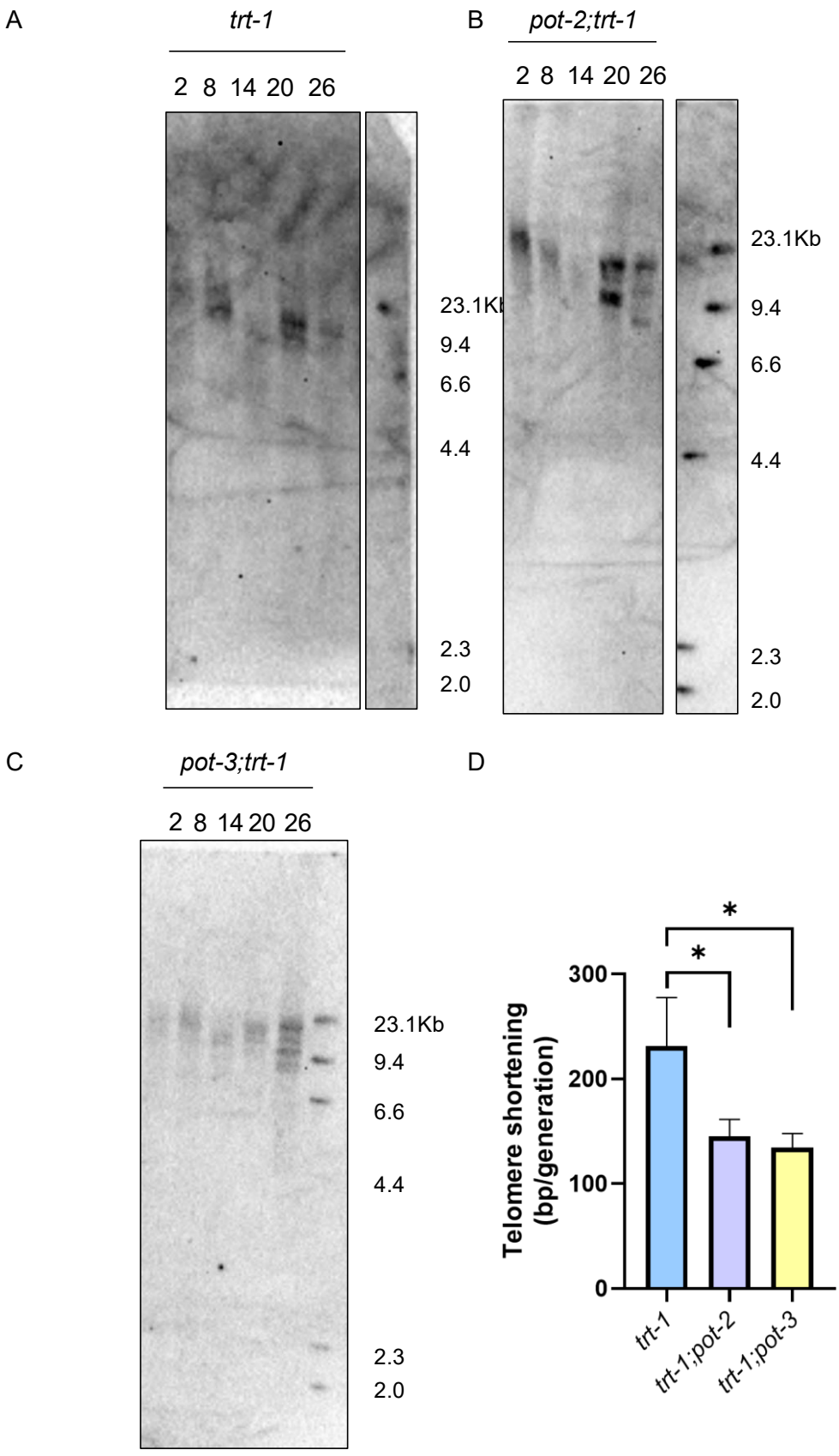

Figure 5.4 Loss of POT-2 and POT-3 decelerates telomere shortening in *trt-1* background worms

A) Telomere Southern blots from genomic DNA of populations of *trt-1* mutants. B) Telomere

Southern blots from genomic DNA of populations of *pot-2;trt-1* double mutants. C) Telomere Southern blots from genomic DNA of populations of *pot-3;trt-1* double mutants. Worms were kept at 20°C. Samples were collected from the 2nd, 8th,14th 20th,and 26th generation. The membrane was probed with DIG-labelled $(TTAGGC)_4$ oligos. D)Statistical analysis of the telomere shortening rate in *trt-1*, *pot-2;trt-1* double mutants, and *pot-3;trt-1* double mutants. The telomere shortening rate indicates the mean of individual telomere shortening rate measurements over indicated generations. Error bars show SEM. *P<0.05 (One-way ANOVA, Tukey's multiple comparisons test).

5.2.5 MRT-1 and TRT-1 behave differently in *exo-1* background

Based on the findings presented in this chapter, even though the loss of POT-3 has been observed to reduce the telomere shortening rate in both *mrt-1* and *trt-1* background worms, the *mrt-1* and *trt-1* strains acted differently in fertility and telomere shortening in response to loss of POT-2 and POT-3. This intriguing result could be attributed to the absence of specific exonuclease activity in *trt-1* compared to *mrt-1*. Exo1 is a protein functioning with 5' to 3' exonuclease activity (Tran et al. 2004). It has been reported that the Exo1 can accelerate the telomere shortening via its interaction with telomeric repeat-containing RNA (TERRA) in *S. cerevisiae* (Pfeiffer and Lingner 2012). In *C. elegans*, EXO-1 was identified as a 5′ to 3′ nuclease to be involved in DSB repair (Yin and Smolikove 2013). Given that MRT-1 possesses 3' to 5' exonuclease activity, we embarked on an investigation to determine whether *mrt-1;exo-1* double mutants and *trt-1;exo-1* are viable.

To assess the viability of these mutant strains, we constructed the double mutant involving *mrt-1(tm1354), trt-1(ok410),* and *exo-1(tm1842)*. We attempted crosses with both *trt-1* males crossing with *exo-1* hermaphrodites or *exo-1* males crossing with *trt-1* hermaphrodites. We were unable to obtain a single *trt-1;exo-1* double mutants among the more than 160 F_2 worms examined. The probability of finding at least one double mutant from 160 F_2 worms was over 99.99%. Conversely, we successfully obtained *mrt-1;exo-1* double mutants at the expected Mendelian ratios (3 in 48 F_2 worms examined – 95% probability of at least one double mutant among 48 F_2 worms). These results indicate that *trt-1;exo-1* double mutants are either inviable or, at the very least, quite sick. Interestingly a *trt-1; exo-1* double mutant strain has been reported before by the lab of Prof. S Ahamed (Longtine, Frenk, and Ahmed 2018). However, this strain was made via a three-factor cross using a balancer chromosome (Prof. S Ahmed, personal communication). This is consistent with our observations that (in contrast to *mrt-1;exo-1)* a *trt-1; exo-1* double mutant strain is not made at the normal Mendelian ratios. This intriguing finding suggests that despite both MRT-1 and TRT-1 being involved in the

telomerase pathway, they play distinct roles in the viability of *C. elegans* with defective exonuclease activity.

5.3 Discussion

5.3.1 The loss of POT-2 or POT-3 cannot rescue the eventual sterility of *mrt-1* mutants or *trt-1* mutants

In this chapter, we explore the influence of POT-2 and POT-3 loss on fertility in *mrt-1* and *trt-1* mutant backgrounds. Notably, *pot-2* mutants and *pot-3* single mutants exhibit longer telomeres compared to wildtype worms and maintain stable brood size over generations without observable reduction in lifespan. Interestingly, loss of POT-2 and POT-3 can significantly elongate the fertility span of *mrt-1* mutant worms while having no effect on *trt-1* mutants. However, the loss of POT-2 and POT-3 cannot rescue the eventual sterility in either mutant background.

It is crucial to note that telomere length has no effect on lifespan in *C. elegans*. Telomere length is believed to have inevitable effects on limiting lifespan, given its role as one of the markers of biological age in various organisms (Vaiserman and Krasnienkov 2021). In *trt-1* mutants, unchanged lifespan regardless of telomere length (whether long or short) and eventual sterility suggest that neither telomere length nor TRT-1 affects postmitotic aging of the soma, even though it is clear that proliferative immortality of the germline is compromised (Meier et al. 2006). Moreover, no difference in lifespan was observed between wildtype *C. elegans* strains and *trt-1* mutants (Meier et al. 2006). This was also indicated by the study of uncoupling lifespan and telomere length in *C. elegans* (Raices et al. 2005). In our study, the telomere shortening rates in *mrt-1* and *trt-1* mutants are comparable to those in previous studies, implying the similar disconnections between telomere length and lifespan. Therefore, the lifespan of these mutants cannot serve as an indicator for the influence of telomere length changes.

On the other hand, telomere length does impact the proliferative immortality of the germline (Meier et al. 2006). In the previous research of *C. elegans trt-1* mutants, apoptosis level were not increased to levels that would induce sterility, but some phenotypes of mitotic failure were observed (Meier et al. 2006). Various phenotypes of chromosome mis-segregation and/or mitotic failure, such as chromosome fusions, protruding vulva, uncoordinated

neuromuscular defects, and occasional slow growth were detected in sterile *trt-1* mutants. These phenotypes were suggested to be the important cause of sterility (Meier et al. 2006). Therefore, in our study, we focused on examining the fertility of *mrt-1* or *trt-1* background mutants as a key parameter to represent the important role of POT-2 or POT-3 in telomere regulation, rather than lifespan.

Our investigation primarily focused on the maximum generation that worms stay fertile (fertility span) as an indicator of the effects caused by telomere shortening over multiple generations. Our findings revealed that the processive sterility was not rescued in *mrt-1* background strains or in *trt-1* background strains when POT-2 or POT-3 was absent. Surprisingly, only the fertility span of *pot-2;mrt-1* and *pot-3;mrt-1* double mutants exhibited an extension compared to *mrt-1* mutants, while the fertility span of *pot-3;trt-1* double mutants and *pot-2;trt-1* double mutants displayed no significant differences compared to *trt-1* mutants. This suggests that the loss of POT-2 and POT-3 play a similar role in partially rescuing the sterility of *mrt-1* mutants, not *trt-1* mutants, with both double mutants exhibiting similar fertility spans rather than demonstrating additive or synergistic effects.

Similarly, in the study of CeOB2 in *C. elegans*, which corresponds to POT-1, the vast majority *trt-1* mutants and *trt-1;ceob2* double mutants lines eventually became sterile, while *trt-1;ceob2* double mutant displayed increased frequency of survivor formation without telomere maintenance compared to *trt-1* mutants (Lackner et al. 2012), which is consistent with our findings of *pot-2* and *pot-3* in *trt-1* background mutants. As mentioned above, the survivor strain of *trt-1* mutants may be attributed to the longer initial telomere length. The survivor strains may inherit longer telomeres from parents, and it may have taken them more time for them to achieve the threshold for cell crisis and sterility.

Additionally, in mammalian studies, shortened telomeres result in an increased the possibility of phenotypes that lead to abnormal germ cells, such as meiotic arrest, segregation abnormalities, and dysjunction (Maser and DePinho 2002). Successive telomere shortening in somatic cells induces senescence both *in vitro* and *in vivo*, while shortened telomeres in male and female germ cells result in germ cell apoptosis and meiotic arrest, respectively (Rodriguez-Brenes and Peskin 2010; Xu et al. 2013). These findings may provide a potential explanation for the mechanism of processive sterility in *C. elegans*, which could be attributed to abnormal germ cells. Further research is needed to confirm these theories and delve deeper into the mechanisms for fertility in telomerase deficient worms.

5.3.2 TRT-1 does not act identically to MRT-1 in telomere maintenance

In our primary experiment, we sought to investigate our hypothesis by constructing crosses between *mrt-1;exo-1* double mutants and the *trt-1;exo-1* double mutants. We successfully obtained *mrt-1;exo-1* double mutants but failed to obtain the *trt-1;exo-1* double mutants. Notably, *trt-1;exo-1* double mutants were previously reported by Ahmed's lab (Longtine, Frenk, and Ahmed 2018), but these mutants were achieved by introducing three marker mutations to balance *trt-1* and *exo-1* (personal communication). Interestingly, the *trt-1;exo-1* double mutants obtained in that study maintained their fertility for a longer duration than *trt-1* mutants and exhibited a high frequency of ALT under crowded conditions (Longtine, Frenk, and Ahmed 2018). The variations in the effort required to construct double mutant *mrt-1;exo-1* and *trt-1;exo-1*, highlight the distinctions in fertility and viability regulation between *mrt-1* and *trt-1* backgrounds.

In the study of MRT-1, it was initially considered to act in the same pathway as TRT-1 in regulating telomere length. MRT-1 is the only POT1 homolog that is essential for telomere-repeat addition by telomerase in *C. elegans*. The *mrt-1* mutants display telomere-erosion phenotypes that are indistinguishable from those of telomerase reverse transcriptase mutants such as *trt-1* and *mrt-2* (Meier et al. 2009). The similarities in telomere shortening rates are also observed in our study. However, the responses to the loss of POT-2 and POT-3 differ between *mrt-1* and *trt-1* mutant worms.

MRT-1 is a dual-domain protein with homology to the human POT1 and to the nuclease domain of the SNM1 family of proteins. Some MRT-1 homologs in other species are also employed in telomere maintenance. In humans, Apollo does have clear telomeric phenotypes, but complete knockout causes rapid telomere shortening. Patients with point mutations in Apollo also show telomere fragility and clinical phenotypes linked to telomere dysfunction such as bone marrow failure (Kermasson et al. 2022). Curiously, human Apollo also lacks an OB-fold, but it does have a domain that binds TRF2 protein with which targets to telomeres (van Overbeek and de Lange 2006). On the contrary, in budding yeast, Pso2p appears to have no telomeric phenotypes (Munari et al. 2013). Pso2p also lacks the OB fold domain found in MRT-1. These suggest that the OB-fold of *C. elegans* MRT-1 is the telomere targeting domain, which is consistent with the preference for telomeric ssDNA shown in the previous study (Meier et al. 2009).

It is worth noting that the strains used for measuring telomere shortening rate in the research described previously, *trt-1(yp2)* and *trt-1(e2661)*, differ from the strain we used, *trt-1(tm1354)* (*trt-1(tm1354)* was also used, but did not show the actual telomere shortening rate). Consequently, the telomere shortening rate may be slightly different between these strains, *trt-1(yp2)* (106 ± 35 bp/generation, Mean ± SD), *trt-1(e2661)* (114 ± 26 bp/generation, Mean ± SD) (Meier et al. 2009), and *trt-1(tm1354)* (200.2 ± 23.58 bp/generation, Mean ± SEM) in our study, respectively. These differences could be attributed to the initial telomere length in each strain. In our research, we calculated the telomere shortening rate based on the isogeneic *trt-1* mutant resulting from the crosses between *pot-2* and *trt-1* or *pot-3* and *trt-1*, which possessed longer initial telomere lengths (stronger telomere signals from high-molecular weight). However, the similar initial telomere lengths observed in *pot-2;mrt-1* double mutants, *pot-3;mrt-1* double mutants, and *pot-2;pot-3;mrt-1* triple mutants help eliminate potential effects resulting from different telomere shortening rates, which is also applicable in *trt-1* background mutants.

Previous research indicated that *mrt-1*, *trt-1*, and *mrt-2* function within the same genetic pathway of telomere elongation (Meier et al. 2006; 2009). It was reported that the TRT-1 and MRT-2 both contribute to telomerase-dependent telomere replication. This was supported by observations that *mrt-1*;*mrt-2* double mutants and *mrt-1*;*trt-1* double mutants displayed telomere shortening rate similar to those in *trt-1* mutants and *mrt-2* mutants (Meier et al. 2009). However, unlike the significant change in telomere shortening rate observed between *trt-1* mutant and *pot-2;trt-1* double mutant, no such difference was noted between *mrt-1* mutant and *pot-2;mrt-1* double mutants. This suggests that MRT-1 may not function identically to TRT-1 in POT-2-dependent telomere elongation. Furthermore, our finding implies that POT-2 shares a pathway with MRT-1 in telomere length regulation, given the similarity in telomere shortening rates observed in *mrt-1* mutants and *pot-2;mrt-1* double mutants. Therefore, the roles of these proteins in telomere maintenance may be more complex than previously concluded in the previous research, which needs to be further confirmed. In the future studies, constructing double or triple mutants in an *mrt-2* background may help elucidate the role of the POT proteins in the processive sterility phenotype in *C. elegans*.

In this chapter, we can conclude that the TRT-1 does not act identically to MRT-1 in telomere maintenance. The effects observed upon the loss of POT-2 and POT-3, which repress the telomerase activity and the telomere elongations, suggest a telomerase-dependent mechanism. This difference may be explained by the following model. In *mrt-1* mutants,

telomerase still act weakly to elongate the critically short telomeres without the repression of POT-2 and POT-3, leading to extended fertility span. On the contrary, in *trt-1* mutants, the telomeres cannot be elongated by telomerase because of the lack of the catalytic subunit of telomerase. This suggests that MRT-1 is needed for fully functional telomerase-dependent telomere maintenance, while TRT-1 is essential for this process.

5.3.3 Shortest telomere length not average length is the key to cell crisis

It is widely believed that the activation of cell senescence (replicative and cellular senescence) or cell apoptosis once the telomere length reaches a certain critical threshold leads to the limitation of fertility in organisms (Victorelli and Passos 2017). In theory, if worms with longer initial length remain similar telomere shortening rates, their span of fertility should be extended.

However, the observations in our research in *mrt-1* background worms were not fully consistent with this hypothesis. We notice that *mrt-1* mutants and *pot-2;mrt-1* double mutants displayed similar initial telomere length and similar telomere length shortening rates. Surprisingly, the fertility span of *mrt-1* mutants was significantly shorter than that of *pot-2;mrt-1* double mutants. The extended fertility span of *pot-2;mrt-1* double mutants cannot solely be attributed to telomere shortening as both mutant groups displayed similar telomere lengths when they reached their fertility limits. Additionally, in *trt-1* background, despite the lower telomere shortening rates in *pot-2;trt-1* and *pot-3;trt-1* double mutants, the fertility spans still remain similar to those of *trt-1* mutants. These results further emphasize the uncoupling of fertility span from average telomere length.

Based on our results in this chapter, we may conclude that the extended fertility span resulting from POT-2 and POT-3 deletions requires the presence of telomerase. Given the conclusion from chapter 3 that POT-2 and POT-3 repress the activity of telomerase, the loss of POT-2 or POT-3 leads to potential enhanced telomerase activity. This theory is consistent with what we observed. In *mrt-1* mutants, the remaining TRT-1 proteins act weakly on critically short telomeres when lacking POT-2/3. This process may lead to the extended fertility span of *pot-2;mrt-1* and *pot-3;mrt-1*. However, the critically short telomere length changes may not be accurately detected in the telomere length measurements in our studies since the method we used are not accurate at short telomeres. Moreover, this elongation activity is very weak, it

might only prolong the time it takes to become sterile but would not prevent the eventual sterility. This theory also helps explain that *mrt-1* and *trt-1* behave differently.

Our use of TRF Southern blot analysis, which can only provide an average telomere length, an overall telomere length distribution within a cell population, has certain limitations. It suggests that the average telomere length may not be the crucial factor in determining fertility span. Previous studies in humans have proposed that the shortest telomere, rather than average telomere length, is the key factor leading to cell crisis such as cell cycle arrest, apoptosis, and cellular senescence (Hanahan and Weinberg 2011; Blackburn and Epel 2012). Similar results were observed in mice that uncompensated telomere shortening leads to telomere dysfunction and subsequent chromosome rearrangement, cell cycle arrest, and apoptosis (Hemann et al. 2001).This concept is also supported by research in *S. cerevisiae*, where the length of the shortest telomere is a critical genetic marker determining senescence (Xu et al. 2013). In light of our conclusions in chapter 4, where we discussed how telomeres inherited from parents are random. The telomere erosion at short telomeres still leads to cell crisis in telomerase-deficient worms, ultimately resulting in eventual sterility. The survivors we observed may attribute to the probability that they inherited the longer telomeres from their parents. In future studies, employing a more accurate telomere length measuring method could help elucidate the connections between cell crisis and short telomeres in *C. elegans* using our survivor strains.

5.3.4 Long-lived survivors were observed in *trt-1* background worms

Our results highlight the significance of telomere shortening rate in both *pot-3;mrt-1* and *pot-3;trt-1* compared to *pot-3* mutants. This suggests that the decrease of telomere shortening rate resulting from loss of POT-3 is not telomerase-dependent. That is consistent with our findings in chapter 3, where we observed that loss of POT-3 leads to recombination and activation of ALT.

In our TRF analysis in *trt-1, pot-2;trt-1,* and *pot-3;trt-1* double mutants, ALT survivor phenotypes were observed. Some generations displayed telomere length increase in these double mutants (shown in appendix, Figure AP.3), similar to the ALT survivors phenotypes previously described in absence of telomerase (Lackner and Karlseder 2013). Similar survivors were noted in double mutants of *pot-1;trt-1* (referred to as *trt-1;ceob2* double mutant) in a previous study. These survivor strains exhibited characteristics similar to late generation *trt-1* mutants, such as reduced brood sizes, genomic instability (including a high incidence of males

(HIM) phenotype), and developmental phenotypes (such as larval arrest and vulva deformations) (Lackner et al. 2012). Some of these characteristics were observed in our survivor strains, such as reduced brood sizes, but systematic analysis would be required to make concrete conclusions on whether these strains activated ALT.

The ALT pathway, as a pathway maintaining telomeres without relying on telomerase, employs recombination-based mechanisms to add telomeric DNA repeats to chromosome ends. ALT is better studied in humans than in *C. elegans*. The characteristic features of human ALT cells include: 1) high rates of exchange between sister chromatids of telomeres, 2) presence of extrachromosomal circular DNA molecules known as C-circles, 3) presence of specialized nuclear structures known as ALT-associated promyelocytic leukemia (PML) bodies (APBs) (Harald Biessmann and Mason 1997; Hou et al. 2022). Notably, APBs cannot be observed in *C. elegans* because *C. elegans* do not have the PML protein. In both *pot-2* mutants and *pot-3* mutants, a higher level of C-circles than wildtype worms were observed. Therefore, the loss of *pot-2* or *pot-3* has important roles in the activation of ALT pathway, especially in the case of *pot-3* mutants, which exhibit a decreased telomere length shortening rate in both *mrt-1* mutants and *trt-1* mutants.

Telomere length heterogeneity is also one of the characteristics feature of ALT cells in various organisms. In humans, ALT cells include long and heterogeneous telomeres, ranging from 2 to greater than 20 kb within an individual cell (Bryan et al. 1995; 1997). In *S. cerevisiae,* type II survivors exhibit significant telomere lengthening and heterogeneity similar to that of the human ALT condition (Teng and Zakian 1999). Similarly, in *C. elegans, pot-1;trt-1* double mutant survivors display increased telomere length heterogeneity, especially in the size of the high-molecular-weight bands (Lackner et al. 2012). Moreover, in our study, increased telomere length heterogeneity was also observed in *pot-2;trt-1*, and *pot-3;trt-1* double mutants, especially in late generations (Figure 5.4). Similarly, *pot-2;mrt-1* double mutants, *pot-3;mrt-1* double mutants, and *pot-2;pot-3;mrt-1* triple mutants all displayed heterogeneous telomeres (Figure 5.2). These findings strongly suggest the activation of the ALT pathway in these mutant strains, which may largely contribute to generating ALT survivors or extending fertility span.

The presence of ALT survivor strains and the activation of the ALT pathway via loss of POT proteins in our research could offer unique tools for further exploration. Hopefully our findings could provide insight to the future studies that aim to elucidate the molecular mechanism of ALT.

Conclusion and future perspectives

In humans, the telomere single-strand DNA binding protein is referred to as Protection of Telomeres 1 (POT1). POT1 proteins play a vital role in binding to the ssDNA overhang at telomeres. POT1 also functions in inhibiting the DNA damage response, generating 3' ssDNA overhangs, and interacting positively and negatively with telomerase. This study focuses on the telomere single-strand DNA binding proteins in *Caenorhabditis elegans*. In *C. elegans*, the human POT1 homologs are POT-1, POT-2, POT-3, and MRT-1. MRT-1 is essential for telomerase-dependent telomere maintenance and serves as a 3' to 5' exonuclease. POT-1 and POT-2 are involved in repressing the telomerase activity and participate in extending telomeric overhang elongations. However, before the start of my PhD, the precise role of POT-3 was still largely unknown.

Firstly, we have successfully identified and characterised POT-3 in *C. elegans*, acting as a paralog of POT-2. We have uncovered its involvement in telomeric functions via a new null allele, *pot-3(syb2415)*. Loss of POT-3 leads to increased telomere length and evaluated C-circle level as observed in *pot-2* mutants without discernible effects on fertility. These findings suggest that POT-3 negatively regulates telomerase and represses telomeric recombination. Moreover, the *pot-2;pot-3* double mutants display milder telomeric phenotypes compared to *pot-2* mutants, and rescue of fertility defects. This *pot-3* suppression of *pot-2* phenotypes suggests that the *pot-3* acts epistatically with *pot-2*. Interestingly, this epistatic relationship between *pot-2* and *pot-3* acts in a POT-1-dependent manner.

Secondly, our results shed light on the telomere length inheritance in *C. elegans*, unveiling it as a stochastic process. The extremely long telomeres of *pot* mutants provided an opportunity to study the inheritance of telomere length in *C. elegans*. Offspring resulting from crosses involving the wildtype strain (N2) and *pot* mutant stains (*pot-2* mutants and *pot-1* mutants) displayed both long telomeres and wildtype length telomeres, regardless of the combination of crosses. It suggests that the initial telomere lengths of the offspring are inherited randomly from both male and hermaphrodite parental chromosomes. This result is further confirmed by the crosses involving the *mrt-1* mutant, which displays distinctively tight TRF bands rather than smeary ones. Moreover, the inherited telomeres undergo rapid telomere lengthening in short ones while stably maintaining the relatively long telomeres.

Thirdly, we have elucidated the roles of POT-2 and POT-3 in telomere length regulation and fertility in the context of *mrt-1* and *trt-1* mutant backgrounds. In the *mrt-1* mutant

background, loss of POT-2 or POT-3 leads to extended fertility span while the loss of POT-3 also decelerates the telomere shorting. On the other hand, in the *trt-1* mutant backgrounds, the loss of POT-2 or POT-3 slows down the telomere shortening but does not extend the number of generations during which worms are fertile. The results further indicate the roles of POT-2 and POT-3 in regulating telomere length and fertility. These observations, along with the viability difference between *mrt-1; exo-1* and *trt-1;exo-1* mutants, suggest that the MRT-1 and TRT-1 do not act identically. These results imply more complicated interactions between these proteins in telomere length regulation.

In this study, we have developed a model to explain the telomere length changes related to POT-2 and POT-3 (Figure CF.1). POT-2 and POT-3 both bind to the G-overhang, while POT-3 has a preference for binding to the 3' end. POT-2 and POT-3 suppress the activity of telomerase via a potential competitive role because TRT-1 and POT-2/3 bind to the same sequences. Moreover, telomere elongation resulting from loss of POT-2 and POT-3 is telomerase-dependent. This can explain the telomere elongation in *pot-2* and *pot-3* mutants. The longer telomere elongation in *pot-2* mutants than in *pot-3* mutants may be attributed to the greater abundance of POT-2 than POT-3. The *pot-2;pot-3* mutants may have a higher probability for telomerase to access the G-overhang. The epistatic relationship of *pot-2* and *pot-3* exists with the essential presence of POT-1. However, the model cannot illustrate how POT-1 is involved in the epistatic relationship of *pot-2* and *pot-3*. It may also be attributed to the conformational changes caused by the presence of POT-1. This theory fits the observation that TEBP-1/2 cannot bind to POT-2 without POT-1, but it needs to be further determined.

In telomerase deficient strains, *mrt-1* and *trt-1*, telomeres shorten through subsequent generations. In *mrt-1*, telomerase is repressed by POT-2 and POT-3. In *mrt-1;pot-2/3* mutants, telomerase may act weakly on the critically short telomeres without the suppression of POT-2 and POT-3, leading to its extended fertility span. However, the telomerase activity in this process needs more evidence to ascertain. In *trt-1* and *trt-1;pot-2/3* mutants, telomere lengths decrease through generations because no telomerase protein is available. The telomere shortening rate in *mrt-1* mutants is about the same as *trt-1* mutants. This suggests that the extension of fertility span does not correlate well with bulk telomere length. Moreover, the activation of ALT caused by the loss of POT-2 and POT-3 could increase the occurrence of survivor strains in *trt-1* mutants.

Furthermore, our study shows that the telomere length inheritance is a stochastic process (Figure CF.2). The telomeres of offspring are randomly inherited from both male and

hermaphrodite parents. This random process has possibility to generate offspring with overall long or short telomeres.

In the future studies, more precise telomere length measurement methods could be employed, such as nanopore sequencing, to enhance our understanding of telomere and overhang length regulation. Our strains, including the new *pot-3* mutant strain, survivor strains, and telomere replication-deficient strains, will serve as powerful tools to further investigate the telomere overhang protection, ALT pathway activation, and the maintenance of genome stability. Our discoveries may also have broader applications in areas like cancer research, particularly in telomerase-positive or ALT-positive cancers, and potentially in the development of novel cancer treatments.

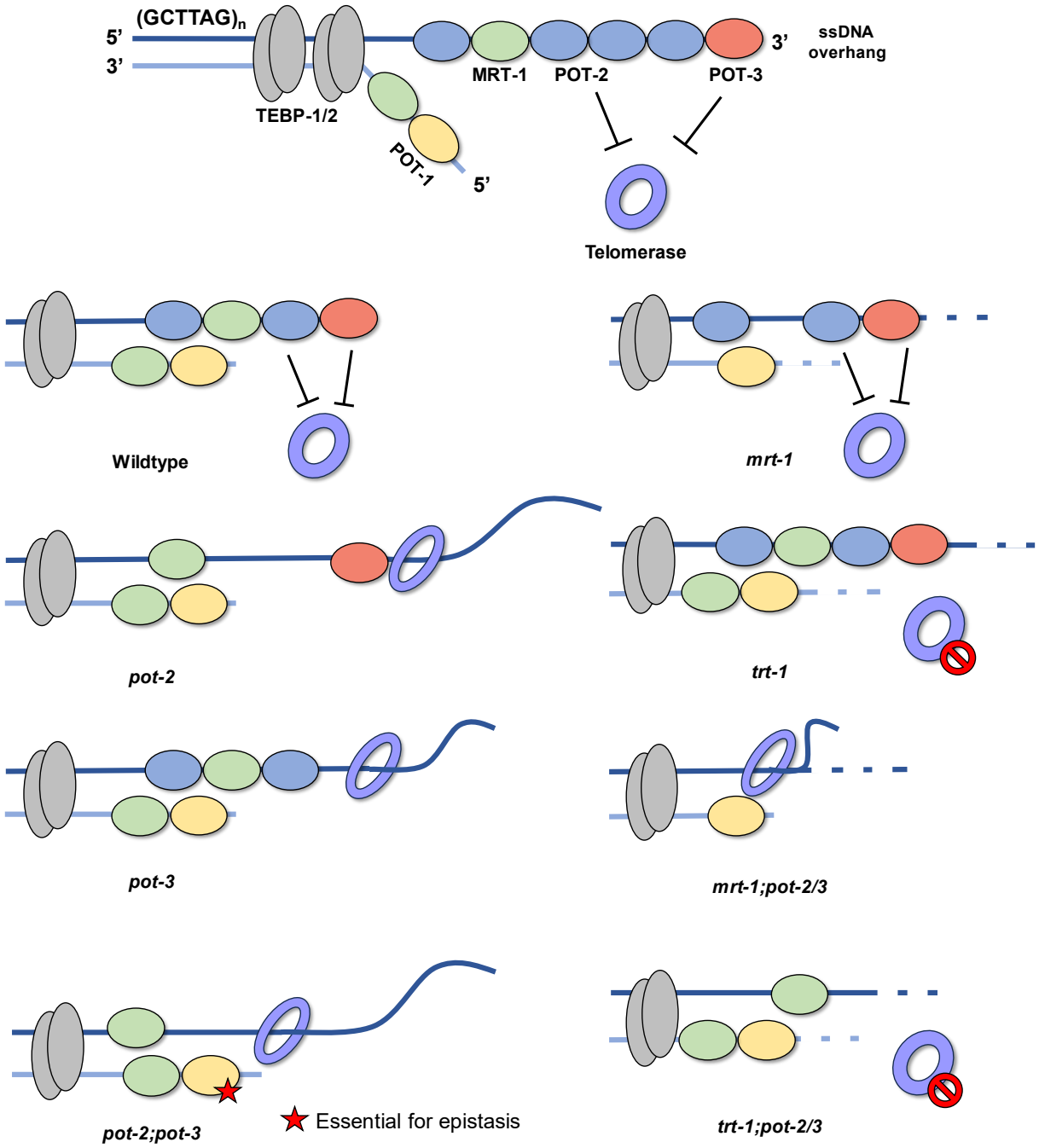

Figure CF.1 POT-2 and POT-3 repress telomerase, and the telomere elongation resulting from loss of POT-2 and POT-3 is telomerase dependent

The telomeric dsDNA is bonded by TEBP-1 and TEBP-2. The POT proteins bind telomeric ssDNA. POT-1 binds C-overhang, while POT-2 and POT-3 bind to G-overhang. MRT-1 can bind both overhangs. In *pot-2, pot-3* and *pot-2;pot-3* mutants, telomerase has higher activity, resulting in elongated telomeres. In *pot-2;pot-3* mutants, POT-1 displays an essential role in the epistatic relationship between *pot-2* and *pot-3* (shown by the red star). In telomerase-deficient strains, *mrt-1* and *trt-1*, telomeres shorten through generations. In *mrt-1*, the telomerase is repressed by POT-2 and POT-3. In *mrt-1;pot-2/3* mutants, telomerase acts weakly leading to elongated fertility span. In *trt-1* and *trt-1;pot-2/3* mutants, telomere lengths decrease through generations. The dashes in the figure show the telomere shortening.

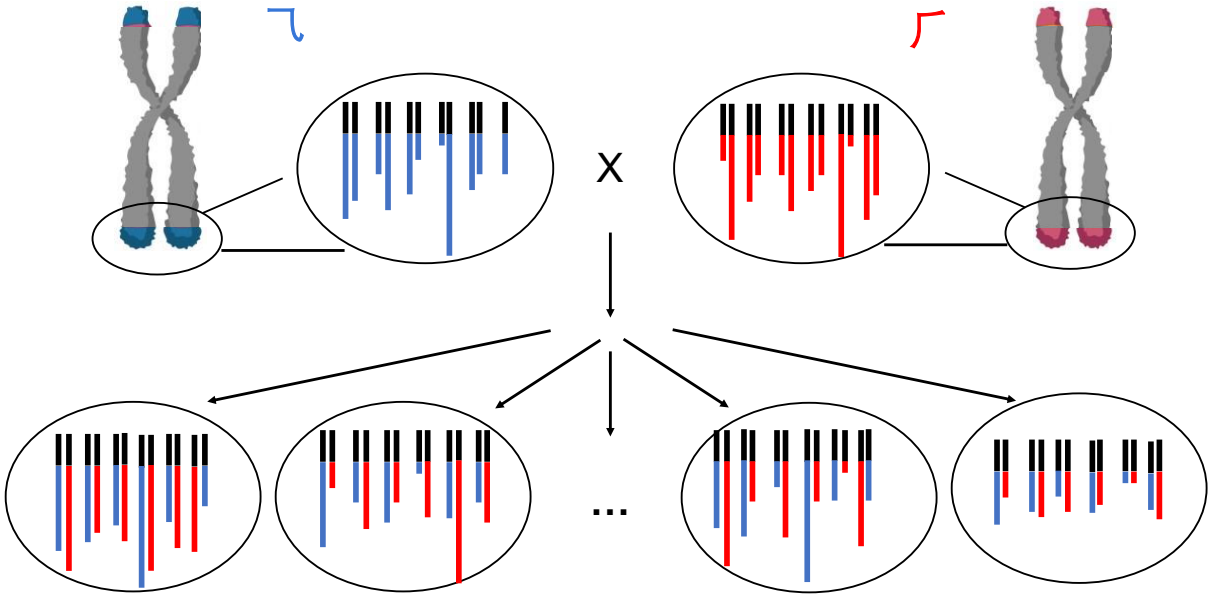

Figure CF.2 The telomere length inheritance in *C. elegans* is a stochastic process

The telomeres in offspring are inherited from both male and hermaphrodite. The blue and red parts indicate the telomeres from males and hermaphrodites, respectively. The offspring inherit random telomeres from parents. There is the possibility that the cells inherit a variety of shorter telomeres or longer telomeres.

References

Abad, José P., Beatriz De Pablos, Kazutoyo Osoegawa, Pieter J. De Jong, Antonia Martín-Gallardo, and Alfredo Villasante. 2004. "TAHRE, a Novel Telomeric Retrotransposon from Drosophila Melanogaster, Reveals the Origin of Drosophila Telomeres." *Molecular Biology and Evolution* 21 (9): 1620–24. https://doi.org/10.1093/molbev/msh180.

Abreu, Eladio, Elena Aritonovska, Patrick Reichenbach, Gaël Cristofari, Brad Culp, Rebecca M. Terns, Joachim Lingner, and Michael P. Terns. 2010. " TIN2-Tethered TPP1 Recruits Human Telomerase to Telomeres In Vivo ." *Molecular and Cellular Biology* 30 (12): 2971–82. https://doi.org/10.1128/mcb.00240-10.

Ahmed, S., and J. Hodgkin. 2000. "MRT-2 Checkpoint Protein Is Required for Germline Immortality and Telomere Replication in C. Elegans." *Nature* 403 (6766): 159–64. https://doi.org/10.1038/35003120.

Alter, Blanche P., Gabriela M. Baerlocher, Sharon A. Savage, Stephen J. Chanock, Babette B. Weksler, Judith P. Willner, June A. Peters, Neelam Giri, and Peter M. Lansdorp. 2007. "Very Short Telomere Length by Flow Fluorescence in Situ Hybridization Identifies Patients with Dyskeratosis Congenita." *Blood* 110 (5): 1439–47. https://doi.org/10.1182/blood-2007-02-075598.

Arnqvist, Jennifer. 2011. "Methodological Development of Human Telomere Sequencing with the Oxford Nanopore Technologies."

Arora, Amit, Mark A. Beilstein, and Dorothy E. Shippen. 2016. "Evolution of Arabidopsis Protection of Telomeres 1 Alters Nucleic Acid Recognition and Telomerase Regulation." *Nucleic Acids Research* 44 (20): gkw807. https://doi.org/10.1093/nar/gkw807.

Asghar, Muhammad, Staffan Bensch, Maja Tarka, Bengt Hansson, and Dennis Hasselquist. 2015. "Maternal and Genetic Factors Determine Early Life Telomere Length." *Proceedings of the Royal Society B: Biological Sciences* 282 (1799). https://doi.org/10.1098/rspb.2014.2263.

Aubert, Geraldine, and Peter M. Lansdorp. 2008. "Telomeres and Aging." *Physiological Reviews* 88 (2): 557–79. https://doi.org/10.1152/physrev.00026.2007.

Aviv, Abraham, Steven C. Hunt, Jue Lin, Xiaojian Cao, Masayuki Kimura, and Elizabeth Blackburn. 2011. “Impartial Comparative Analysis of Measurement of Leukocyte Telomere Length/DNA Content by Southern Blots and QPCR.” *Nucleic Acids Research* 39 (20): 1–5. https://doi.org/10.1093/nar/gkr634.

Baerlocher, Gabriela M., and Peter M. Lansdorp. 2003. “Telomere Length Measurements in Leukocyte Subsets by Automated Multicolor Flow-FISH.” *Cytometry Part A* 55 (1): 1–6. https://doi.org/10.1002/cyto.a.10064.

———. 2004. “Telomere Length Measurements Using Fluorescence in Situ Hybridization and Flow Cytometry.” *Methods in Cell Biology* 2004 (75): 719–50. https://doi.org/10.1016/s0091-679x(04)75031-1.

Baerlocher, Gabriela M, Irma Vulto, Gary de Jong, and Peter M Lansdorp. 2006. “Flow Cytometry and FISH to Measure the Average Length of Telomeres (Flow FISH).” *Nature Protocols* 1 (5): 2365–76. https://doi.org/10.1038/nprot.2006.263.

Baird, Duncan M., Jan Rowson, David Wynford-Thomas, and David Kipling. 2003. “Extensive Allelic Variation and Ultrashort Telomeres in Senescent Human Cells.” *Nature Genetics* 33 (2): 203–7. https://doi.org/10.1038/ng1084.

Barstead, Robert, Gary Moulder, Beth Cobb, Stephen Frazee, Diane Henthorn, Jeff Holmes, Daniela Jerebie, et al. 2012. “Large-Scale Screening for Targeted Knockouts in the Caenorhabditis Elegans Genome.” *G3: Genes, Genomes, Genetics* 2 (11): 1415–25. https://doi.org/10.1534/g3.112.003830.

Basenko, Evelina, Zeki Topcu, and Michael J. Mceachern. 2011. “Recombination Can Either Help Maintain Very Short Telomeres or Generate Longer Telomeres in Yeast Cells with Weak Telomerase Activity.” *Eukaryotic Cell* 10 (8): 1131–42. https://doi.org/10.1128/EC.05079-11.

Bateson, William. 1907. “Facts Limiting the Theory of Heredity.” *Science* 26 (672): 649–60.

Bauch, Christina, Jelle J. Boonekamp, Peter Korsten, Ellis Mulder, and Simon Verhulst. 2019. “Epigenetic Inheritance of Telomere Length in Wild Birds.” *PLoS Genetics* 15 (2): 1–15. https://doi.org/10.1371/journal.pgen.1007827.

Baumann, Peter, and Thomas R. Cech. 2001. “Pot1, the Putative Telomere End-Binding Protein in Fission Yeast and Humans.” *Science* 292 (5519): 1171–75. https://doi.org/10.1126/science.1060036.

Baumann, Peter, and Carolyn Price. 2010. “Pot1 and Telomere Maintenance.” *FEBS Letters* 584 (17): 3779–84. https://doi.org/10.1016/j.febslet.2010.05.024.

Beauséjour, Christian M, Ana Krtolica, Francesco Galimi, Masashi Narita, Scott W Lowe, Paul Yaswen, and Judith Campisi. 2003. “Reversal of Human Cellular Senescence: Roles of the P53 and P16 Pathways.” *The EMBO Journal* 22 (16): 4212–22. https://doi.org/https://doi.org/10.1093/emboj/cdg417.

Bechter, Oliver E., Ying Zou, William Walker, Woodring E. Wright, and Jerry W. Shay. 2004. “Telomeric Recombination in Mismatch Repair Deficient Human Colon Cancer Cells after Telomerase Inhibition.” *Cancer Research* 64 (10): 3444–51. https://doi.org/10.1158/0008-5472.CAN-04-0323.

Behrens, Yvonne Lisa, Kathrin Thomay, Maike Hagedorn, Juliane Ebersold, Lea Henrich, Rainer Nustede, Brigitte Schlegelberger, and Gudrun Göhring. 2017. “Comparison of Different Methods for Telomere Length Measurement in Whole Blood and Blood Cell Subsets: Recommendations for Telomere Length Measurement in Hematological Diseases.” *Genes Chromosomes and Cancer* 56 (9): 700–708. https://doi.org/10.1002/gcc.22475.

Beilstein, Mark A., Nathalie S. Nagalingum, Mark D. Clements, Steven R. Manchester, and Sarah Mathews. 2010. “Dated Molecular Phylogenies Indicate a Miocene Origin for Arabidopsis Thaliana.” *Proceedings of the National Academy of Sciences of the United States of America* 107 (43): 18724–28. https://doi.org/10.1073/pnas.0909766107.

Beilstein, Mark A., Kyle B. Renfrew, Xiangyu Song, Eugene V. Shakirov, Michael J. Zanis, and Dorothy E. Shippen. 2015. “Evolution of the Telomere-Associated Protein POT1a in Arabidopsis Thaliana Is Characterized by Positive Selection to Reinforce Protein-Protein Interaction.” *Molecular Biology and Evolution* 32 (5): 1329–41. https://doi.org/10.1093/molbev/msv025.

Bender, Hannah S., Elizabeth P. Murchison, Hilda A. Pickett, Janine E. Deakin, Margaret A. Strong, Carly Conlan, Daniel A. McMillan, et al. 2012. “Extreme Telomere Length Dimorphism in the Tasmanian Devil and Related Marsupials Suggests Parental

Control of Telomere Length." *PLoS ONE* 7 (9): 1–10. https://doi.org/10.1371/journal.pone.0046195.

Bendix, Laila, Peer Bendix Horn, Uffe Birk Jensen, Ivica Rubelj, and Steen Kolvraa. 2010. "The Load of Short Telomeres, Estimated by a New Method, Universal STELA, Correlates with Number of Senescent Cells." *Aging Cell* 9 (3): 383–97. https://doi.org/10.1111/j.1474-9726.2010.00568.x.

Bhaumik, Pranami, Mandar Bhattacharya, Priyanka Ghosh, Sujay Ghosh, and Subrata Kumar Dey. 2017. "Telomere Length Analysis in Down Syndrome Birth." *Mechanisms of Ageing and Development* 164: 20–26. https://doi.org/10.1016/j.mad.2017.03.006.

Bianchi, Alessandro, and David Shore. 2007. "Early Replication of Short Telomeres in Budding Yeast." *Cell* 128 (6): 1051–62. https://doi.org/10.1016/j.cell.2007.01.041.

Biessmann, H., L. E. Champion, M. O'Hair, K. Ikenaga, B. Kasravi, and J. M. Mason. 1992. "Frequent Transpositions of Drosophila Melanogaster HeT-A Transposable Elements to Receding Chromosome Ends." *EMBO Journal* 11 (12): 4459–69. https://doi.org/10.1002/j.1460-2075.1992.tb05547.x.

Biessmann, Harald, and James M. Mason. 1997. "Telomere Maintenance without Telomerase." *Chromosoma* 106 (2): 63–69. https://doi.org/10.1007/s004120050225.

Bilaud, Thomas, Christine Brun, Katia Ancelin, Catherine Elaine Koering, Thierry Laroche, and Eric Gilson. 1997. "Telobox Protein" 17 (october): 155–58.

Blackburn, Elizabeth H., and Elissa S. Epel. 2012. "Too Toxic to Ignore." *Nature* 490 (7419): 169–71. https://doi.org/10.1038/490169a.

Blackburn, Elizabeth H., and Joseph G. Gall. 1978. "A Tandemly Repeated Sequence at the Termini of the Extrachromosomal Ribosomal RNA Genes in Tetrahymena." *Journal of Molecular Biology* 120 (1): 33–53. https://doi.org/10.1016/0022-2836(78)90294-2.

Blasco, María A., Han Woong Lee, M. Prakash Hande, Enrique Samper, Peter M. Lansdorp, Ronald A. DePinho, and Carol W. Greider. 1997. "Telomere Shortening and Tumor Formation by Mouse Cells Lacking Telomerase RNA." *Cell* 91 (1): 25–34. https://doi.org/10.1016/S0092-8674(01)80006-4.

Bluyssen, Hans A.R., Roselinde I. Van Os, Nicole C. Naus, Iris Jaspers, Jan H.J. Hoeijmakers, and Annelies De Klein. 1998. “A Human and Mouse Homolog of the Schizosaccharomyces Pombe Rad1+ Cell Cycle Checkpoint Control Gene.” *Genomics* 54 (2): 331–37. https://doi.org/10.1006/geno.1998.5582.

Bodnar, Andrea G., Michel Ouellette, Maria Frolkis, Shawn E. Holt, Choy Pik Chiu, Gregg B. Morin, Calvin B. Harley, Jerry W. Shay, Serge Lichtsteiner, and Woodring E. Wright. 1998. “Extension of Life-Span by Introduction of Telomerase into Normal Human Cells.” *Science* 279 (5349): 349–52. https://doi.org/10.1126/science.279.5349.349.

Brenes, Alejandro, Vackar Afzal, Robert Kent, and Angus I. Lamond. 2018. “The Encyclopedia of Proteome Dynamics: A Big Data Ecosystem for (Prote)Omics.” *Nucleic Acids Research* 46 (D1): D1202–9. https://doi.org/10.1093/nar/gkx807.

Brenner, S. 1974. “THE GENETICS OF CAENORHABDITIS ELEGANS.” *Genetics* 77 (1): 71–94. https://doi.org/10.1093/genetics/77.1.71.

Broer, Linda, Veryan Codd, Dale R. Nyholt, Joris Deelen, Massimo Mangino, Gonneke Willemsen, Eva Albrecht, et al. 2013. “Meta-Analysis of Telomere Length in 19 713 Subjects Reveals High Heritability, Stronger Maternal Inheritance and a Paternal Age Effect.” *European Journal of Human Genetics* 21 (10): 1163–68. https://doi.org/10.1038/ejhg.2012.303.

Bryan, Tracy M., Anna Englezou, Jyothi Gupta, Silvia Bacchetti, and Roger R. Reddel. 1995. “Telomere Elongation in Immortal Human Cells without Detectable Telomerase Activity.” *EMBO Journal* 14 (17): 4240–48. https://doi.org/10.1002/j.1460-2075.1995.tb00098.x.

Bryan, Tracy M, Anna Englezou, Luciano Dalla-Pozza, Melissa A Dunham, and Roger R Reddel. 1997. “Evidence for an Alternative Mechanism for Maintaining Telomere Length in Human Tumors and Tumor-Derived Cell Lines.” *Nature Medicine* 3 (11): 1271–74. https://doi.org/10.1038/nm1197-1271.

Campisi, Judith, and Fabrizio d’Adda di Fagagna. 2007. “Cellular Senescence: When Bad Things Happen to Good Cells.” *Nature Reviews Molecular Cell Biology* 8 (9): 729–40. https://doi.org/10.1038/nrm2233.

Canela, Andrés, Elsa Vera, Peter Klatt, and María A. Blasco. 2007. “High-Throughput Telomere Length Quantification by FISH and Its Application to Human Population Studies.” *Proceedings of the National Academy of Sciences of the United States of America* 104 (13): 5300–5305. https://doi.org/10.1073/pnas.0609367104.

Casacuberta, E., and M. L. Pardue. 2005. “HeT-A and TART, Two Drosophila Retrotransposons with a Bona Fide Role in Chromosome Structure for More than 60 Million Years.” *Cytogenetic and Genome Research* 110 (1–4): 152–59. https://doi.org/10.1159/000084947.

Cawthon, Richard M. 2002. “Telomere Measurement by Quantitative PCR.” *Nucleic Acids Research* 30 (10): 1–6. https://doi.org/10.1093/nar/30.10.e47.

———. 2009. “Telomere Length Measurement by a Novel Monochrome Multiplex Quantitative PCR Method.” *Nucleic Acids Research* 37 (3): 1–7. https://doi.org/10.1093/nar/gkn1027.

Celli, Giulia B., and Titia de Lange. 2005. “DNA Processing Is Not Required for ATM-Mediated Telomere Damage Response after TRF2 Deletion.” *Nature Cell Biology* 7 (7): 712–18. https://doi.org/10.1038/ncb1275.

Cesare, Anthony J., and Jack D. Griffith. 2004. “Telomeric DNA in ALT Cells Is Characterized by Free Telomeric Circles and Heterogeneous T-Loops.” *Molecular and Cellular Biology* 24 (22): 9948–57. https://doi.org/10.1128/mcb.24.22.9948-9957.2004.

Chaires, Jonathan B., Robert D. Gray, William L. Dean, Robert Monsen, Lynn W. Deleeuw, Vilius Stribinskis, and John O. Trent. 2020. “Human POT1 Unfolds G-Quadruplexes by Conformational Selection.” *Nucleic Acids Research* 48 (9): 4976–91. https://doi.org/10.1093/nar/gkaa202.

Chalapati, Sachin, Conor A Crosbie, Dixita Limbachiya, Nimesh Pinnamaneni, and Fumihito Miura. 2021. “Direct Oligonucleotide Sequencing with Nanopores [Version 1; Peer Review: 1 Approved with Reservations] Report,” 1–15. https://doi.org/10.12688/openreseurope.13578.1.

Chen, Cong, Peili Gu, Jian Wu, Xianyun Chen, Shuangshuang Niu, Hong Sun, Lijie Wu, et al. 2017. “Structural Insights into POT1-TPP1 Interaction and POT1 C-Terminal Mutations in Human Cancer.” *Nature Communications* 8. https://doi.org/10.1038/ncomms14929.

Chen, Qijun, Arne Ijpma, and Carol W. Greider. 2001. “Two Survivor Pathways That Allow Growth in the Absence of Telomerase Are Generated by Distinct Telomere Recombination Events.” *Molecular and Cellular Biology* 21 (5): 1819–27. https://doi.org/10.1128/mcb.21.5.1819-1827.2001.

Cheng, Chen, Ludmila Shtessel, Megan M. Brady, and Shawn Ahmed. 2012. “Caenorhabditis Elegans POT-2 Telomere Protein Represses a Mode of Alternative Lengthening of Telomeres with Normal Telomere Lengths.” *Proceedings of the National Academy of Sciences of the United States of America* 109 (20): 7805–10. https://doi.org/10.1073/pnas.1119191109.

Cheung, Iris, Michael Schertzer, Ann Rose, and Peter M. Lansdorp. 2006a. “High Incidence of Rapid Telomere Loss in Telomerase-Deficient Caenorhabditis Elegans.” *Nucleic Acids Research* 34 (1): 96–103. https://doi.org/10.1093/nar/gkj417.

Cheung, Iris, Michael Schertzer, Ann Rose, and Peter M Lansdorp. 2006b. “High Incidence of Rapid Telomere Loss in Telomerase-Deficient Caenorhabditis Elegans.” *Nucleic Acids Research* 34 (1): 96–103. https://doi.org/10.1093/nar/gkj417.

Cheung, Iris, Mike Schertzer, Agnes Baross, Ann M Rose, Peter M Lansdorp, and Duncan M Baird. 2004. “Strain-Specific Telomere Length Revealed by Single Telomere Length Analysis in Caenorhabditis Elegans.” *Nucleic Acids Research* 32 (11): 3383–91. https://doi.org/10.1093/nar/gkh661.

Chong, Laura, Bas Van Steensel, Dominique Broccoli, Hediye Erdjument-Bromage, John Hanish, Paul Tempst, and Titia De Lange. 1995. “A Human Telomeric Protein.” *Science* 270 (5242): 1663–67. https://doi.org/10.1126/science.270.5242.1663.

Chung, Inn, Sarah Osterwald, Katharina I. Deeg, and Karsten Rippe. 2012. “PML Body Meets Telomere.” *Nucleus* 3 (3): 263–75. https://doi.org/10.4161/nucl.20326.

Churikov, Dmitri, and Carolyn M. Price. 2008. “Pot1 and Cell Cycle Progression Cooperate in Telomere Length Regulation.” *Nature Structural and Molecular Biology* 15 (1): 79–84. https://doi.org/10.1038/nsmb1331.

Cicconi, Alessandro, Emanuela Micheli, Fiammetta Vernì, Alison Jackson, Ana Citlali Gradilla, Francesca Cipressa, Domenico Raimondo, et al. 2017. “The Drosophila Telomere-Capping Protein Verrocchio Binds Single-Stranded DNA and Protects

Telomeres from DNA Damage Response." *Nucleic Acids Research* 45 (6): 3068–85. https://doi.org/10.1093/nar/gkw1244.

Cohen, Scott B, Mark E Graham, George O Lovrecz, Nicolai Bache, Phillip J Robinson, and Roger R Reddel. 2007. "Protein Composition of Catalytically Active Human Telomerase from Immortal Cells." *Science* 315 (5820): 1850–53. https://doi.org/10.1126/science.1138596.

Cohn, Marita. 2008. "Molecular Diversity of Telomeric Sequences." *Origin and Evolution of Telomeres. Landes Bioscience*, 70–82.

Collins, Kathleen. 2006. "The Biogenesis and Regulation of Telomerase Holoenzymes." *Nature Reviews Molecular Cell Biology* 7 (7): 484–94. https://doi.org/10.1038/nrm1961.

Cranert, Stacey, Serena Heyse, Benjamin R. Linger, Rachel Lescasse, and Carolyn Price. 2014. "Tetrahymena Pot2 Is a Developmentally Regulated Paralog of Pot1 That Localizes to Chromosome Breakage Sites but Not to Telomeres." *Eukaryotic Cell* 13 (12): 1519–29. https://doi.org/10.1128/EC.00204-14.

Cristofari, Gaël, and Joachim Lingner. 2006. "Telomere Length Homeostasis Requires That Telomerase Levels Are Limiting." *EMBO Journal* 25 (3): 565–74. https://doi.org/10.1038/sj.emboj.7600952.

D'Adda Di Fagagna, Fabrizio, Philip M Reaper, Lorena Clay-Farrace, Heike Fiegler, Philippa Carr, Thomas Von Zglinicki, Gabriele Saretzki, Nigel P. Carter, and Stephen P. Jackson. 2003. "A DNA Damage Checkpoint Response in Telomere-Initiated Senescence." *Nature* 426 (6963): 194–98. https://doi.org/10.1038/nature02118.

Dargahi, Daryanaz, David Baillie, and Frederic Pio. 2013. "Bioinformatics Analysis Identify Novel OB Fold Protein Coding Genes in C. Elegans." *PLoS ONE* 8 (4). https://doi.org/10.1371/journal.pone.0062204.

Dean, Frank B., Lubing Lian, and Mike O'Donnell. 1998. "CDNA Cloning and Gene Mapping of Human Homologs for Schizosaccharomyces Pombe Rad17, Rad1, and Hus1 and Cloning of Homologs from Mouse, Caenorhabditis Elegans, and Drosophila Melanogaster." *Genomics* 54 (3): 424–36. https://doi.org/10.1006/geno.1998.5587.

Denchi, Eros Lazzerini, and Titia De Lange. 2007. “Protection of Telomeres through Independent Control of ATM and ATR by TRF2 and POT1.” *Nature* 448 (7157): 1068–71. https://doi.org/10.1038/nature06065.

Depeursinge, Adrien, Daniel Racoceanu, Jimison Iavindrasana, Gilles Cohen, Alexandra Platon, Pierre-Alexandre Poletti, Henning Muller, et al. 2004. “A Dynamic Molecular Link between the Telomere Length Regulator TRF1 and the Chromosome End Protector TRF2.” *Current Biology* 14 (18): 1621–31. https://doi.org/10.1016/j.cub.2004.08.052.

Dietz, Sabrina, Miguel Vasconcelos Almeida, Emily Nischwitz, Jan Schreier, Nikenza Viceconte, Albert Fradera-Sola, Christian Renz, et al. 2021. “The Double-Stranded DNA-Binding Proteins TEBP-1 and TEBP-2 Form a Telomeric Complex with POT-1.” *Nature Communications* 12 (1): 1–20. https://doi.org/10.1038/s41467-021-22861-2.

Dietz, Sabrina, Miguel Vasconcelos Almeida, Emily Nischwitz, Jan Schreier, Nikenza Viceconte, Albert Fradera Sola, Christian Renz, et al. 2020. “The Double-Stranded DNA-Binding Proteins TEBP-1 and TEBP-2 Form a Telomeric Complex with POT-1.” *Nature Communications*, no. 2021: 2020.08.19.256388. https://doi.org/10.1038/s41467-021-22861-2.

Diotti, Rafaella, and Diego Loayza. 2011. “Shelterin Complex and Associated Factors at Human Telomeres.” *Nucleus*. Taylor and Francis Inc. https://doi.org/10.4161/nucl.2.2.15135.

Draskovic, Irena, Nausica Arnoult, Villier Steiner, Silvia Bacchetti, Patrick Lomonte, and Arturo Londoño-Vallejo. 2009. “Probing PML Body Function in ALT Cells Reveals Spatiotemporal Requirements for Telomere Recombination.” *Proceedings of the National Academy of Sciences* 106 (37): 15726–31. https://doi.org/10.1073/pnas.0907689106.

Eisenberg, Dan T.A. 2014. “Inconsistent Inheritance of Telomere Length (TL): Is Offspring TL More Strongly Correlated with Maternal or Paternal TL.” *European Journal of Human Genetics* 22 (1): 8–9. https://doi.org/10.1038/ejhg.2013.202.

Elbers, Clara C., Melissa E. Garcia, Masayuki Kimura, Steven R. Cummings, Mike A. Nalls, Anne B. Newman, Vicki Park, et al. 2014. “Comparison between Southern Blots and QPCR Analysis of Leukocyte Telomere Length in the Health ABC Study.” *Journals*

of Gerontology - Series A Biological Sciences and Medical Sciences 69 A (5): 527–31. https://doi.org/10.1093/gerona/glt121.

Episkopou, Harikleia, Irena Draskovic, Amandine Van Beneden, Gaëlle Tilman, Marina Mattiussi, Matthieu Gobin, Nausica Arnoult, Arturo Londoño-Vallejo, and Anabelle Decottignies. 2014. "Alternative Lengthening of Telomeres Is Characterized by Reduced Compaction of Telomeric Chromatin." *Nucleic Acids Research* 42 (7): 4391–4405. https://doi.org/10.1093/nar/gku114.

Erdel, Fabian, Katja Kratz, Smaranda Willcox, Jack D Griffith, Eric C Greene, and Titia de Lange. 2017. "Telomere Recognition and Assembly Mechanism of Mammalian Shelterin." *Cell Reports* 18 (1): 41–53. https://doi.org/10.1016/j.celrep.2016.12.005.

Evans, Sara K., and Victoria Lundblad. 1999. "Est1 and Cdc13 as Comediators of Telomerase Access." *Science* 286 (5437): 117–20. https://doi.org/10.1126/science.286.5437.117.

Farmery, James H.R., Mike L. Smith, Aarnoud Huissoon, Abigail Furnell, Adam Mead, Adam P. Levine, Adnan Manzur, et al. 2018. "Telomerecat: A Ploidy-Agnostic Method for Estimating Telomere Length from Whole Genome Sequencing Data." *Scientific Reports* 8 (1): 1–17. https://doi.org/10.1038/s41598-017-14403-y.

Ferreira, Helder C., Benjamin D. Towbin, Thibaud Jegou, and Susan M. Gasser. 2013. "The Shelterin Protein POT-1 Anchors Caenorhabditis Elegans Telomeres through SUN-1 at the Nuclear Periphery." *Journal of Cell Biology* 203 (5): 727–35. https://doi.org/10.1083/jcb.201307181.

Flynn, Rachel Litman, Richard C. Centore, Roderick J. O'Sullivan, Rekha Rai, Alice Tse, Zhou Songyang, Sandy Chang, Jan Karlseder, and Lee Zou. 2011. "TERRA and HnRNPA1 Orchestrate an RPA-to-POT1 Switch on Telomeric Single-Stranded DNA." *Nature* 471 (7339): 532–38. https://doi.org/10.1038/nature09772.

Force, Allan, Michael Lynch, F. Bryan Pickett, Angel Amores, Yi Lin Yan, and John Postlethwait. 1999. "Preservation of Duplicate Genes by Complementary, Degenerative Mutations." *Genetics* 151 (4): 1531–45. https://doi.org/10.1093/genetics/151.4.1531.

Freire, Raimundo, Jose R. Murguía, Madalina Tarsounas, Noel F. Lowndes, Peter B. Moens, and Stephen P. Jackson. 1998. "Human and Mouse Homologs of Schizosaccharomyces Pombe Rad1+ and Saccharomyces Cerevisiae Rad17: Linkage to

Checkpoint Control and Mammalian Meiosis." *Genes and Development* 12 (16): 2560–73. https://doi.org/10.1101/gad.12.16.2560.

Garvik, B, M Carson, and L Hartwell. 1995. "Single-Stranded DNA Arising at Telomeres in Cdc13 Mutants May Constitute a Specific Signal for the RAD9 Checkpoint." *Molecular and Cellular Biology* 15 (11): 6128–38. https://doi.org/10.1128/mcb.15.11.6128.

Garvik, Barbara, Michael Carson, and Leland Hartwell. 1995. "Single-Stranded DNA Arising at Telomeres in Cdc13 Mutants May Constitute a Specific Signal for the RAD9 Checkpoint." *Molecular and Cellular Biology* 15 (11): 6128–38. https://doi.org/10.1128/mcb.15.11.6128.

Giardini, Miriam Aparecida, Marcela Segatto, Marcelo Santos Da Silva, Vinícius Santana Nunes, and Maria Isabel Nogueira Cano. 2014. "Telomere and Telomerase Biology." In *Progress in Molecular Biology and Translational Science*, 125:1–40. Elsevier B.V. https://doi.org/10.1016/B978-0-12-397898-1.00001-3.

Gong, Yi, and Titia de Lange. 2010. "A Shld1-Controlled POT1a Provides Support for Repression of ATR Signaling at Telomeres through RPA Exclusion." *Molecular Cell* 40 (3): 377–87. https://doi.org/10.1016/j.molcel.2010.10.016.

Graakjaer, Jesper, Héra Der-Sarkissian, Annette Schmitz, Jan Bayer, Gilles Thomas, Steen Kolvraa, and José Arturo Londoño-Vallejo. 2006. "Allele-Specific Relative Telomere Lengths Are Inherited." *Human Genetics* 119 (3): 344–50. https://doi.org/10.1007/s00439-006-0137-x.

Grandin, Nathalie, Aymeric Bailly, and Michel Charbonneau. 2005. "Activation of Mrc1, a Mediator of the Replication Checkpoint, by Telomere Erosion." *Biology of the Cell* 97 (10): 799–814. https://doi.org/https://doi.org/10.1042/BC20040526.

Grandin, Nathalie, Christelle Damon, and Michel Charbonneau. 2000. "Cdc13 Cooperates with the Yeast Ku Proteins and Stn1 To Regulate Telomerase Recruitment." *Molecular and Cellular Biology* 20 (22): 8397–8408. https://doi.org/10.1128/mcb.20.22.8397-8408.2000.

Greider, Carol W. 1996. "Telomere Length Regulation." *Annual Review of Biochemistry* 65 (1): 337–65. https://doi.org/10.1146/annurev.biochem.65.1.337.

———. 2016. “Regulating Telomere Length from the inside out: The Replication Fork Model.” *Genes and Development* 30 (13): 1483–91. https://doi.org/10.1101/gad.280578.116.

Greider, Carol W., and Elizabeth H. Blackburn. 1985. “Identification of a Specific Telomere Terminal Transferase Activity in Tetrahymena Extracts.” *Cell* 43 (2 PART 1): 405–13. https://doi.org/10.1016/0092-8674(85)90170-9.

———. 1989. “A Telomeric Sequence in the RNA of Tetrahymena Telomerase Required for Telomere Repeat Synthesis.” *Nature* 337 (6205): 331–37. https://doi.org/10.1038/337331a0.

Hanahan, Douglas, and Robert A. Weinberg. 2011. “Hallmarks of Cancer: The next Generation.” *Cell* 144 (5): 646–74. https://doi.org/10.1016/j.cell.2011.02.013.

Hayflick, L, and P S Moorhead. 1961. “The Serial Cultivation of Human Diploid Cell Strains.” *Experimental Cell Research* 25 (3): 585–621. https://doi.org/https://doi.org/10.1016/0014-4827(61)90192-6.

He, Hua, Asha S. Multani, Wilfredo Cosme-Blanco, Hidetoshi Tahara, Jin Ma, Sen Pathak, Yibin Deng, and Sandy Chang. 2006. “POT1b Protects Telomeres from End-to-End Chromosomal Fusions and Aberrant Homologous Recombination.” *EMBO Journal* 25 (21): 5180–90. https://doi.org/10.1038/sj.emboj.7601294.

Hemann, Michael T., Margaret A. Strong, Ling Yang Hao, and Carol W. Greider. 2001. “The Shortest Telomere, Not Average Telomere Length, Is Critical for Cell Viability and Chromosome Stability.” *Cell* 107 (1): 67–77. https://doi.org/10.1016/S0092-8674(01)00504-9.

Henson, Jeremy D, Ying Cao, Lily I Huschtscha, Andy C Chang, Amy Y.M. Au, Hilda A Pickett, and Roger R Reddel. 2009a. “DNA C-Circles Are Specific and Quantifiable Markers of Alternative- Lengthening-of-Telomeres Activity.” *Nature Biotechnology* 27 (12): 1181–85. https://doi.org/10.1038/nbt.1587.

Henson, Jeremy D, Ying Cao, Lily I Huschtscha, Andy C Chang, Amy Y M Au, Hilda A Pickett, and Roger R Reddel. 2009b. “DNA C-Circles Are Specific and Quantifiable Markers of Alternative-Lengthening-of-Telomeres Activity.” *Nature Biotechnology* 27 (12): 1181–85. https://doi.org/10.1038/nbt.1587.

Hockemeyer, Dirk, Jan Peter Daniels, Hiroyuki Takai, and Titia de Lange. 2006. “Recent Expansion of the Telomeric Complex in Rodents: Two Distinct POT1 Proteins Protect Mouse Telomeres.” *Cell* 126 (1): 63–77. https://doi.org/10.1016/j.cell.2006.04.044.

Horn, Thorsten, Bruce C. Robertson, Margaret Will, Daryl K. Eason, Graeme P. Elliott, and Neil J. Gemmell. 2011. “Inheritance of Telomere Length in a Bird.” *PLoS ONE* 6 (2): 1–5. https://doi.org/10.1371/journal.pone.0017199.

Hou, Kailong, Yuyang Yu, Duda Li, Yanduo Zhang, Ke Zhang, Jinkai Tong, Kunxian Yang, and Shuting Jia. 2022. “Alternative Lengthening of Telomeres and Mediated Telomere Synthesis.” *Cancers* 14 (9). https://doi.org/10.3390/cancers14092194.

IJpma, Arne S, and Carol W Greider. 2003. “Short Telomeres Induce a DNA Damage Response InSaccharomyces Cerevisiae.” *Molecular Biology of the Cell* 14 (3): 987–1001. https://doi.org/10.1091/mbc.02-04-0057.

Jacob, Naduparambil K., Rachel Lescasse, Benjamin R. Linger, and Carolyn M. Price. 2007. “Tetrahymena POT1a Regulates Telomere Length and Prevents Activation of a Cell CycleCheckpoint.” *Molecular and Cellular Biology* 27 (5): 1592–1601. https://doi.org/10.1128/mcb.01975-06.

Jaiswal, Amit, and P. T.V. Lakshmi. 2015. “Molecular Inhibition of Telomerase Recruitment Using Designer Peptides: An in Silico Approach.” *Journal of Biomolecular Structure and Dynamics* 33 (7): 1442–59. https://doi.org/10.1080/07391102.2014.953207.

Jaskelioff, Mariela, Florian L. Muller, Ji Hye Paik, Emily Thomas, Shan Jiang, Andrew C. Adams, Ergun Sahin, et al. 2011. “Telomerase Reactivation Reverses Tissue Degeneration in Aged Telomerase-Deficient Mice.” *Nature* 469 (7328): 102–7. https://doi.org/10.1038/nature09603.

Jiang, Jiansen, Yaqiang Wang, Lukas Sušac, Henry Chan, Ritwika Basu, Z. Hong Zhou, and Juli Feigon. 2018. “Structure of Telomerase with Telomeric DNA.” *Cell* 173 (5): 1179-1190.e13. https://doi.org/10.1016/j.cell.2018.04.038.

Joeng, Kyu Sang, Eun Joo Song, Kong Joo Lee, and Junho Lee. 2004. “Long Lifespan in Worms with Long Telomeric DNA.” *Nature Genetics* 36 (6): 607–11. https://doi.org/10.1038/ng1356.

Joseph, Immanual, Dingwu Jia, and Arthur J Lustig. 2005. “Ndj1p-Dependent Epigenetic Resetting of Telomere Size in Yeast Meiosis.” *Current Biology* 15 (3): 231–37.

Kabir, Shaheen, Dirk Hockemeyer, and Titia de Lange. 2014. “TALEN Gene Knockouts Reveal No Requirement for the Conserved Human Shelterin Protein Rap1 in Telomere Protection and Length Regulation.” *Cell Reports* 9 (4): 1273–80. https://doi.org/10.1016/j.celrep.2014.10.014.

Kelleher, Colleen, Isabel Kurth, and Joachim Lingner. 2005. “Human Protection of Telomeres 1 (POT1) Is a Negative Regulator of Telomerase Activity In Vitro.” *Molecular and Cellular Biology* 25 (2): 808–18. https://doi.org/10.1128/mcb.25.2.808-818.2005.

Kellogg, Elizabeth A. 1998. “Relationships of Cereal Crops and Other Grasses.” *Proceedings of the National Academy of Sciences of the United States of America* 95 (5): 2005–10. https://doi.org/10.1073/pnas.95.5.2005.

Kermasson, Laëtitia, Dmitri Churikov, Aya Awad, Riham Smoom, Elodie Lainey, Fabien Touzot, Séverine Audebert-Bellanger, et al. 2022. “Inherited Human Apollo Deficiency Causes Severe Bone Marrow Failure and Developmental Defects.” *Blood* 139 (16): 2427–40. https://doi.org/10.1182/blood.2021010791.

Khadaroo, Basheer, M. Teresa Teixeira, Pierre Luciano, Nadine Eckert-Boulet, Susanne M. Germann, Marie Noelle Simon, Irene Gallina, et al. 2009. “The DNA Damage Response at Eroded Telomeres and Tethering to the Nuclear Pore Complex.” *Nature Cell Biology* 11 (8): 980–87. https://doi.org/10.1038/ncb1910.

Kibe, Tatsuya, Gail A. Osawa, Catherine E. Keegan, and Titia de Lange. 2010. “Telomere Protection by TPP1 Is Mediated by POT1a and POT1b.” *Molecular and Cellular Biology* 30 (4): 1059–66. https://doi.org/10.1128/mcb.01498-09.

Kim, Hyeung, Feng Li, Quanyuan He, Tingting Deng, Jun Xu, Feng Jin, Cristian Coarfa, Nagireddy Putluri, Dan Liu, and Zhou Songyang. 2017. “Systematic Analysis of Human Telomeric Dysfunction Using Inducible Telosome/Shelterin CRISPR/Cas9 Knockout Cells.” *Cell Discovery* 3 (September). https://doi.org/10.1038/celldisc.2017.34.

Kim, Sahn-ho, Patrick Kaminker, and Judith Campisi. 1999. “TIN2, a New Regulator of Telomere Length in Human Cells.” *Nature Genetics* 23 (4): 405–12. https://doi.org/10.1038/70508.

Kim, Sahn Ho, Albert R. Davalos, Seok Jin Heo, Francis Rodier, Ying Zou, Christian Beausejour, Patrick Kaminker, Steven M. Yannone, and Judith Campisi. 2008. “Telomere Dysfunction and Cell Survival: Roles for Distinct TIN2-Containing Complexes.” *Journal of Cell Biology* 181 (3): 447–60. https://doi.org/10.1083/jcb.200710028.

Kimura, Masayuki, Rivka C. Stone, Steven C. Hunt, Joan Skurnick, Xiaobin Lu, Xiaojian Cao, Calvin B. Harley, and Abraham Aviv. 2010. “Measurement of Telomere Length by the Southern Blot Analysis of Terminal Restriction Fragment Lengths.” *Nature Protocols* 5 (9): 1596–1607. https://doi.org/10.1038/nprot.2010.124.

Kipling, D, and H J Cooke. 1990. “Hypervariable Ultra-Long Telomeres in Mice.” *Nature* 347 (6291): 400–402. https://doi.org/10.1038/347400a0.

Klebanov-Akopyan, Olga, Amartya Mishra, Galina Glousker, Yehuda Tzfati, and Joseph Shlomai. 2018. “Trypanosoma Brucei UMSBP2 Is a Single-Stranded Telomeric DNA Binding Protein Essential for Chromosome End Protection.” *Nucleic Acids Research* 46 (15): 7757–71. https://doi.org/10.1093/nar/gky597.

Kobayashi, Callie R., Claudia Castillo-González, Yulia Survotseva, Elijah Canal, Andrew D.L. Nelson, and Dorothy E. Shippen. 2019. “Recent Emergence and Extinction of the Protection of Telomeres 1c Gene in Arabidopsis Thaliana.” *Plant Cell Reports* 38 (9): 1081–97. https://doi.org/10.1007/s00299-019-02427-9.

Kockler, Zachary W., Josep M. Comeron, and Anna Malkova. 2021. “A Unified Alternative Telomere-Lengthening Pathway in Yeast Survivor Cells.” *Molecular Cell* 81 (8): 1816-1829.e5. https://doi.org/10.1016/j.molcel.2021.02.004.

Konishi, Akimitsu, and Titia De Lange. 2008. “Cell Cycle Control of Telomere Protection and NHEJ Revealed by a Ts Mutation in the DNA-Binding Domain of TRF2.” *Genes and Development* 22 (9): 1221–30. https://doi.org/10.1101/gad.1634008.

Kratz, Katja, and Titia de Lange. 2018. “Protection of Telomeres 1 Proteins POT1a and POT1b Can Repress ATR Signaling by RPA Exclusion, but Binding to CST Limits ATR Repression by POT1b.” *The Journal of Biological Chemistry* 293 (37): 14384–92. https://doi.org/10.1074/jbc.RA118.004598.

Lackner, Daniel H., and Jan Karlseder. 2013. “ C. Elegans Survivors without Telomerase .” *Worm* 2 (1): e21073. https://doi.org/10.4161/worm.21073.

Lackner, Daniel H., Marcela Raices, Hugo Maruyama, Candy Haggblom, and Jan Karlseder. 2012. “Organismal Propagation in the Absence of a Functional Telomerase Pathway in Caenorhabditis Elegans.” *EMBO Journal* 31 (8): 2024–33. https://doi.org/10.1038/emboj.2012.61.

Lai, Tsung Po, Woodring E. Wright, and Jerry W. Shay. 2018. “Comparison of Telomere Length Measurement Methods.” *Philosophical Transactions of the Royal Society B: Biological Sciences* 373 (1741). https://doi.org/10.1098/rstb.2016.0451.

Lai, Tsung Po, Ning Zhang, Jungsik Noh, Ilgen Mender, Enzo Tedone, Ejun Huang, Woodring E. Wright, Gaudenz Danuser, and Jerry W. Shay. 2017. “A Method for Measuring the Distribution of the Shortest Telomeres in Cells and Tissues.” *Nature Communications* 8 (1): 1–13. https://doi.org/10.1038/s41467-017-01291-z.

Lange, Titia de. 2018. “Shelterin-Mediated Telomere Protection.” *Annual Review of Genetics* 52 (1): 223–47. https://doi.org/10.1146/annurev-genet-032918-021921.

Lansdorp, Peter M, Nico P Verwoerd, Frans M Van De Rijke, Visia Dragowska, Marie-térèse Little, Roeland W Dirks, Anton K Raap, and Hans J Tanke. 1996. “Heterogeneity in Telomere Length of Human Chromosomes” 5 (5): 685–91.

Latrick, Chrysa M., and Thomas R. Cech. 2010. “POT1-TPP1 Enhances Telomerase Processivity by Slowing Primer Dissociation and Aiding Translocation.” *EMBO Journal* 29 (5): 924–33. https://doi.org/10.1038/emboj.2009.409.

Le, Siyuan, J. Kent Moore, James E. Haber, and Carol W. Greider. 1999. “RAD50 and RAD51 Define Two Pathways That Collaborate to Maintain Telomeres in the Absence of Telomerase.” *Genetics* 152 (1): 143–52. https://doi.org/10.1093/genetics/152.1.143.

Lee, Michael, Christine E. Napier, Sile F. Yang, Jonathan W. Arthur, Roger R. Reddel, and Hilda A. Pickett. 2017. “Comparative Analysis of Whole Genome Sequencing-Based Telomere Length Measurement Techniques.” *Methods* 114: 4–15. https://doi.org/10.1016/j.ymeth.2016.08.008.

Lei, Ming, Elaine R. Podell, and Thomas R. Cech. 2004. “Structure of Human POT1 Bound to Telomeric Single-Stranded DNA Provides a Model for Chromosome End-Protection.” *Nature Structural and Molecular Biology* 11 (12): 1223–29. https://doi.org/10.1038/nsmb867.

Lemmens, Bennie B L G, and Marcel Tijsterman. 2011. “DNA Double-Strand Break Repair in Caenorhabditis Elegans.” *Chromosoma* 120 (1): 1–21. https://doi.org/10.1007/s00412-010-0296-3.

Li, Bibo, and Arthur J Lustig. 1996. “A Novel Mechanism for Telomere Size Control in Saccharomyces Cerevisiae.” *Genes & Development* 10 (11): 1310–26.

Li, Bibo, Stephanie Oestreich, and Titia De Lange. 2000. “Identification of Human Rap1: Implications for Telomere Evolution.” *Cell* 101 (5): 471–83. https://doi.org/10.1016/S0092-8674(00)80858-2.

Lin, Jue, Dana L. Smith, Kyle Esteves, and Stacy Drury. 2019. “Telomere Length Measurement by QPCR – Summary of Critical Factors and Recommendations for Assay Design.” *Psychoneuroendocrinology* 99 (September 2018): 271–78. https://doi.org/10.1016/j.psyneuen.2018.10.005.

Lindrose, Alyssa R., Lauren W.Y. McLester-Davis, Renee I. Tristano, Leila Kataria, Shahinaz M. Gadalla, Dan T.A. Eisenberg, Simon Verhulst, and Stacy Drury. 2021. “Method Comparison Studies of Telomere Length Measurement Using QPCR Approaches: A Critical Appraisal of the Literature.” *PLoS ONE* 16 (1 January): 1–23. https://doi.org/10.1371/journal.pone.0245582.

Liu, Dan, Amin Safari, Matthew S. O’Connor, Doug W. Chan, Andrew Laegeler, Jun Qin, and Zhou Songyang. 2004. “PTOP Interacts with POT1 and Regulates Its Localization to Telomeres.” *Nature Cell Biology* 6 (7): 673–80. https://doi.org/10.1038/ncb1142.

Loayza, Diego, and Titia De Lange. 2003. “POT1 as a Terminal Transducer of TRF1 Telomere Length Control.” *Nature* 423 (6943): 1013–18. https://doi.org/10.1038/nature01688.

Londoño-Vallejo, J. Arturo, Héra Der-Sarkissian, Lucien Cazes, Silvia Bacchetti, and Roger R Reddel. 2004. “Alternative Lengthening of Telomeres Is Characterized by High Rates of Telomeric Exchange.” *Cancer Research* 64 (7): 2324–27. https://doi.org/10.1158/0008-5472.CAN-03-4035.

Longtine, Charlie, Stephen Frenk, and Shawn Ahmed. 2018. “Small RNA-Mediated Genomic Silencing Promotes Telomere Stability in the Absence of Telomerase.” *BioRxiv*, 1–46.

Lossaint, G, E Besnard, D Fisher, J Piette, and V Dulić. 2011. “Chk1 Is Dispensable for G2 Arrest in Response to Sustained DNA Damage When the ATM/P53/P21 Pathway Is Functional.” *Oncogene* 30 (41): 4261–74. https://doi.org/10.1038/onc.2011.135.

Lundblad, Victoria, and Elizabeth H. Blackburn. 1993. “An Alternative Pathway for Yeast Telomere Maintenance Rescues Est1- Senescence.” *Cell* 73 (2): 347–60. https://doi.org/10.1016/0092-8674(93)90234-H.

Lynch, Michael, and Allan Force. 2000. “The Probability of Duplicate Gene Preservation by Subfunctionalization.” *Genetics* 154 (1): 459–73. https://doi.org/10.1093/genetics/154.1.459.

Malik, Harmit S., William D. Burke, and Thomas H. Eickbush. 2000. “Putative Telomerase Catalytic Subunits from Giardia Lamblia and Caenorhabditis Elegans.” *Gene* 251 (2): 101–8. https://doi.org/10.1016/S0378-1119(00)00207-9.

Marcand, Stéphane, Vanessa Brevet, and Eric Gilson. 1999. “Progressive Cis-Inhibition of Telomerase upon Telomere Elongation.” *EMBO Journal* 18 (12): 3509–19. https://doi.org/10.1093/emboj/18.12.3509.

Marcand, Stéphane, Eric Gilson, and David Shore. 1997. “A Protein-Counting Mechanism for Telomere Length Regulation in Yeast.” *Science* 275 (5302): 986–90. https://doi.org/10.1126/science.275.5302.986.

Mary Kironmai, K., and K. Muniyappa. 1997. “Alteration of Telomeric Sequences and Senescence Caused by Mutations in RAD50 of Saccharomyces Cerevisiae.” *Genes to Cells* 2 (7): 443–55. https://doi.org/10.1046/j.1365-2443.1997.1330331.x.

Maser, Richard S, and Ronald A DePinho. 2002. “Connecting Chromosomes, Crisis, and Cancer.” *Science* 297 (5581): 565–69. https://doi.org/10.1126/science.297.5581.565.

Mason, James M., and Harald Biessmann. 1995. “The Unusual Telomeres of Drosophila.” *Trends in Genetics* 11 (2): 58–62. https://doi.org/10.1016/S0168-9525(00)88998-2.

Meier, Bettina, Louise J. Barber, Yan Liu, Ludmila Shtessel, Simon J. Boulton, Anton Gartner, and Shawn Ahmed. 2009. “The MRT-1 Nuclease Is Required for DNA Crosslink Repair and Telomerase Activity in Vivo in Caenorhabditis Elegans.” *EMBO Journal* 28 (22): 3549–63. https://doi.org/10.1038/emboj.2009.278.

Meier, Bettina, Iuval Clejan, Yan Liu, Mia Lowden, Anton Gartner, Jonathan Hodgkin, and Shawn Ahmed. 2006. “Trt-1 Is the Caenorhabditis Elegans Catalytic Subunit of Telomerase.” *PLoS Genetics* 2 (2): 187–97. https://doi.org/10.1371/journal.pgen.0020018.

Melnikova, Larisa, Harald Biessmann, and Pavel Georgiev. 2005. “The Ku Protein Complex Is Involved in Length Regulation of Drosophila Telomeres.” *Genetics* 170 (1): 221–35. https://doi.org/10.1534/genetics.104.034538.

Meneely, Philip M, Caroline L Dahlberg, and Jacqueline K Rose. 2019. “Working with Worms : Caenorhabditis Elegans as a Model Organism,” 1–35. https://doi.org/10.1002/cpet.35.

Meng, Xiangzhou, and Xiaolan Zhao. 2017. “Replication Fork Regression and Its Regulation.” *FEMS Yeast Research* 17 (1): 1–10. https://doi.org/10.1093/femsyr/fow110.

Meyer, Tim De, Ernst R. Rietzschel, Marc L. De buyzere, Dirk De Bacquer, Wim Van Criekinge, Guy G. De Backer, Thierry C. Gillebert, Patrick Van Oostveldt, and Sofie Bekaert. 2007. “Paternal Age at Birth Is an Important Determinant of Offspring Telomere Length.” *Human Molecular Genetics* 16 (24): 3097–3102. https://doi.org/10.1093/hmg/ddm271.

Meyer, Tim De, Katrien Vandepitte, Simon Denil, Marc L. De Buyzere, Ernst R. Rietzschel, and Sofie Bekaert. 2014. “A Non-Genetic, Epigenetic-like Mechanism of Telomere Length Inheritance.” *European Journal of Human Genetics* 22 (1): 10–11. https://doi.org/10.1038/ejhg.2013.255.

Meyne, J., R. L. Ratliff, and R. K. Moyzis. 1989. “Conservation of the Human Telomere Sequence (TTAGGG)(n) among Vertebrates.” *Proceedings of the National Academy of Sciences of the United States of America* 86 (18): 7049–53. https://doi.org/10.1073/pnas.86.18.7049.

Mikhailovsky, Stanislav, Tatyana Belenkaya, and Pavel Georgiev. 1999. “Broken Chromosomal Ends Can Be Elongated by Conversion in Drosophila Melanogaster.” *Chromosoma* 108 (2): 114–20. https://doi.org/10.1007/s004120050358.

Moyzis, R. K., J. M. Buckingham, L. S. Cram, M. Dani, L. L. Deaven, M. D. Jones, J. Meyne, R. L. Ratliff, and J. R. Wu. 1988. “A Highly Conserved Repetitive DNA Sequence, (TTAGGG)(n), Present at the Telomeres of Human Chromosomes.”

Proceedings of the National Academy of Sciences of the United States of America 85 (18): 6622–26. https://doi.org/10.1073/pnas.85.18.6622.

MULLER, Hermann Joseph. 1938. “The Remaking of Chromosomes.” *Collecting Net* 8: 198.

Munari, Fernanda Mosena, Temenouga Nikolova Guecheva, Diego Bonatto, and João Antônio Pêgas Henriques. 2013. “New Features on Pso2 Protein Family in DNA Interstrand Cross-Link Repair and in the Maintenance of Genomic Integrity in Saccharomyces Cerevisiae.” *Fungal Genetics and Biology* 60: 122–32. https://doi.org/https://doi.org/10.1016/j.fgb.2013.09.003.

Myler, Logan R., Charles G. Kinzig, Nanda K. Sasi, George Zakusilo, Sarah W. Cai, and Titia de Lange. 2021. “The Evolution of Metazoan Shelterin.” *Genes & Development* 35 (23–24): 1625–41. https://doi.org/10.1101/gad.348835.121.

Nandakumar, Jayakrishnan, Caitlin F. Bell, Ina Weidenfeld, Arthur J. Zaug, Leslie A. Leinwand, and Thomas R. Cech. 2012. “The TEL Patch of Telomere Protein TPP1 Mediates Telomerase Recruitment and Processivity.” *Nature* 492 (7428): 285–89. https://doi.org/10.1038/nature11648.

Nandakumar, Jayakrishnan, and Thomas R. Cech. 2013. “Finding the End: Recruitment of Telomerase to Telomeres.” *Nature Reviews Molecular Cell Biology* 14 (2): 69–82. https://doi.org/10.1038/nrm3505.

Nawrot, Tim S., Jan A. Staessen, Jeffrey P. Gardner, and Abraham Aviv. 2004. “Telomere Length and Possible Link to X Chromosome.” *Lancet* 363 (9408): 507–10. https://doi.org/10.1016/S0140-6736(04)15535-9.

Nersisyan, Lilit, and Arsen Arakelyan. 2015. “Computel: Computation of Mean Telomere Length from Whole-Genome next-Generation Sequencing Data.” *PLoS ONE* 10 (4): 1–14. https://doi.org/10.1371/journal.pone.0125201.

Njajou, Omer T., Richard M. Cawthon, Coleen M. Damcott, Shih Hsuan Wu, Sandy Ott, Michael J. Garant, Elizabeth H. Blackburn, Braxton D. Mitchell, Alan R. Shuldiner, and Wen Chi Hsueh. 2007. “Telomere Length Is Paternally Inherited and Is Associated with Parental Lifespan.” *Proceedings of the National Academy of Sciences of the United States of America* 104 (29): 12135–39. https://doi.org/10.1073/pnas.0702703104.

Nordfjäll, Katarina, Åsa Larefalk, Petter Lindgren, Dan Holmberg, and Göran Roos. 2005. “Telomere Length and Heredity: Indications of Paternal Inheritance.” *Proceedings of the National Academy of Sciences of the United States of America* 102 (45): 16374–78. https://doi.org/10.1073/pnas.0501724102.

Nordfjäll, Katarina, Ulrika Svenson, Karl Fredrik Norrback, Rolf Adolfsson, and Göran Roos. 2010. “Large-Scale Parent-Child Comparison Confirms a Strong Paternal Influence on Telomere Length.” *European Journal of Human Genetics* 18 (3): 385–89. https://doi.org/10.1038/ejhg.2009.178.

Nugent, Constance I., Timothy R. Hughes, Neal F. Lue, and Victoria Lundblad. 1996. “Cdc13p: A Single-Strand Telomeric DNA-Binding Protein with a Dual Role in Yeast Telomere Maintenance.” *Science* 274 (5285): 249–52. https://doi.org/10.1126/science.274.5285.249.

O’Callaghan, Nathan J., and Michael Fenech. 2011. “A Quantitative PCR Method for Measuring Absolute Telomere Length.” *Biological Procedures Online* 13 (1): 1–10. https://doi.org/10.1186/1480-9222-13-3.

Olovnikov, A M. 1973. “A Theory of Marginotomy: The Incomplete Copying of Template Margin in Enzymic Synthesis of Polynucleotides and Biological Significance of the Phenomenon.” *Journal of Theoretical Biology* 41 (1): 181–90. https://doi.org/https://doi.org/10.1016/0022-5193(73)90198-7.

Olsson, Mats, Angela Pauliny, Erik Wapstra, Tobias Uller, Tonia Schwartz, and Donald Blomqvist. 2011. “Sex Differences in Sand Lizard Telomere Inheritance: Paternal Epigenetic Effects Increases Telomere Heritability and Offspring Survival.” *PLoS ONE* 6 (4). https://doi.org/10.1371/journal.pone.0017473.

Overbeek, Megan van, and Titia de Lange. 2006. “Apollo, an Artemis-Related Nuclease, Interacts with TRF2 and Protects Human Telomeres in S Phase.” *Current Biology* 16 (13): 1295–1302. https://doi.org/10.1016/j.cub.2006.05.022.

Palm, Wilhelm, Dirk Hockemeyer, Tatsuya Kibe, and Titia de Lange. 2009. “Functional Dissection of Human and Mouse POT1 Proteins.” *Molecular and Cellular Biology* 29 (2): 471–82. https://doi.org/10.1128/mcb.01352-08.

Pardue, Mary-Lou, and P G DeBaryshe. 2003. “Retrotransposons Provide an Evolutionarily Robust Non-Telomerase Mechanism to Maintain Telomeres.” *Annual*

Review of Genetics 37 (1): 485–511. https://doi.org/10.1146/annurev.genet.38.072902.093115.

Paterson, A. H., J. E. Bowers, and B. A. Chapman. 2004. "Ancient Polyploidization Predating Divergence of the Cereals, and Its Consequences for Comparative Genomics." *Proceedings of the National Academy of Sciences of the United States of America* 101 (26): 9903–8. https://doi.org/10.1073/pnas.0307901101.

Pfeiffer, Verena, and Joachim Lingner. 2012. "TERRA Promotes Telomere Shortening through Exonuclease 1-Mediated Resection of Chromosome Ends." *PLoS Genetics* 8 (6). https://doi.org/10.1371/journal.pgen.1002747.

Pham, Kenneth, Neda Masoudi, Eduardo Leyva-Díaz, and Oliver Hobert. 2021. "A Nervous System-Specific Subnuclear Organelle in Caenorhabditis Elegans." *Genetics* 217 (1). https://doi.org/10.1093/GENETICS/IYAA016.

Phillips, Jane A., Angela Chan, Katrin Paeschke, and Virginia A. Zakian. 2015. "The Pif1 Helicase, a Negative Regulator of Telomerase, Acts Preferentially at Long Telomeres." *PLoS Genetics* 11 (4): 1–19. https://doi.org/10.1371/journal.pgen.1005186.

Poon, Steven S.S., and Peter M. Lansdorp. 2001. "Measurements of Telomere Length on Individual Chromosomes by Image Cytometry." *Methods in Cell Biology* 64 (64): 69–96. https://doi.org/10.1016/s0091-679x(01)64007-x.

Poon, Steven S.S., Uwe M. Martens, Rabab K. Ward, and Peter M. Lansdorp. 1999. "Telomere Length Measurements Using Digital Fluorescence Microscopy." *Cytometry* 36 (4): 267–78. https://doi.org/10.1002/(SICI)1097-0320(19990801)36:4<267::AID-CYTO1>3.0.CO;2-O.

Raices, Marcela, Hugo Maruyama, Andrew Dillin, and Jan Kariseder. 2005. "Uncoupling of Longevity and Telomere Length in C, Elegans." *PLoS Genetics* 1 (3): 295–301. https://doi.org/10.1371/journal.pgen.0010030.

Raices, Marcela, Ramiro E. Verdun, Sarah A. Compton, Candy I. Haggblom, Jack D. Griffith, Andrew Dillin, and Jan Karlseder. 2008. "C. Elegans Telomeres Contain G-Strand and C-Strand Overhangs That Are Bound by Distinct Proteins." *Cell* 132 (5): 745–57. https://doi.org/10.1016/j.cell.2007.12.039.

Rakha, A. 2015. "Cloning Efficiency and a Comparison between Donor Cell Types." *Clon. Transgen* 2: 141.

Reichert, S., E. R. Rojas, S. Zahn, J. P. Robin, F. Criscuolo, and S. Massemin. 2015. “Maternal Telomere Length Inheritance in the King Penguin.” *Heredity* 114 (1): 10–16. https://doi.org/10.1038/hdy.2014.60.

Rice, Cory, Prashanth Krishna Shastrula, Andrew V. Kossenkov, Robert Hills, Duncan M. Baird, Louise C. Showe, Tzanko Doukov, Susan Janicki, and Emmanuel Skordalakes. 2017. “Structural and Functional Analysis of the Human POT1-TPP1 Telomeric Complex.” *Nature Communications* 8: 1–13. https://doi.org/10.1038/ncomms14928.

Riddle, Donald L, Thomas Blumenthal, Barbara J Meyer, and James R Priess. 1997. “C. Elegans II.”

Rodriguez-Brenes, Ignacio A., and Charles S. Peskin. 2010. “Quantitative Theory of Telomere Length Regulation and Cellular Senescence.” *Proceedings of the National Academy of Sciences of the United States of America* 107 (12): 5387–92. https://doi.org/10.1073/pnas.0914502107.

Rossignol, Pascale, Sarah Collier, Max Bush, Peter Shaw, and John H. Doonan. 2007. “Arabidopsis POT1A Interacts with TERT-V(18), an N-Terminal Splicing Variant of Telomerase.” *Journal of Cell Science* 120 (20): 3678–87. https://doi.org/10.1242/jcs.004119.

Rufer, Nathalie, Wieslawa Dragowska, Gayle Thornbury, Eddy Roosnek, and Peter M Lansdorp. 1998. “Flow Cyton1Etry,” 743–47.

Saint-Leandre, Bastien, and Mia T. Levine. 2020. “The Telomere Paradox: Stable Genome Preservation with Rapidly Evolving Proteins.” *Trends in Genetics* 36 (4): 232–42. https://doi.org/10.1016/j.tig.2020.01.007.

Sanjuán, Rafael, and Santiago F Elena. 2006. “Epistasis Correlates to Genomic Complexity.” *Proceedings of the National Academy of Sciences* 103 (39): 14402–5. https://doi.org/10.1073/pnas.0604543103.

Schaetzlein, Sonja, Andrea Lucas-Hahn, Erika Lemme, Wilfried A. Kues, Martina Dorsch, Michael P. Manns, Heiner Niemann, and K. Lenhard Rudolph. 2004. “Telomere Length Is Reset during Early Mammalian Embryogenesis.” *Proceedings of the National Academy of Sciences of the United States of America* 101 (21): 8034–38. https://doi.org/10.1073/pnas.0402400101.

Schmutz, Isabelle, and Titia de Lange. 2016. “Shelterin.” *Current Biology* 26 (10): R397–99. https://doi.org/10.1016/j.cub.2016.01.056.

Schmutz, Isabelle, and Titia De Lange. 2016. “Current Biology Shelterin.” *Current Biology*. Vol. 26. https://doi.org/10.1016/j.cub.2016.01.056.

Sfeir, Agnel J., Weihang Chai, Jerry W. Shay, and Woodring E. Wright. 2005. “Telomere-End Processing: The Terminal Nucleotidesof Human Chromosomes.” *Molecular Cell* 18 (1): 131–38. https://doi.org/10.1016/j.molcel.2005.02.035.

Sfeir, Agnel, Shaheen Kabir, Megan van Overbeek, Giulia B Celli, Titia de Lange, B K Kobilka, L Hein, et al. 2010. “Loss of Rap1 Induces Telomere Recombination in the Absence of NHEJ or a DNA Damage Signal.” *Science* 327 (5973): 1657–61. https://doi.org/10.1126/science.1185100.

Sfeir, Agnel, Settapong T. Kosiyatrakul, Dirk Hockemeyer, Sheila L. MacRae, Jan Karlseder, Carl L. Schildkraut, and Titia de Lange. 2009. “Mammalian Telomeres Resemble Fragile Sites and Require TRF1 for Efficient Replication.” *Cell* 138 (1): 90–103. https://doi.org/10.1016/j.cell.2009.06.021.

Shakirov, E. V., S. L. Salzberg, M. Alam, and D. E. Shippen. 2008. “Analysis of Carica Papaya Telomeres and Telomere-Associated Proteins: Insights into the Evolution of Telomere Maintenance in Brassicales.” *Tropical Plant Biology* 1 (3–4): 202–15. https://doi.org/10.1007/s12042-008-9018-x.

Shakirov, Eugene V., Thomas D. McKnight, and Dorothy E. Shippen. 2009. “POT1-Independent Single-Strand Telomeric DNA Binding Activities in Brassicaceae.” *Plant Journal* 58 (6): 1004–15. https://doi.org/10.1111/j.1365-313X.2009.03837.x.

Shakirov, Eugene V., Pierre François Perroud, Andrew D. Nelson, Maren E. Cannell, Ralph S. Quatrano, and Dorothy E. Shippen. 2010. “Protection of Telomeres 1 Is Required for Telomere Integrity in the Moss Physcomitrella Patens.” *Plant Cell* 22 (6): 1838–48. https://doi.org/10.1105/tpc.110.075846.

Shakirov, Eugene V., Yulia V. Surovtseva, Nathan Osbun, and Dorothy E. Shippen. 2005. “ The Arabidopsis Pot1 and Pot2 Proteins Function in Telomere Length Homeostasis and Chromosome End Protection .” *Molecular and Cellular Biology* 25 (17): 7725–33. https://doi.org/10.1128/mcb.25.17.7725-7733.2005.

Shay, Jerry W, Olivia M Pereira-Smith, and Woodring E Wright. 1991. “A Role for Both RB and P53 in the Regulation of Human Cellular Senescence.” *Experimental Cell Research* 196 (1): 33–39. https://doi.org/https://doi.org/10.1016/0014-4827(91)90453-2.

Sholes, Samantha L., Kayarash Karimian, Ariel Gershman, Thomas J. Kelly, Winston Timp, and Carol W. Greider. 2022. “Chromosome-Specific Telomere Lengths and the Minimal Functional Telomere Revealed by Nanopore Sequencing.” *Genome Research* 32 (4): 616–28. https://doi.org/10.1101/gr.275868.121.

Shtessel, Ludmila, Mia Rochelle Lowden, Chen Cheng, Matt Simon, Kyle Wang, and Shawn Ahmed. 2013. “Caenorhabditis Elegans POT-1 and POT-2 Repress Telomere Maintenance Pathways.” *G3: Genes, Genomes, Genetics* 3 (2): 305–13. https://doi.org/10.1534/g3.112.004440.

Skopp, Rose, Wenlan Wang, and Carolyn Price. 1996. “RTP: A Candidate Telomere Protein That Is Associated with DNA Replication.” *Chromosoma* 105 (2): 82–91. https://doi.org/10.1007/BF02509517.

Slijepcevic, Predrag. 2001. “Telomere Length Measurement by Q-FISH.” *Methods in Cell Science* 23 (1–3): 17–22. https://doi.org/10.1023/A:1013177128297.

Smoom, Riham, Catherine Lee May, Vivian Ortiz, Mark Tigue, Hannah M Kolev, Melissa Rowe, Yitzhak Reizel, et al. 2023. “Telomouse – a Mouse Model with Human-Length Telomeres Generated by a Single Amino Acid Change in RTEL1.” *BioRxiv*, January, 2021.06.06.447246. https://doi.org/10.1101/2021.06.06.447246.

Sobinoff, Alexander P, Joshua AM Allen, Axel A Neumann, Sile F Yang, Monica E Walsh, Jeremy D Henson, Roger R Reddel, and Hilda A Pickett. 2017. “BLM and SLX4 Play Opposing Roles in Recombination-dependent Replication at Human Telomeres.” *The EMBO Journal* 36 (19): 2907–19. https://doi.org/10.15252/embj.201796889.

Steensel, Bas van, and Titia de Lange. 1997. “Control of Telomere Length by the Human Telomeric Protein TRF1 Bas.” *Nature* 385 (February): 740–43.

Surovtseva, Yulia V., Dmitri Churikov, Kara A. Boltz, Xiangyu Song, Jonathan C. Lamb, Ross Warrington, Katherine Leehy, Michelle Heacock, Carolyn M. Price, and Dorothy E. Shippen. 2009. “Conserved Telomere Maintenance Component 1 Interacts with STN1 and Maintains Chromosome Ends in Higher Eukaryotes.” *Molecular Cell* 36 (2): 207–18. https://doi.org/10.1016/j.molcel.2009.09.017.

Surovtseva, Yulia V., Eugene V. Shakirov, Laurent Vespa, Nathan Osbun, Xiangyu Song, and Dorothy E. Shippen. 2007. “Arabidopsis POT1 Associates with the Telomerase RNP and Is Required for Telomere Maintenance.” *EMBO Journal* 26 (15): 3653–61. https://doi.org/10.1038/sj.emboj.7601792.

Takai, Hiroyuki, Emma Jenkinson, Shaheen Kabir, Riyana Babul-Hirji, Nasrin Najm-Tehrani, David A. Chitayat, Yanick J. Crow, and Titia de Lange. 2016. “A POT1 Mutation Implicates Defective Telomere End Fill-in and Telomere Truncations in Coats Plus.” *Genes and Development* 30 (7): 812–26. https://doi.org/10.1101/gad.276873.115.

Takai, Kaori K, Tatsuya Kibe, Jill R Donigian, David Frescas, and Titia de Lange. 2011. “Telomere Protection by TPP1/POT1 Requires Tethering to TIN2.” *Molecular Cell* 44 (4): 647–59. https://doi.org/10.1016/j.molcel.2011.08.043.

Takai, Kaori K., Sarah Hooper, Stephanie Blackwood, Rita Gandhi, and Titia de Lange. 2010a. “In Vivo Stoichiometry of Shelterin Components.” *Journal of Biological Chemistry* 285 (2): 1457–67. https://doi.org/10.1074/jbc.M109.038026.

Takai, Kaori K, Sarah Hooper, Stephanie Blackwood, Rita Gandhi, and Titia de Lange. 2010b. “In Vivo Stoichiometry of Shelterin Components.” *Journal of Biological Chemistry* 285 (2): 1457–67. https://doi.org/10.1074/jbc.M109.038026.

Tan, Kar-Tong, Michael K Slevin, Matthew Meyerson, and Heng Li. 2022. “Identifying and Correcting Repeat-Calling Errors in Nanopore Sequencing of Telomeres.” *Genome Biology* 23 (1): 1–16.

Tarik, Mohamad, Lakshmy Ramakrishnan, Harshpal S. Sachdev, Nikhil Tandon, Ambuj Roy, Santosh K. Bhargava, and Ravindra M. Pandey. 2018. “Validation of Quantitative Polymerase Chain Reaction with Southern Blot Method for Telomere Length Analysis.” *Future Science OA* 4 (4). https://doi.org/10.4155/fsoa-2017-0115.

Teixeira, M. Teresa, Milica Arneric, Peter Sperisen, and Joachim Lingner. 2004. “Telomere Length Homeostasis Is Achieved via a Switch between Telomerase-Extendible and -Nonextendible States.” *Cell* 117 (3): 323–35. https://doi.org/10.1016/S0092-8674(04)00334-4.

Teixeira, Maria Teresa. 2013. “Saccharomyces Cerevisiae as a Model to Study Replicative Senescence Triggered by Telomere Shortening.” *Frontiers in Oncology* 3. https://www.frontiersin.org/journals/oncology/articles/10.3389/fonc.2013.00101.

Teng, Shu-Chun, and Virginia A. Zakian. 1999. “ Telomere-Telomere Recombination Is an Efficient Bypass Pathway for Telomere Maintenance in Saccharomyces Cerevisiae .” *Molecular and Cellular Biology* 19 (12): 8083–93. https://doi.org/10.1128/mcb.19.12.8083.

Teng, Shu Chun, Jason Chang, Bradley McCowan, and Virginia A. Zakian. 2000. “Telomerase-Independent Lengthening of Yeast Telomeres Occurs by an Abrupt Rad50p-Dependent, Rif-Inhibited Recombinational Process.” *Molecular Cell* 6 (4): 947–52. https://doi.org/10.1016/S1097-2765(05)00094-8.

Tham, Cheng Yong, Lai Fong Poon, Ting Dong Yan, Javier Yu Peng Koh, Muhammad Khairul Ramlee, Vania Swee Imm Teoh, Suihan Zhang, et al. 2023. “High-Throughput Telomere Length Measurement at Nucleotide Resolution Using the PacBio High Fidelity Sequencing Platform.” *Nature Communications* 14 (1). https://doi.org/10.1038/s41467-023-35823-7.

Tischler, Julia, Ben Lehner, Nansheng Chen, and Andrew G Fraser. 2006. “Combinatorial RNA Interference in Caenorhabditis Elegans Reveals That Redundancy between Gene Duplicates Can Be Maintained for More than 80 Million Years of Evolution.” *Genome Biology* 7 (8): R69. https://doi.org/10.1186/gb-2006-7-8-r69.

Torrance, Victoria, and David Lydall. 2018. “Overlapping Open Reading Frames Strongly Reduce Human and Yeast STN1 Gene Expression and Affect Telomere Function.” *PLoS Genetics* 14 (8): 1–20. https://doi.org/10.1371/journal.pgen.1007523.

Tran, Phuoc T., Naz Erdeniz, Lorraine S. Symington, and R. Michael Liskay. 2004. “EXO1-A Multi-Tasking Eukaryotic Nuclease.” *DNA Repair* 3 (12): 1549–59. https://doi.org/10.1016/j.dnarep.2004.05.015.

Vaiserman, Alexander, and Dmytro Krasnienkov. 2021. “Telomere Length as a Marker of Biological Age: State-of-the-Art, Open Issues, and Future Perspectives.” *Frontiers in Genetics* 11 (January). https://doi.org/10.3389/fgene.2020.630186.

Verdun, Ramiro E., and Jan Karlseder. 2007. “Replication and Protection of Telomeres.” *Nature* 447 (7147): 924–31. https://doi.org/10.1038/nature05976.

Victorelli, Stella, and João F. Passos. 2017. “Telomeres and Cell Senescence - Size Matters Not.” *EBioMedicine* 21: 14–20. https://doi.org/10.1016/j.ebiom.2017.03.027.

Vitis, Marco De, Francesco Berardinelli, and Antonella Sgura. 2018. “Telomere Length Maintenance in Cancer: At the Crossroad between Telomerase and Alternative Lengthening of Telomeres (ALT).” *International Journal of Molecular Sciences* 19 (2). https://doi.org/10.3390/ijms19020606.

Vizlin-Hodzic, Dzeneta, Jessica Ryme, Stina Simonsson, and Tomas Simonsson. 2009. “Developmental Studies of Xenopus Shelterin Complexes: The Message to Reset Telomere Length Is Already Present in the Egg.” *The FASEB Journal* 23 (8): 2587–94. https://doi.org/10.1096/fj.09-129619.

Wageningen, Sake Van, Patrick Kemmeren, Philip Lijnzaad, Thanasis Margaritis, Joris J. Benschop, Inês J. De Castro, Dik Van Leenen, et al. 2010. “Functional Overlap and Regulatory Links Shape Genetic Interactions between Signaling Pathways.” *Cell* 143 (6): 991–1004. https://doi.org/10.1016/j.cell.2010.11.021.

Wang, Feng, Elaine R. Podell, Arthur J. Zaug, Yuting Yang, Paul Baciu, Thomas R. Cech, and Ming Lei. 2007. “The POT1-TPP1 Telomere Complex Is a Telomerase Processivity Factor.” *Nature* 445 (7127): 506–10. https://doi.org/10.1038/nature05454.

Wang, Richard C, Agata Smogorzewska, and Titia De Lange. 2004. “Homologous Recombination Generates T-Loop-Sized Deletions at Human Telomeres (Marciniak et Al We Document That HR Can Delete Large Segments of Telomeric DNA in Human and Mouse Cells Meric Segments Resulting in Rapid Shortening of Telo-2 Present Address: D.” *Cell* 119: 355–68. http://www.

Wang, Yisong, Natalie Erdmann, Richard J. Giannone, Jun Wu, Marla Gomez, and Yie Liu. 2005. “An Increase in Telomere Sister Chromatid Exchange in Murine Embryonic Stem Cells Possessing Critically Shortened Telomeres.” *Proceedings of the National Academy of Sciences of the United States of America* 102 (29): 10256–60. https://doi.org/10.1073/pnas.0504635102.

Wellinger, R. J., and D. Sen. 1997. “The DNA Structures at the Ends of Eukaryotic Chromosomes.” *European Journal of Cancer Part A* 33 (5): 735–49. https://doi.org/10.1016/S0959-8049(97)00067-1.

Wellinger, Raymund J. 2010. “When the Caps Fall off: Responses to Telomere Uncapping in Yeast.” *FEBS Letters* 584 (17): 3734–40. https://doi.org/10.1016/j.febslet.2010.06.031.

Wu, Ling, Asha S. Multani, Hua He, Wilfredo Cosme-Blanco, Yu Deng, Jian Min Deng, Olga Bachilo, et al. 2006. “Pot1 Deficiency Initiates DNA Damage Checkpoint Activation and Aberrant Homologous Recombination at Telomeres.” *Cell* 126 (1): 49–62. https://doi.org/10.1016/j.cell.2006.05.037.

Wu, Peng, Hiroyuki Takai, and Titia De Lange. 2012. “Telomeric 3′ Overhangs Derive from Resection by Exo1 and Apollo and Fill-in by POT1b-Associated CST.” *Cell* 150 (1): 39–52. https://doi.org/10.1016/j.cell.2012.05.026.

Xin, Huawei, Dan Liu, Ma Wan, Amin Safari, Hyeung Kim, Wen Sun, Matthew S. O’Connor, and Zhou Songyang. 2007. “TPP1 Is a Homologue of Ciliate TEBP-β and Interacts with POT1 to Recruit Telomerase.” *Nature* 445 (7127): 559–62. https://doi.org/10.1038/nature05469.

Xu, Zhou, Khanh Dao Duc, David Holcman, and Maria Teresa Teixeira. 2013. “The Length of the Shortest Telomere as the Major Determinant of the Onset of Replicative Senescence.” *Genetics* 194 (4): 847–57. https://doi.org/10.1534/genetics.113.152322.

Yamamoto, Io, Kexin Zhang, Jingjing Zhang, Egor Vorontsov, and Hiroki Shibuya. 2021. “Telomeric Double-Strand Dna-Binding Proteins Dtn-1 and Dtn-2 Ensure Germline Immortality in Caenorhabditis Elegans.” *ELife* 10: 1–21. https://doi.org/10.7554/eLife.64104.

Ye, Jeffrey Zheng Sheng, and Titia De Lange. 2004. “TIN2 Is a Tankyrase 1 PARP Modulator in the TRF1 Telomere Length Control Complex.” *Nature Genetics* 36 (6): 618–23. https://doi.org/10.1038/ng1360.

Yeager, Thomas R, Axel A Neumann, Anna Englezou, Lily I Huschtscha, Jane R Noble, and Roger R Reddel. 1999. “Telomerase-Negative Immortalized Human Cells Contain a Novel Type of Promyelocytic Leukemia (PML) Body.” *Cancer Research* 59 (17): 4175–79.

Yin, Yizhi, and Sarit Smolikove. 2013. “Impaired Resection of Meiotic Double-Strand Breaks Channels Repair to Nonhomologous End Joining in Caenorhabditis Elegans.” *Molecular and Cellular Biology* 33 (14): 2732–47. https://doi.org/10.1128/MCB.00055-13.

Yong, Wang Jin, Lan Jing, Zhao Jiugang, Chen Lei, and Liu Yonggang. 2012. “A Novel Porcine Gene, POT1, Differentially Expressed in the Longissimus Muscle Tissues

from Wujin and Large White Pigs." *Cytokine* 59 (1): 22–26. https://doi.org/10.1016/j.cyto.2012.03.028.

Yu, Xupeng, Sean Gray, and Helder C Ferreira. 2023. "POT-3 Preferentially Binds the Terminal DNA-Repeat on the Telomeric G-Overhang." *Nucleic Acids Research* 51 (2): 610–18. https://doi.org/10.1093/nar/gkac1203.

Zhang, Tianpeng, Zepeng Zhang, Gong Shengzhao, Xiaocui Li, Haiying Liu, and Yong Zhao. 2019. "Strand Break-Induced Replication Fork Collapse Leads to C-Circles, C-Overhangs and Telomeric Recombination." *PLoS Genetics* 15 (2). https://doi.org/10.1371/journal.pgen.1007925.

Zhang, Ze-Hao, Sheng Hu Qian, Dengguo Wei, and Zhen-Xia Chen. 2023. "In Vivo Dynamics and Regulation of DNA G-Quadruplex Structures in Mammals." *Cell & Bioscience* 13 (1): 117.

Zhong, Z, L Shiue, S Kaplan, and T de Lange. 1992. "A Mammalian Factor That Binds Telomeric TTAGGG Repeats in Vitro." *Molecular and Cellular Biology* 12 (11): 4834–43. https://doi.org/10.1128/mcb.12.11.4834-4843.1992.

Appendix

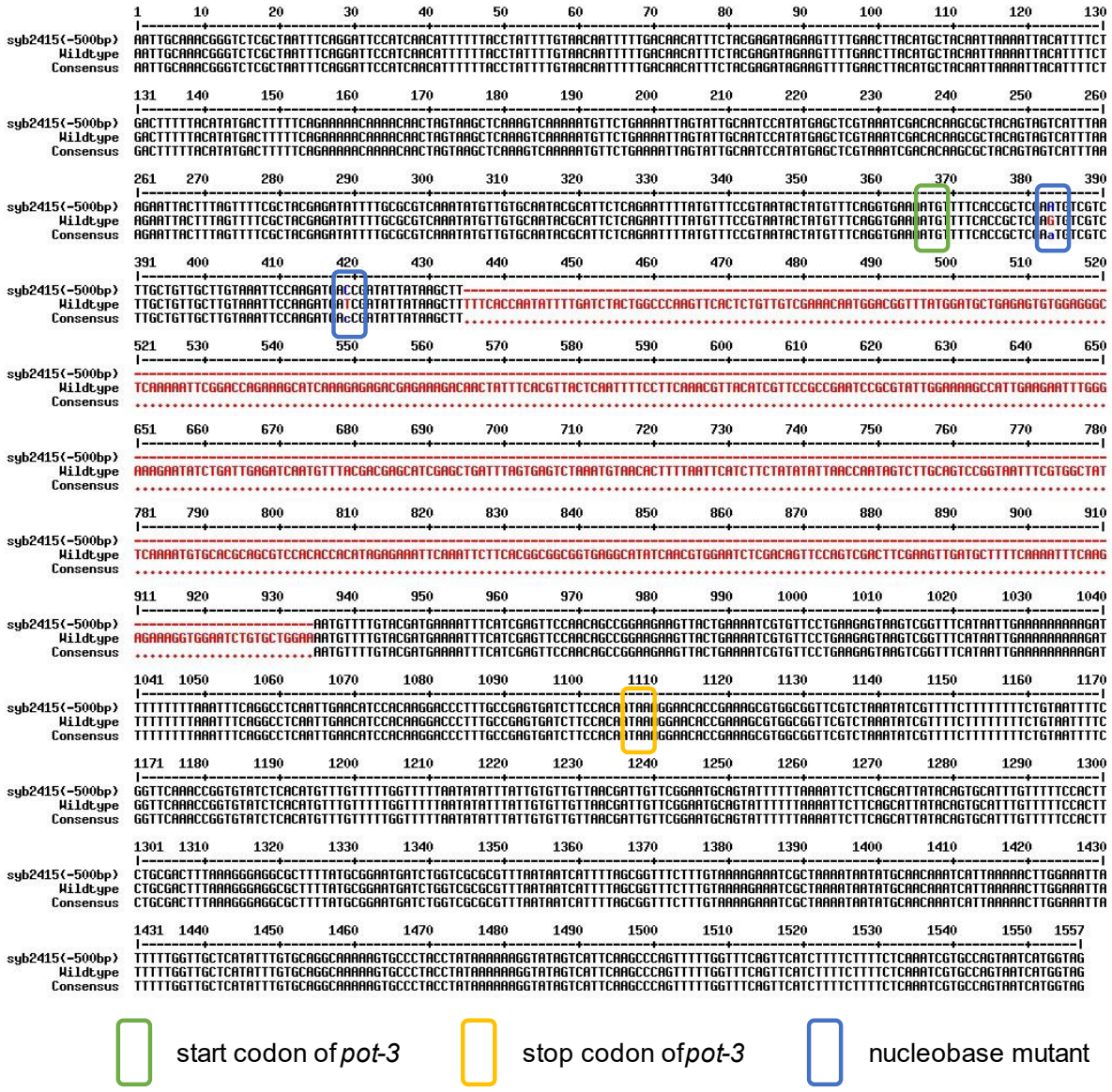

Figure AP.1 *pot-3(syb2415)* mutant stain has OB-fold deletion

The sequence of *pot-3(syb2415)* and upstream/downstream area. The red sequence indicates the deletion region. The green square indicates the start codon of the *pot-3* CDS. The yellow square indicates the stop codon of the *pot-3* CDS. The blue squares indicate the mutant nucleobases, which do not change the amino acid sequence after translation.

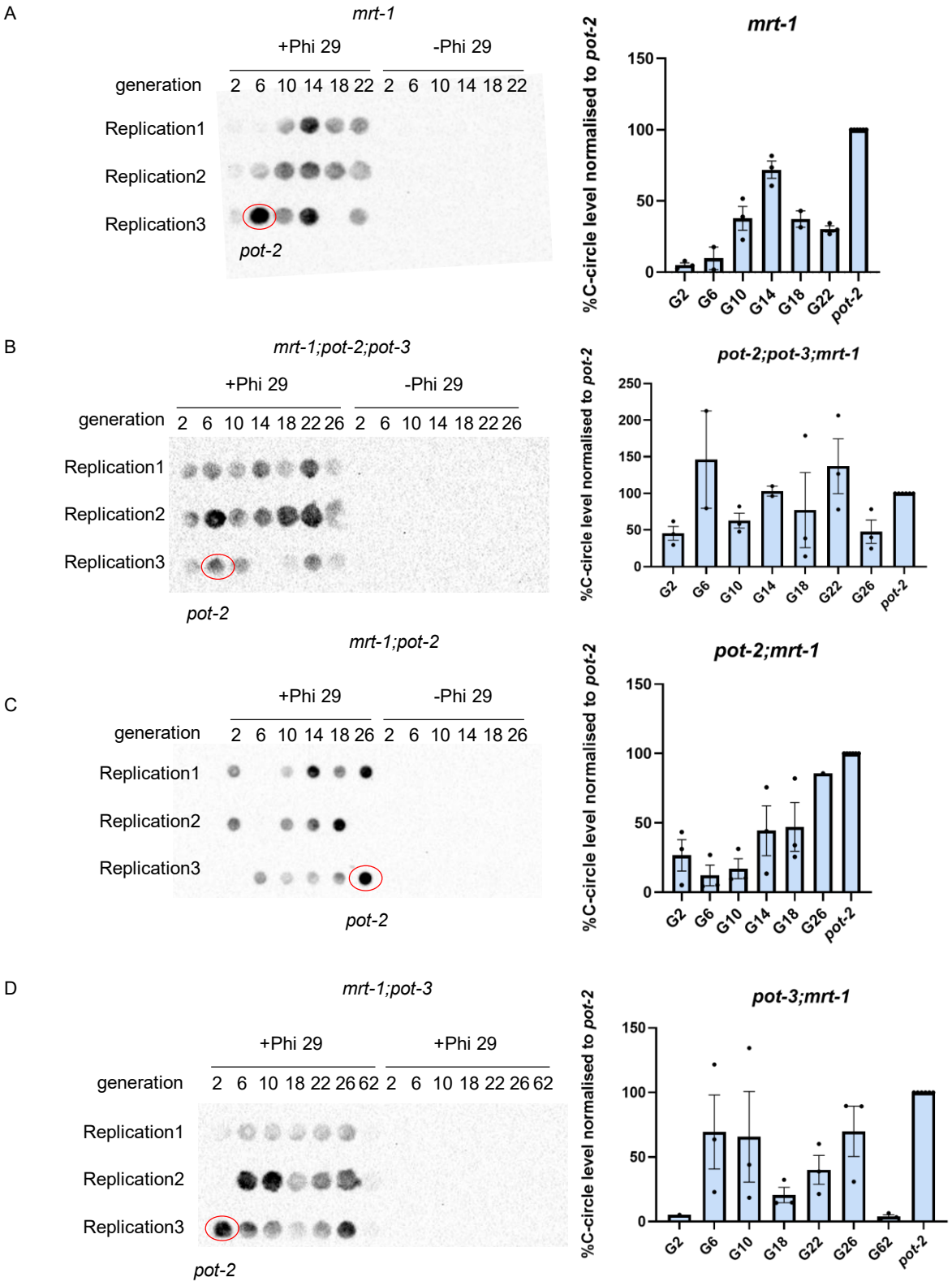

Figure AP.2 The C-circle assay of crosses involving *mrt-1*, *pot-2;mrt-1*, *pot-3;mrt-1*, and *pot-2;pot-3;mrt-1* display no discernible consistent pattern

A) C-circle assay from genomic DNA of populations of *mrt-1* mutants. Samples were collected from the 2nd, 6th, 10th,14th 18th, and 22nd generation. B) C-circle assay from genomic DNA of populations of *pot-2;pot-3;mrt-1* triple mutants. Samples were collected from the 2nd, 6th, 10th,14th, 22nd, and 26th generation. C) C-circle assay from genomic DNA of populations of *mrt-*

1;pot-2 double mutants. Samples were collected from the 2nd, 6th, 10th,14th 18th,22nd and 26th generation. D) C-circle assay from genomic DNA of populations of *mrt-1;pot-3* double mutants. Samples were collected from the 2nd, 6th, 10th,14th, 22nd, 26th, and 62nd generation. Animals were kept at 20°C. Membrane was probed with DIG-labelled $(TTAGGC)_4$ oligos. Statistical analysis of the telomere shortening rate in *mrt-1*, *pot-2;mrt-1* double mutants, *pot-3;mrt-1* double mutants, and *pot-2;pot-3;mrt-1* triple mutants. The quantification indicates the mean of individual C-circle level measurements over indicated generations. Error bars show SEM.

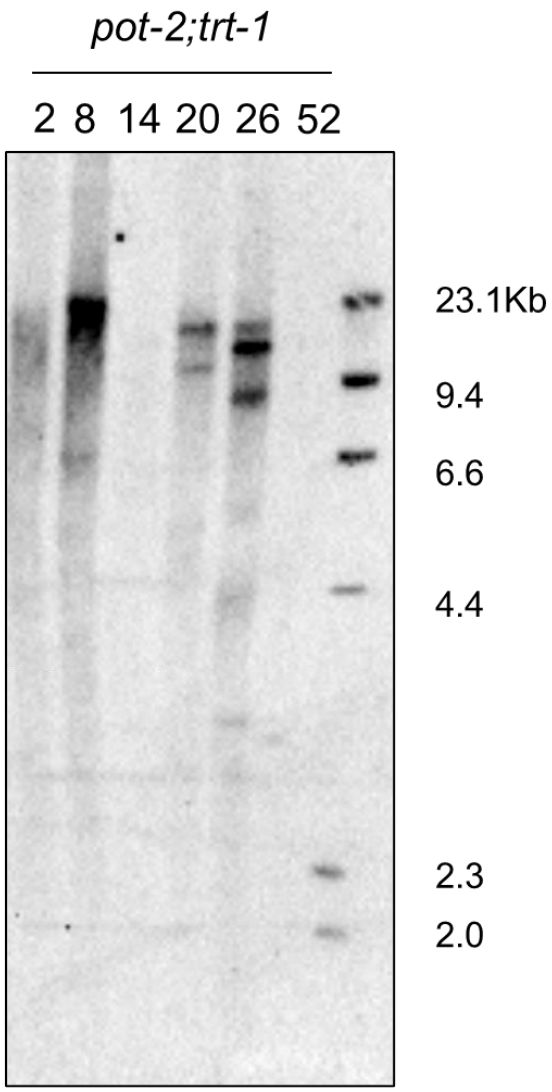

Figure AP.3 Telomere length of *pot-2;trt-1* shows ALT telomere length elongation phenotype

A TRF Southern blot of telomere length changes intergenerationally involving *pot-2;trt-1*. Worms were kept at 20°C. Samples were collected from the 2nd, 8th, 14th, 20th,26th, and 52nd generation. The membrane was probed with DIG-labelled $(TTAGGC)_4$ oligos. The telomere length of this strain displayed the telomere length increase in the strongest telomeric signals in the 8th generation.